SUCCESS: A 6 Unit CubeSat Bus Development Effort

Mechanical Engineering
UNIVERSITY OF COLORADO BOULDER

D03: Final Report
May 7, 2015

COSGC
COLORADO SPACE GRANT CONSORTIUM

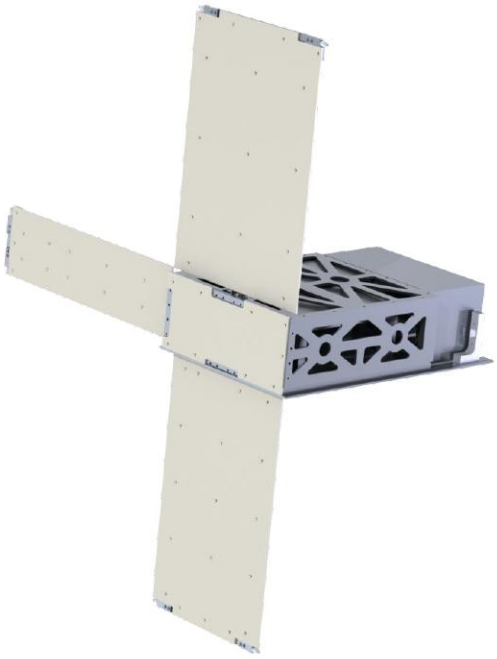

Khalid AlDossary –
Nicholas Merten –
Andrew Ohlig –
William Pardee
Dan Waltermire –
Hongyu Zhang –

University of Colorado at Boulder

Department of Mechanical Engineering

Table of Contents

Table of Figures

Table of Tables

1 Executive Summary

CubeSats are an inexpensive solution to science missions in space due to their small size and universal design specifications. This makes them popular among academic institutions and other organizations that lack the enormous budgets to send full-scale satellites. Colorado Space Grant Consortium (COSGC) is a state-wide program that seeks to provide Colorado students access to space science through a variety of courses and projects. COSGC has fielded a number of successful CubeSat missions, such as DANDE and ALL-STAR. The CubeSat concept meets the needs of COSGC on many levels, and the program is continually researching and developing new projects. Most CubeSats are size 3U or smaller, but the 6U size is becoming more common, and has a number of benefits.

SUCCESS is the response to COSGC's interest in the 6U standard. SUCCESS stands for Six Unit Canisterized Cubic Exploratory Satellite Structure, and it is a Mechanical Engineering senior design project. The overall goal of this project was to design and manufacture a 6U CubeSat structure as part of the start of a bus development effort. This entails the design of the structure, solar array deployment system, and mass simulators for spacecraft systems. After fabricating the design, the prototype was to be verified with a fit check and test deployment with the candidate deployment system, the Planetary Systems Canisterized Satellite Dispenser. The final step in verifying the design is a random vibration test of the structure within a test CSD.

Starting in September of 2014, the team began an accelerated design process that required a crash course in spacecraft design. The critical design review occurred just three months after the start of the project in November, where the first full iteration of the design was scrutinized by a panel of industry engineers. The design was further refined and reviewed once more at a manufacturing review in December, and was approved for continuation into the manufacturing phase.

The design is made up of six structural plates, three mass simulators (payload, avionics stack, and additional volume), and the solar array deployment system. The total mass of the designed assembly is 11.6 kg, with the structure comprising 1.7 kg of that. The bus portion of the structure has an internal volume of approximately 5200 cubic centimeters (24.5 cm $\times$ 22.4 cm $\times$ 9.4 cm), and the payload portion of the structure supports a volume of 2300 cubic centimeters (10.9 cm $\times$ 21.1 cm $\times$ 10.0 cm). There is substantial volume within the bus portion to support larger payload volumes and specialized bus systems. The avionics stack used as reference was designed for a 3U CubeSat, so an adequate bus system would likely consume more volume, but there is still excess. This space was occupied by an additional volume mass simulator designed to bring the total mass near the 12 kg maximum.

The majority of the parts were fabricated in house with Mechanical Engineering resources. Several parts had to be outsourced due to machine shop limitations. The full assembly consists of 26+ unique parts, and in order to meet schedule goals, it was decided to outsource additional parts. The total cost of the project including all material and machining costs was $2,793. Cleanliness and certifications that would be needed for flight were not considered, as this is an engineering development unit. Fabricating equivalent hardware for flight would likely cost significantly more than this listed cost. Additionally, COSGC paid to have this project as a Mechanical Engineering senior design project, so there is additional cost that may be equivalent to labor costs.

After extensive dimensional verification and some redesign and rework, the model was ready for a fit check and deployment. This took place on April 15, 2015 at the Space Symposium in Colorado Springs. The full mass unit was tested for fit and a mass relieved version was successfully deployed from the Planetary Systems CSD. The next step for the project is a random vibration test. This will hopefully be carried out by a Space Grant team over the summer.

2 Introduction

2.1 CubeSat Background

CubeSat design specifications were first developed in 1999 to facilitate the design and manufacture of low-cost miniaturized satellites for use in scientific and other missions. Since then, over 100 CubeSats have been launched into space. One of the primary benefits of the CubeSat specification is that designs conform to certain size standards. This allows the reuse of bus designs for various payloads and the ability to purchase components from suppliers that build to the standard, reducing the cost significantly. As a result, the CubeSat format has become popular among academic institutions and smaller organizations that don't have the resources to build and launch conventional satellites. The Colorado Space Grant Consortium (COSGC) is a NASA funded organization that focuses on educational and scientific outreach through a number of space technology programs. As such, Space Grant is involved and interested in the development of CubeSats and the scientific inquiries made possible with their use.

The most common CubeSat configuration is a one unit (1U) satellite, which has the dimensions 10 x 10 x 10 cm. Satellites with more than one unit typically maintain the 10 x 10 cm profile, but are extended in one axis to 20 cm or 30 cm (2U and 3U respectively). Figure 1 is a 3U CubeSat designed by students for Colorado Space Grant. This platform has been used for one successful mission, and has several future missions in the works. The portion of the satellite with deployable solar arrays is the length of a 3U, but there is an additional section that extends from within the structure to allow for more solar array surface and exposure for spacecraft instruments. Figure 2 is an example of a 1U CubeSat from Montana State University.

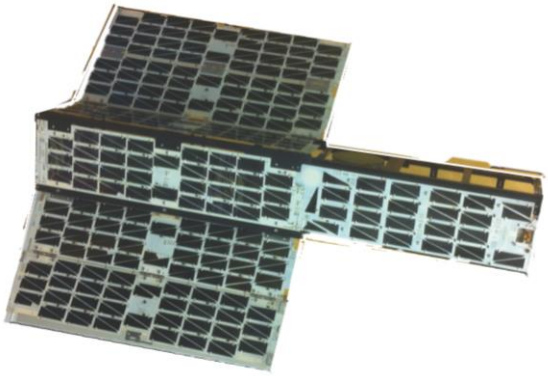

Figure 1: COSGC 3U ALL-STAR Bus

Figure 2: Montana State 1U Explorer-1 CubeSat [1]

It can be seen from these examples that the design is fundamentally changed based on the size of the CubeSat. Simple designs can be propagated to larger form factors, but the best approach is to look at the size difference and really leverage it to the advantage of the mission. The 1U size typically does not need deployable solar arrays as are seen in the 3U, and much larger payloads can be supported with the 3U design.

CubeSats larger than 3U have been proposed, such as 6U or 12U, but not many have been built. The main benefit to a bigger satellite configuration is the extra space for payloads and spacecraft systems. In particular, it allows for greater focal lengths and lens diameters in optical instruments. A robust 6U (10 x 20 x 30 cm) design is the next logical step in the evolution of CubeSat configurations, and COSGC is interested in developing a 6U satellite bus for future missions.

Each satellite consists of a bus and payload. The bus is the structure and systems needed to power and control the satellite after launch, and the payload is the instrumentation or devices that serve the

purposes of the given mission. COSGC has requested the design of a novel structure as well as a solar array deployment system for use in a 6U CubeSat. The electronics and other bus systems that would be necessary for flight are not included within the project scope. Only the mechanical elements of the structure and solar array deployment system are developed, though considerations were made for the accommodation of the other bus systems.

2.2 Design Reference Mission

It is difficult to develop a useful bus design without a clear mission in mind. Although CubeSats are fundamentally simple and aim to be modular, each mission must tailor the bus design to meet its needs. For this project, a Design Reference Mission (DRM) was established to guide design efforts. The bus design is not intended to meet all requirements for the DRM, but many common requirements for a typical mission are pulled from the DRM to this project.

The DRM for this project is the COSGC Phoenix mission. Phoenix involves the development and test of a 2U MWIR camera payload. The mission objective for Phoenix is to capture a sequence of images of the Bennu asteroid, and measure the observed angular velocity of the asteroid using imaging. In order to accurately capture images, the payload will utilize a 3.5µm wavelength nBn detector (Lockheed Martin Santa Barbara Focalplane). The sensor is a 1.3 Megapixel (1280 x 1024) detector which has an operating temperature of roughly 140K. This payload will be utilized by Lockheed Martin Space Systems Company in their first internal CubeSat mission of this type. Lockheed Martin is developing a 6U bus to support the payload that will host a structure of a single part of laser sintered Titanium.

From this mission, the main requirements that apply to the project are the dynamic envelope of the payload, a similar attachment scheme, and accommodation of thermal barriers and other specific requirements.

2.3 Related Work and Current Designs

Currently, in the nano-satellite industry, the standard has not been fully established for the 6U CubeSat configuration. There are only defined standards for up to 3U CubeSats. It is proposed, however, that the standard for the 6U to be that of two 3U CubeSats side by side (10 x 20 x 30 cm). There are several designs suggested and some have already been produced. Two notable design references are the 6U structure by Innovative Solutions In Space (ISIS) and the 6U structure developed by Pumpkin Inc. One of the most significant foundations for the 6U structure design is the candidate satellite dispenser system, the Canisterized Satellite Dispenser (CSD) by Planetary Systems Corporation. This dispenser dictates many of the overall requirements for the structure as is explained in the driving requirements section.

2.3.1 Innovative Solutions in Space (ISIS)

ISIS has developed a 6U structure that is available for purchase at $8,185. The design incorporates the side-by-side 3U CubeSat configuration. It houses the payload with an outer volume of (100 x 226.3 x 340.5 mm), an inner volume of (96 x 96 x 89.4 mm), to a weight limit of 11 kg. It has the capability of integrating 6 1-Unit PCBs to the structure in multiple possible orientations and mounting points. It also has a 10 mm room for mounting external systems or deployables such as solar array panels. This design is shown in Figure 3.

Figure 3: ISIS 6U Structure [2]

The structure has a total mass of 1100 grams, but requires a significant amount of added components before it would be ready for flight. It can be seen from the image that the structure is most likely not designed for use with the Planetary Systems CSD because it features rails instead of tabs.

2.3.2 Pumpkin Inc. Supernova

The Pumpkin Inc. Supernova structure is similar to the system designed for this project in several ways. It is designed specifically for the Planetary Systems CSD to be a modular bus solution for the 6U form factor. Pumpkin Inc. is also developing a full bus system to go along with the structure. The full bus ejecting from the Planetary Systems is shown in Figure 4 and the isolated structure is shown in Figure 5.

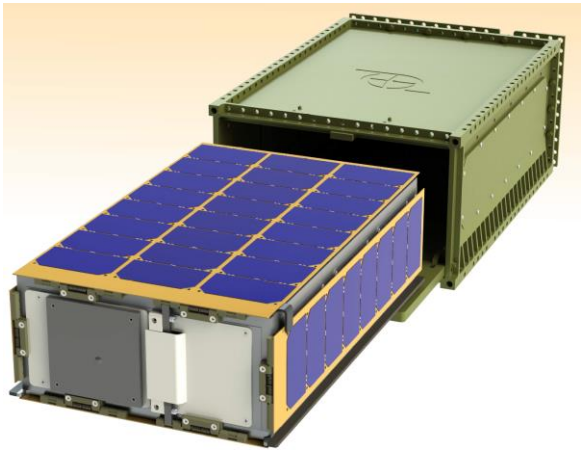

Figure 4: Full Supernova with CSD [3]

Figure 5: 6U Supernova Structure [3]

The structure has a mass of 1,640 grams before the addition of other components. This is comparable to the total mass of the structure designed in this project, and serves as a good benchmark.

2.3.3 Planetary Systems Corporation

The Planetary Systems Corporation proposed a standard for the 6U-CubeSats in the 25th annual AIAA/Utah State University conference on Small Satellites through their design of the canisterized satellite dispenser (CSD). The design parameters, mass and volume, are a maximum of 12 kg and roughly 12 x 24 x 36 cm,

respectively. Other parameters, i.e. center of mass, maximum payload depth, external load on payload, are specified depending on the method of payload attachment to the canister (rails vs. tabs). Although this standard suggested shows an increase in density of the structure compared to six 1U CubeSats, it is justified as this increase will better the orbit lifespan [4].

The proposed interface to the CSD is a tab system that is clamped prior to the payload ejection. This system allows for a very rigid connection to the launch vehicle. This allows for much easier analysis due to the clear load path and constraints. Another benefit of the CSD is the ability to constrain deployables with the CSD walls. This removes the need for actuators and other electronics that may fail or have other problems. It allows for a much simpler implementation of the solar array deployment system.

2.3.4 Conclusions

As was stated in the design reference mission, Lockheed Martin is also developing a 6U bus. Their structure design is proprietary, but it has been suggested that the structure will be made of laser sintered Titanium.

These examples demonstrate that the 6U format is under serious consideration by several notable organizations. The team is not the first to design a structure for a 6U CubeSat, but this effort is an essential part of COSGC's plan to leverage existing designs and its student workforce to prepare for future missions utilizing the 6U configuration.

2.4 Team Roles and Responsibilities

The members of the team were given specific roles to better dictate their responsibilities in the project. These roles were fairly flexible though, as most of the group members worked on a wide variety of tasks across roles.

Project Manager: Dan Waltermire

The team manager is responsible for the scheduling and execution of the project, as well as providing organizational and emotional support for every member involved. The manager must also direct the team's efforts in a way that ensures quality engineering while meeting budgetary and scheduling constraints.

Communications Director: Zach Pardee

The communications director is responsible for team coordination and all internal and external interactions. As part of the job, the communications director must create agendas, organize meetings, and record decisions made in an orderly fashion.

Design and Test Engineer: Andrew Ohlig

The role of the design and test engineer is to develop all CAD models, cooperate with the manufacturing engineer to layout manufacturing and assembly instructions, and work with the systems engineer to carry out testing procedures.

Financial Manager: Hongyu Zhang

The financial manager oversees the budget of the project, keeping a close eye on all expenses. In addition to meticulously keeping track of the project monetary flow, the financial manager must plan out a budget and adjust it to suit the needs of the team and client.

Manufacturing Engineer: Khalid Al Dossary

The manufacturing engineer connects the team with the machine shop and vendor as well as helping to personally machine and assemble any necessary prototypes. The manufacturing engineer oversees the engineering prints and their manufacturability by communicating with the machine shop supervisors and the design engineer to carry the project to prototyping.

Systems Engineer: Nick Merten

The systems engineer is responsible for overseeing system assembly, integration, and test as well as managing requirements and flowing them into design. The systems engineer can be seen as the chief engineer and serves as the final authority on technical aspects of the project.

Faculty Director: Carl Himpsel, Laboratory for Atmospheric and Space Physics

The director helped to guide the efforts of the group members and provide advice and resources for solving problems. The director can be seen as a higher management level that monitors the team performance.

Client: Brian Sanders, Colorado Space Grant Consortium

The client was the primary source of requirements and overall goals for the project. He developed an idea of what was expected of the project and how the project goals were fulfilled. He was also a source of resources and knowledge.

3 Driving Requirements

The design of the CubeSat structure was highly dependent on requirements. Almost every design decision was in part influenced by requirements – there were many constraints. These constraints come from the environments that the CubeSat must survive, both on launch and in operation. There were also many dimensional and functional requirements specified by Planetary Systems for proper interfacing with the CSD. Interfaces and other requirements for the DRM payload were also part of the design process. Beyond environments, there are functional requirements that must be considered for the CubeSat operation such as electrical power supply for all of the components. The driving requirements fall primarily into three categories: environments, interfaces, and operational requirements.

Some of the more immediately important requirements and their verification are discussed in the testing and verification section of this report as well as in more detail in the testing document *D02: SUCCESS Testing and Verification Document*.

3.1 Design Factors and Acceptance

Prior to incorporating loads and other requirements into the design process, standards must be established for factors of safety and other appropriate margins that must be taken into account. Table 1 is table of recommended uncertainty factors from *Elements of Spacecraft Design* by Charles Brown.

Table 1: Recommended Loads Uncertainty Factors [5]

Factor	Starting Point	Ending Point
1.40	Start of program	Sufficient development testing or CDR level design maturity
1.25	Development testing or CDR level design maturity	Correlation of finite element model with flight hardware static or modal test
1.10	Correlation of finite element model	Launch

For experienced engineers working full-time on a spacecraft design, a factor of 1.4 is appropriate as a starting design factor. Because this is a student project at the very early stages of development, it was decided to increase this factor to 2.0. After future analysis and testing to refine the design further, this factor of safety may be relaxed to a more standard level.

3.2 Launch Environment

The most demanding structural environments seen by the CubeSat occur during launch. This section will focus primarily on those loads and the specific requirements they entail.

3.2.1 Quasi-Static Load

During launch the spacecraft is exposed to nearly steady accelerations. To encompass the variability in launch vehicles, several candidate systems were studied. The maximum design load factors for typical missions of the three most likely launch vehicles are shown in Table 2.

Table 2: Quasi-steady-state LV Load Factors

LV	Axial Load	Lateral Load
SpaceX Falcon 9 [6]	±2 G	6 G compression, 2.5 G tension
ULA Delta IV Medium [7]	±2 G	6.5 G compression, 2 G tension
ULA Atlas V 500 [8]	±2 G	5.5 G compression, 2 G tension

The reference axes used in this case axial and lateral refer to the axial direction of the launch vehicle (along its long axis) and the lateral direction of the launch vehicle (transverse to its long axis).

It must be noted that axial and lateral loads can be applied simultaneously, so the spacecraft must be able to survive this combined load. Furthermore, because of the rideshare nature of CubeSats, the canister

may be oriented in strange ways. This can increase the accelerations seen by the CubeSat significantly. To account for this additional variability, a factor of 1.5 was applied to the maximum loads.

The CubeSat structure and mechanisms shall be designed to survive ±3 G in the axial direction, 9 G in lateral compression, and 3.75 G in lateral tension. The CubeSat shall be designed to survive a combined load comprised of the maximum loads seen in each direction of axial and lateral acceleration. To take a conservative approach, it was decided to set the requirement to be 9 G of acceleration in each of the translational axes. The CubeSat survival of this environment is determined with finite element analysis and partially validated with hand calculations.

3.2.2 Vibration

During launch the CubeSat will experience sinusoidal vibration inputs due to numerous transients and oscillatory flight events. The maximum predicted flight level vibration inputs for the Delta IV and Atlas V launch vehicles are shown in Table 3. SpaceX did not provide vibration levels in their Falcon 9 LV user's guide, but rather stated that the levels must be determined via a coupled loads analysis. It should be noted that vibration levels depend on the payload mass properties.

Table 3: LV Vibration Levels

LV	Axis	Frequency (Hz)	Maximum flight levels
ULA Delta IV [7]	Axial	5 to 6.2	1.0 g (zero to peak)
	Lateral	6.2 to 100	0.7 g (zero to peak)
Atlas V [8]	Axial	5 to 100	0.9 g
	Lateral	5 to 100	0.6 g

The CubeSat shall be able to survive the vibration levels presented in the two ULA LV specifications documents. The most significant vibration levels output by the launch vehicles are within the 0-100 Hz range. To ensure that the CubeSat will not couple with these vibrations, it will be designed to fundamental frequency greater than 100 Hz.

Further guidelines are determined from the NASA General Environmental Verification Standard. The random vibration levels that the CubeSat must ultimately be tested to are encompassed by the 22.7 kg curve shown in Figure 6.

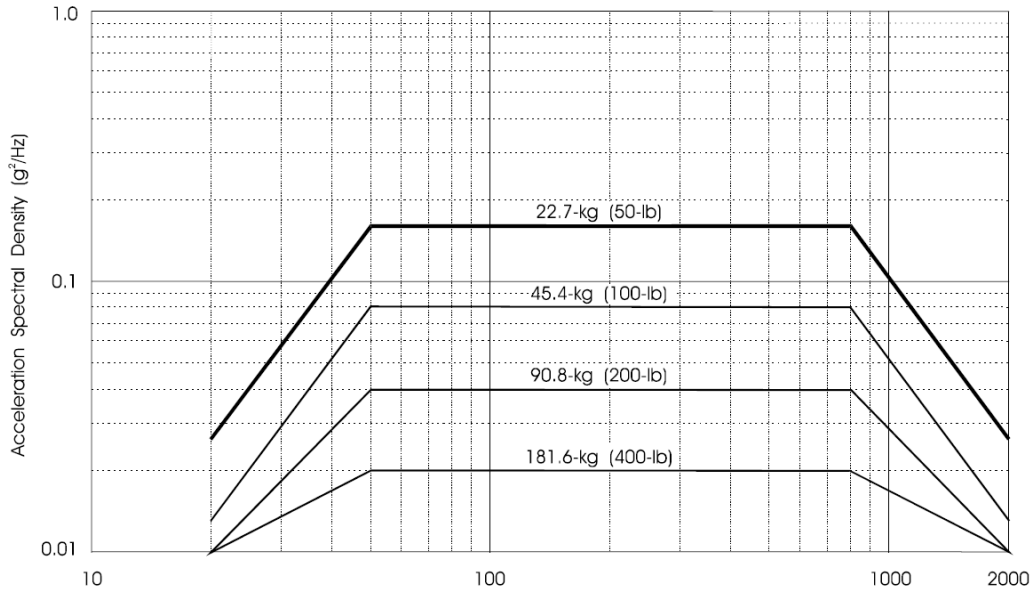

Figure 6: GEVS Acceleration Spectral Density Plot [9]

3.2.3 Acoustic and Shock

During launch the payload is exposed to high frequency acoustic loads. The maximum acoustic environments are specified as one-third octave-band sound pressure levels (dB) versus one-third octave-band center frequency in the LV documentation.

Events during flight such as the payload fairing separation lead to shock loads on the CubeSat. These loads are specified as acceleration vs. frequency curves in the LV documentation.

The CubeSat shall be able to survive the acoustic and shock levels presented in the three LV specifications documents. Most of these high frequency loads are unlikely to reach the CubeSat structure through the launch vehicle interface and CSD. To fully verify the CubeSat's ability to survive these loads, a random vibration test must be carried out to characterize the response of the system at these levels. Typically, the low-frequency levels are the design driver for the spacecraft, but there may be sensitive components within the payload or bus systems that respond at these levels.

3.3 Interfaces

3.3.1 Canisterized Satellite Dispenser

The single most significant design driver for the project was the CSD. There are many dimensional requirements that the CubeSat must exhibit to fit and deploy from the canister properly. Figure 7 shows the reference faces of the CubeSat as defined by Planetary Systems, as well as a number of features of the CSD.

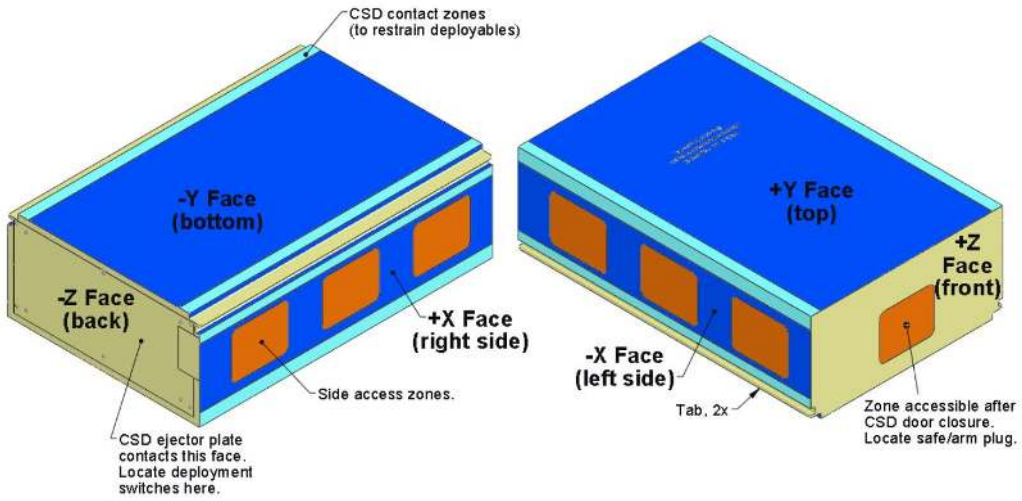

Figure 7: CSD CubeSat Reference Faces and Features [10]

The ejector plate of the CSD contacts the CubeSat at its –Z face, where the electrical connector is located. There are access zones distributed throughout the CSD that can be used once the CubeSat is integrated with the dispenser. The light blue regions reflect the contact zones of the CSD, where deployables may interface with the CSD.

Not all of the requirements from the CSD are included in this report. The CSD Payload specification document should be referenced for the full requirement list. This document is available on the Planetary Systems website.

3.3.1.1 Dynamic Envelope

The CubeSat and deployables must fit within a dynamic envelope as specified by Planetary Systems. This envelope is described by Figure 8 and Table 4. Note that Figure 10 is the tab detail view from Figure 8.

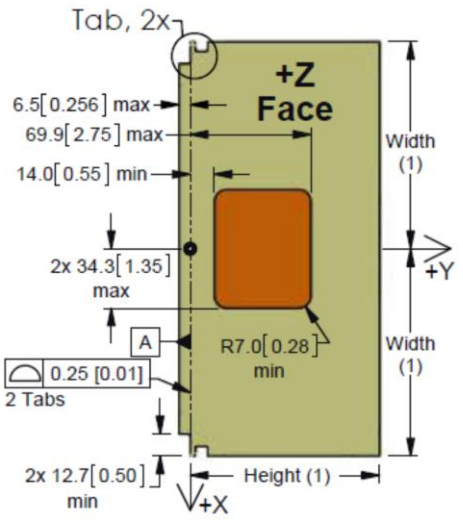

Figure 8: CSD Dynamic Envelope [10]

Table 4: CSD Dynamic Envelope [10]

Parameter	Min	Max
Height	0	109.7 mm
Width	0	119.7 mm
Length	361 mm	366 mm

Figure 8 shows the width and height dimensions given in the table. The dimensioning scheme uses an origin at the +Z face, at the top of the bottom plate, in the middle of the CubeSat in the X direction.

3.3.1.2 Tab Interface

Firstly, the CubeSat structure shall interface with the CSD via fully continuous tabs of aluminum alloy 7075-T7 (or stronger) with a hard anodized surface per MIL-A-8625F or similar. Within the CSD, the tabs will be clamped with a high preload to ensure a rigid support. The tab thickness is critical to this process – the tabs shall be within the range 0.116-0.120 inches in thickness. The CubeSat tabs run along the long axis of the structure on the bottom edge of the satellite where they meet the CSD clamps. This interface can be seen in Figure 9, and the full dimensioning of the tab interface is shown in Figure 10.

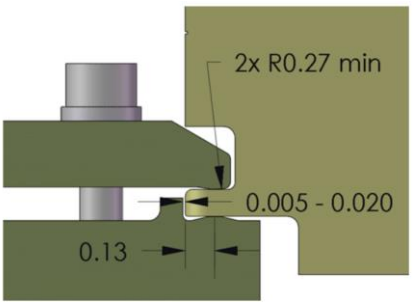

Figure 9: CSD tab interface [10]

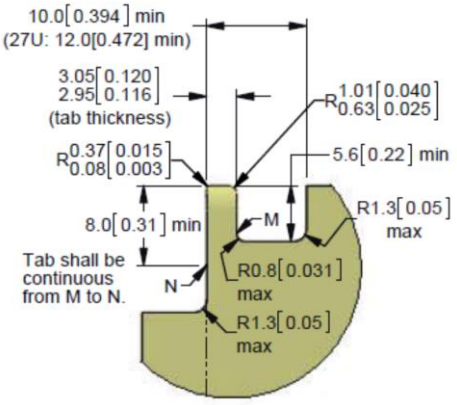

Figure 10: Detailed Tab Dimensions [10]

The dimensions in Figure 9 are in inches, and the dimensions in Figure 10 are in mm with inch dimensions in brackets. These tabs shall run the entire length of the CubeSat, with no portion of the CubeSat extending beyond the tabs in the +Z or –Z directions.

3.3.1.3 Ejection Plate Contact Zone

Another important area of the CSD specification is the ejection plate contact zone. The ejection plate contacts the –Z face of the CubeSat, and requires at least three contact points that envelope the location of the center of mass as projected to the –Z face. There is also a specific envelope in which these contact points must exist as shown in Figure 11.

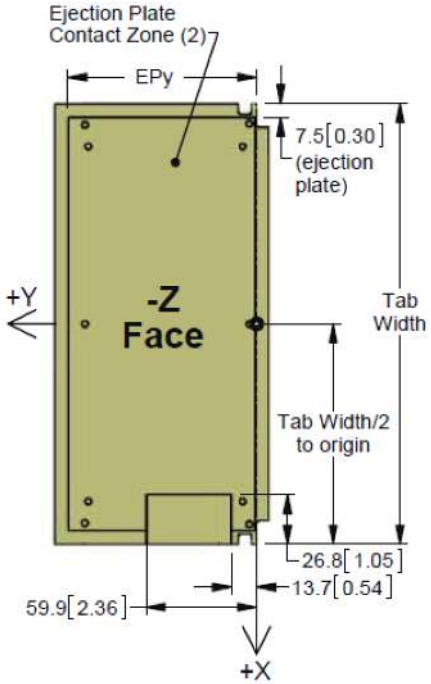

Figure 11: Ejection Plate Contact Zone [10]

The contact points may not be lower in the Y direction than the tabs, which must also contact the ejection plate. There is a small window cut out of the contact zone for the electrical connector location. The ejection plate is of the same size as this contact zone, and there is a gap where the connector resides on the interior of the deployer.

3.3.1.4 Deployables Contact Zones

There are specific regions on the CSD where the constrained deployables can contact the interior surfaces. These seem arbitrary at first, but they are actually dictated by the design of the CSD. The contact zones for the +Y and –Y faces, for example, are ledges built into the interior of the CSD. Not remaining on those zones means the deployable will over-deploy and likely catch. The contact zones for the +X and –X faces depend on the location of the access windows on the CSD as seen in Figure 7. Contacting outside of those zones will lead to catching on the recesses for those windows. Table 5 contains the required dimensions for these contact zones.

Table 5: Deployables Contact Zones [10]

Parameter	Min	Max
Deployable contact zone with CSD, ±X face near +Y face	91.4 mm	-
Deployable contact zone with CSD, ±X face near -Y face	-	20.3 mm
Deployable contact zone with CSD, +Y face (1)	107.00 mm	-
Deployable contact zone with CSD, -Y face (1)	94.3 mm	-

Note that the contact zones are still limited by the overall width and height dimensions. These dimensions are with respect to the defined origin.

3.3.2 Payload

The Phoenix payload is contained within its own 2U structure and has its own specific requirements that are not fully defined. The CubeSat structure shall interface with the payload volume structure, providing the same level of support as throughout the CubeSat bus to survive launch and other environments. Additionally, the interface shall allow for EPS and C&DH attachments and have the necessary thermal damping that the payload instruments require.

3.3.3 Spacecraft Systems

The CubeSat structure shall accommodate the spacecraft systems needed for the DRM. Table 4 is a list of the expected spacecraft systems and their estimated volume requirements and other spatial constraints that must be taken into account. Thermal Control (TC) systems are not considered in this section because it is assumed the volume and spatial requirements are negligible as far as the structure is concerned. It is likely that the TC system will be passive (Kapton tape or similar insulation).

3.4 Operational Requirements

3.4.1 Mass Properties

The mass properties of the structure affect loads incurred on launch, and attitude control once the satellite is in operation. The total mass limit for the CubeSat is 12 kg. The structure designed by ISIS has a mass of 1100 grams, but does not incorporate many of the specific requirements for the DRM so it cannot be used as an adequate reference. Given a 90% light-weighted aluminum block with the dimensions of a 6U, the mass will be 2.8 kg. Additionally, the similar Pumpkin Inc. Supernova bus structure has a total mass of 1640 grams. The total mass requirement for the structure is no greater than 2 kg.

Table 6 is a preliminary budget of the spacecraft system masses. It can be seen that this is well below the anticipated 12 kg limit. The structure mass as built, however, has the following mass values in Table 7.

Table 6: Preliminary Mass Budget

Subsystem	Mass (g)	Reference
Structure	2,800	-
ACS	850	[14]
Phoenix	2,660	-
EPS	233	[11]
COMM	95	[12]
C&DH	88.3	[13]
Total	6,726.3	

Table 7: As-built Mass Budget

Subsystem	Mass (g)
Structure	1,698
Phoenix	2,633
Avionics	1,801
Additional Volume	3,946
Total	10,078

Note that the additional volume mass simulator was added to get the structure close to the maximum allowed mass of 12 kg in order to conduct a vibe test at maximum load. The mass of the solar arrays, backbones and fasteners will add up the total mass to 11.6 kg.

3.4.2 Electrical Power System

3.4.2.1 Power Budget

The power generated must be enough to meet the power requirements of the Phoenix mission. The payload has a nominal consumption of 5W and a maximum of 10W. Other major subsystems that will be considered are EPS, COMM, C&DH and ACS.

Table 8 demonstrates power consumption of the subsystems during the Insolated Phase (67% in duration of the orbit) and the Eclipse Phase (33% in duration of the orbit) for a Low Earth Orbit (LEO). The solar array system shall provide 16 W throughout orbit.

Table 8: Preliminary Power Budget

	Power (mW)	
Subsystem	**Insolated**	**Eclipse**
ACS	1,800	1,800
Phoenix	5,000	5,000
EPS	8,040	100
COMM	700	700
C&DH	340	340
Total	15,880	7,940
Available	22,166	14,226
Margin	28.4%	44.2%

It can be seen in the table that it is enough to power the subsystems during orbit. All subsystems are assumed to be operating throughout the orbit at nominal power.

These subsystems were specified by the team to be used for a typical mission but the team was instructed by their client to use the avionics stack used in the ALL-STAR mission. The reason why the team recommends using subsystems different from the ALL-STAR avionics stack is mainly because of the ACS and the power it can provide to a heavier structure and its lower power consumption. Table 9 is the power budget for the components in the ALL-STAR stack.

Table 9: Actual Power Budget

	Power (mW)
Subsystem	**Eclipse**
ACS	5,750
Phoenix	5,000
EPS	838
COMM	2,370
C&DH	1,390
Total	15,348
Available	22,062
Margin	33.4%

The ALL-STAR avionics stack is slightly less efficient than the larger components, but it can be seen that there is still significant power margin given the power gathered by the solar arrays.

3.4.2.2 Power Storage

When the satellite is in eclipse, it needs to draw power from a battery. Assuming LEO with a total eclipse time of 35 minutes, the battery needs to have a capacity of 7.94 W for 35 minutes which yields a capacity of 8.5 Whr assuming 30% depth of discharge. If Lithium Ion cells are used, a 10% fade per year is considered. The batteries specified are rated to 2.552 Ahr and the minimum battery Ahr required is 3.34 Ahr. Therefore, the EPS specified shall accommodate a series of batteries rated to at least a combined 3.34 Ahr.

For the used configuration of subsystems, it is recommended to use at least three batteries of the specified 2.552 Ahr capacity as the capacity needed is 6.46 Ahr as the needed power is 15.35 W with an assumption of the standard 30% depth of discharge.

3.4.2.3 Solar Array Sizing

The solar array sizing is based on the power consumption by the subsystems and payload. By using the *Elements of Spacecraft Design* book, the team was able to calculate the power generated from a solar array given the size, orbit elevation, efficiency and losses. The total surface area used for solar arrays is 1515 cm^2 with an efficiency of 29.5% (Emcore). The total power generated under operational conditions is 36.77 W but with taking 60% of that value to better approximate the Orbit Average Power (OAP), the power is 22.06 W (Power Budgets for Mission Success). The calculations and parameters used are shown in the following equation.

$$\mathrm{P_c} = P_L * \mu_{rad} * \mu_{uv} * \mu_s * \mu_{cy} * \mu_{con} * \mu_t * \mu_{packing} * Hl * L_p$$

Where:

- P_L is the power delivered by one cell under lab conditions in W
- μ_{rad} is the power loss caused by radiation damage=0.9
- μ_{uv} is the power loss caused by UV discoloration=0.98
- μ_s is the power loss caused by shadowing=1.0
- μ_{cy} is the power loss by thermal cycling=0.99
- μ_{con} is power loss caused by contamination from all sources=0.99
- μ_t is the power adjustment for operation temperature=1.0
- Hl is the adjustment for solar intensity at orbit positon ≅1.0
- L_p is the array pointing loss factor=cos(α), α=±0.007deg
- $\mu_{packing}$ is the packing factor ≅0.7

4 Design

The following section contains an overview of the design aspects of the SUCCESS CubeSat bus. This section is separated into three major sections in an effort to remain organized and convey information easier. The first section of the design description includes an overview of the primary structural components of the bus, the second includes an overview of the solar array deployment system and solar arrays, and the third overviews the primary contact interfaces with the planetary systems CSD. There is also a section on the mass simulator design, and other miscellaneous design considerations. Each of these designs were finalized after a multitude of revisions.

4.1 Primary Structure

In order to meet all design requirements, the group decided on a 6 piece external structure, with a structural plate representing each primary face of the CubeSat excepting the negative Y face. Most of these plates demonstrate a unique, light-weighting pattern that provides the necessary structural support for the entire bus. Most of the plates are constructed from 6061-T6 aluminum, but the bottom plate has been constructed from 7075-T6 aluminum.

4.1.1 Primary Design Elements

While there were a multitude of specific design constraints associated with the design of the external structure, the following list is an overview of the major constraints designed for by the team. Any other questions about driving requirements are answered in section 3 of this report.

4.1.1.1 Loads and Fastening

One of the primary design drivers for the external structure of the 6U bus is the fact that the external structure had to be the primary load path for any applied force. Meaning all loads applied to the structure cannot go through the solar arrays, payloads, or connector. The forces will be applied along the tabs of the bottom plate, P1005. As the door of the CSD closes, clamps in the CSD will exert a force to hold the tabs in place. During launch this is the only part of the CubeSat that will be constrained, and therefore it needed to be able to carry this load. This is part of the reason why the material for the bottom plate was required to be Aluminum 7075-T6 or stronger. The tabs also needed to be fairly hard to not deform from the clamping load.

This also meant the pieces of the structure that were constrained to the bottom plate needed to be designed to withstand the load that would travel through the bottom plate and initially the plates were

thinner. The group decided to increase the thickness of the plates after taking the analysis into account. The bottom plate can be seen below in Figure 12.

Figure 12: Bottom Plate

The thickness of the plates were not the only part of the design that was changed due to the load path. The amount of fasteners and where they were placed was a large part of the design. When choosing the amount of fasteners the original idea was to put as many as possible to constrain the plates in all directions. Then after doing some analysis, the amount of fasteners in the plates could be reduced. After some trial and error of removing fasteners an optimal amount was chosen for each plate.

Before doing analysis, the group had a specific design for where the fasteners would be placed. The group met with the director of the project, Carl Himpsel, and discussed the concept of "over constraining" parts, and what exactly is required to support the CubeSat structurally. The idea was to ensure the tolerance the tolerance stack up would not hinder the group's ability to constrain a part, but still be able to constrain a part in all directions and axes of rotation. This discussion guided the team's efforts in terms of placing fasteners, and in which axes the fasteners were place. Each of the structural parts is supported in all translational and rotational axes, and there is minimal over constraint. There are fasteners fixing the side plates to the top and bottom plates, and this is the only example of over constraint. This is inevitable due to the fact that the structure is a 6 sided cuboid. There is no way to join the pieces without some over constraint. Figure 14 and Figure 13 demonstrate this fastening concept in one of the side plates.

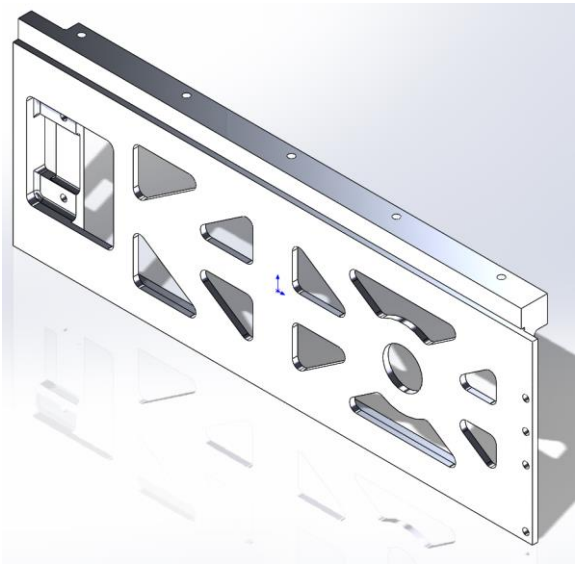

Figure 14: Side Plate Constraints

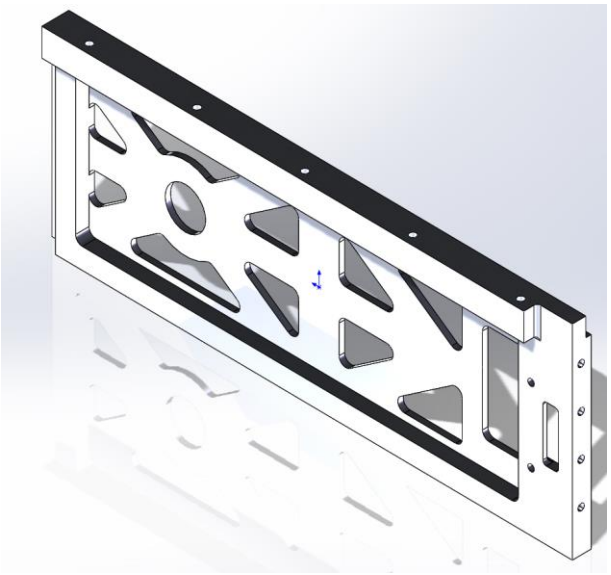

Figure 13: Side Plate Constraints 2

4.1.1.2 Modularity

One of the largest design drivers for the CubeSat was the aim for a modular design. In order for this design to be useful, it must be able to accommodate whatever payload that would use this bus.

The bottom plate is a good example of this goal. This part does not have many openings to increase the surface area. The increased surface area is able to improve the mounting point abilities and accommodate any mounting pattern necessary from a battery, avionics, or any payload that could possibly be used in the future. The large surface area can be seen on the bottom plate in Figure 15.

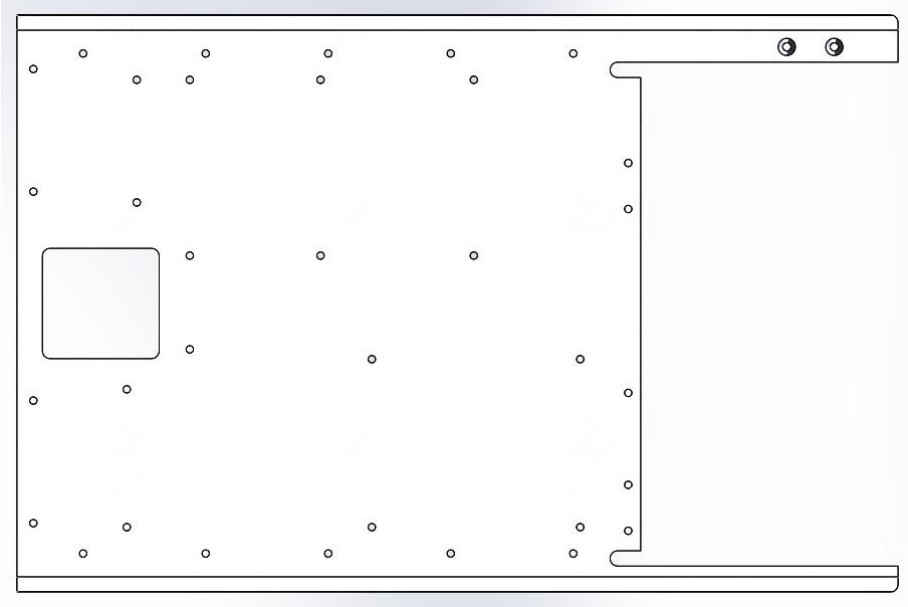

Figure 15: Bottom Plate Surface Area

The initial design for the plate also featured the light weighting pattern seen in the other plates, but because this part is seen in several of the resonant modes, the opening were removed to improve stiffness.

The unique pattern that can be seen on the side, front, and top plates was also influenced by the modular design concept. The goal was to be able to maximize the amount of mass that could go to the payload or anything going into the bus, by decreasing the amount of mass taken up by the CubeSat structure. With that in mind it was decided the walls of the structure would need to be lighter while still being able to withstand the 9 G loading, and maintain a fundamental frequency greater than 100 Hz. This can be seen in Figure 16.

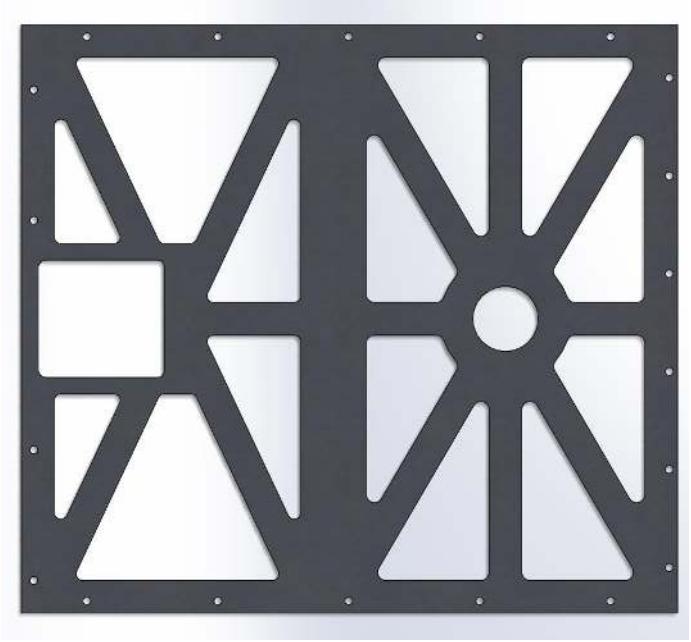

Figure 16: Top Plate Pattern

A consideration was made in the pattern of the +X face to accommodate a star tracker. It can be seen in the design the two side plates are primarily similar, except for a couple of design changes. This includes the platform for the hinge assembly on the –X face, but that design will be discussed later. The other main difference between the two plates is an opening near the center of the plate. This gap corresponds to the location of the star tracker in the ALL-STAR avionics stack. This can be seen in Figure 17.

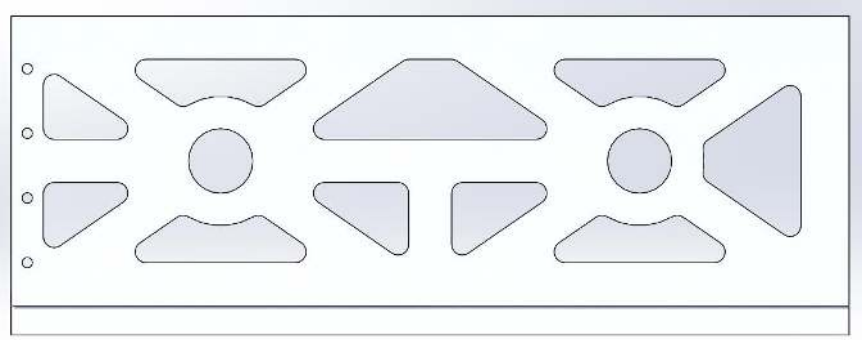

Figure 17: Star Tracker Gap

The maximum amount of mass Planetary Systems allowed in the CubeSat was 12 kg. To maintain the modular concept, the worst possible mass case must be considered. The total amount of mass inside the CubeSat was maximized, so the entire structure including the mass simulators were designed to be as close as possible to 12 kg. This design was intended to accommodate a heavy payload or specialized bus systems in a future mission.

4.1.1.3 Payload Interface

Another major requirement for the project was to design the structure to accommodate the DRM payload, and other potential future payloads. The Phoenix senior design team gave the model for their structure early in the design process to guide this effort. The middle frame (P1006), otherwise known as the payload interface plate, was designed to accommodate the Phoenix payload. The payload interface can be seen in the payload mass simulator design (P1302).

The middle frame is a fairly simple part to manufacture and can be replaced quickly. This is useful because if there is a need to change the mounting holes in the design it can be done without large impacts to the rest of the structural design. This further increases the modularity of the CubeSat giving it the chance to mount a different payload onto the CubeSat. The middle frame and can be seen in Figure 18.

Figure 18: Payload Interface Plate

4.1.1.4 Solar Array Deployment Accommodations

Another major design driver for the structure was the mounting system for the solar arrays. The system had to integrate with the structure in a sound manner, while also minimizing the total volume consumed. This was a challenge for the team because the amount of space within the CSD was limited, and the deployment system had to integrate very tightly with the structure.

The hinge design required moving parts that needed to be easily accessible, but nested within the profile of the structure. In the –X side plate design it can be seen that the hinge mechanism is incorporated in the plate itself. This was done to simplify and stiffen the design, and the intended thickness of the plate was large enough to fit the mounting system for the spring hinge.

The hinge mechanism was mounted to a seat (P1202) attached to the front plate for the top and bottom solar arrays. Integrating this seat into the top and bottom plates would have greatly increased the difficulty of machining those parts. A future design may choose to do this if there is less of a limitation on manufacturing resources.

4.1.1.5 Ease of Assembly

One requirement the client gave the group was to create a design that could be easily assembled and disassembled. This guided the concept of the top plate design. It was only constrained in one direction by the fasteners, and is a plate that can be easily removed. The structure then serves as a simple kind of box, where the top plate may be removed to access the internal components. This way if there is a last minute need to change a payload or a need to get into the CubeSat structure for some other reason; it will be easy to accomplish. The easy accessibility of the mass simulators or payload is shown in Figure 19.

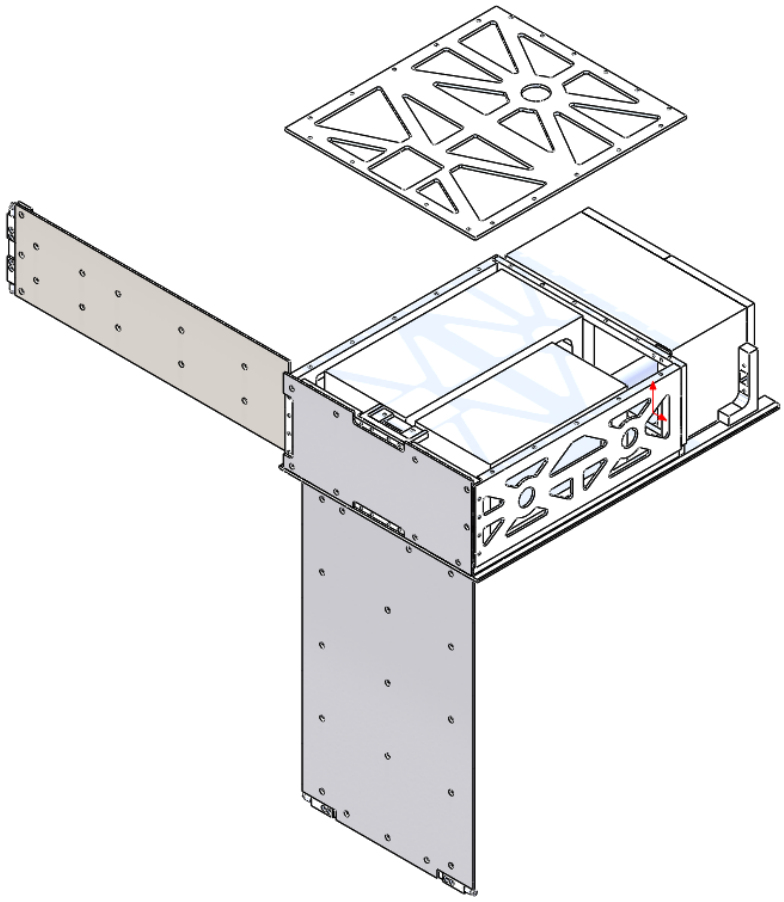

Figure 19: Top Plate Easy Accessibility

4.2 Solar Array Deployment System

4.2.1 Primary Design Elements

4.2.1.1 Hinge Assembly

One of the principle design goals of the project from the client was to have deployable solar arrays. At first the group thought about doing some type of controls system for the solar array system, and possibly solar arrays that can rotate with the sun light. This was decided against due to the complexity, and the group did not want to risk having an unnecessary electrical failure. The simplest solution to the problem is a spring driven hinge. The torsional spring idea was a simple but effective idea; allowing the solar arrays to deploy with little complication coming from any control system. The torsional springs in the hinge assembly can be seen in Figure 20.

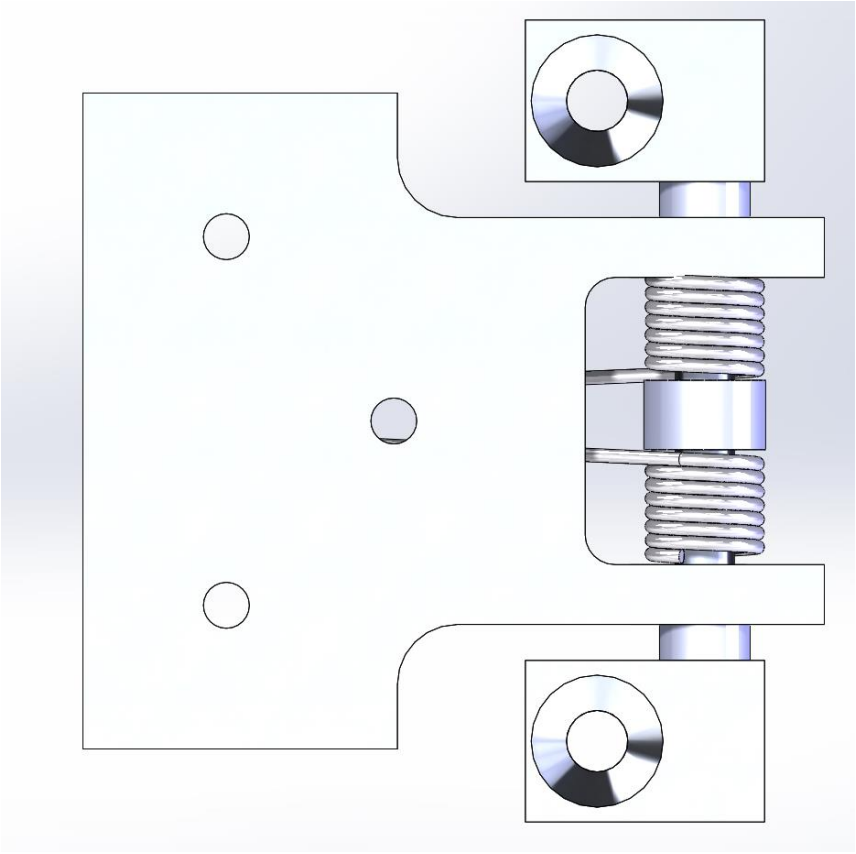

Figure 20: Hinge Assembly

The springs apply a force to the back of the hinge arm to rotate the solar arrays. The Hinge Rod (P1101) was chosen to be stainless steel instead of aluminum due to the thickness of the rod. In order to assure the solar arrays can deploy it was decided that the rod should be made of a stronger material due to the small radius of the part. This material also interfaces well with aluminum in terms of galling and low friction. This design should not require any lubrication to operate properly. The rod does not bear significant loads, but it was important to take a pre-caution and assure the rod does not break during launch or during the deployment of the solar arrays.

After the hinge assembly was built, it was noticed that the two springs used were rotating and twisting along the hinge rod, and a concern was raised about the springs exerting some of their force into each other and losing preload torque. If the springs are exerting force into each other instead of putting all their energy into moving the hinge arm then the solar arrays have a greater chance of not deploying. The hinge spacer (P1107) was then made to keep the springs aligned throughout deployment. The hinge spacer is a simple piece of delrin, and its design can be seen in Figure 21.

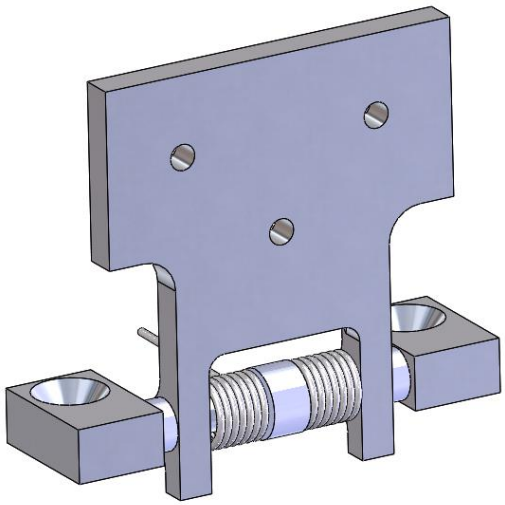

Figure 21: Hinge Assembly

There are also two smaller spacers to the sides of the hinge arm, and these are to keep the hinge arm aligned with the hinge seat, and also keep the assembly from sliding along the hinge rod.

The hinge deployment is stopped when the two ends of the arm hit the stop in the hinge seats. Figure 23 and Figure 22 show how the hinge is stopped.

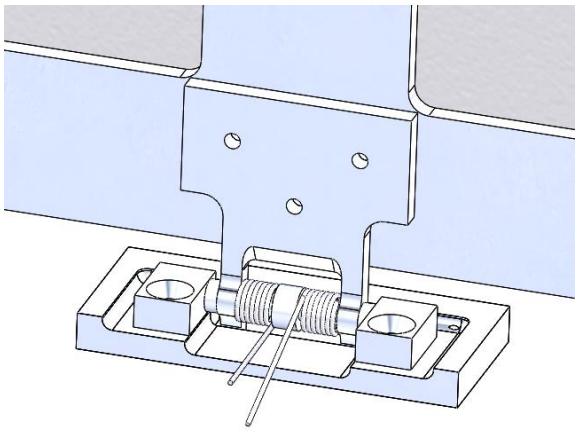

Figure 23: Hinge Stop Front View

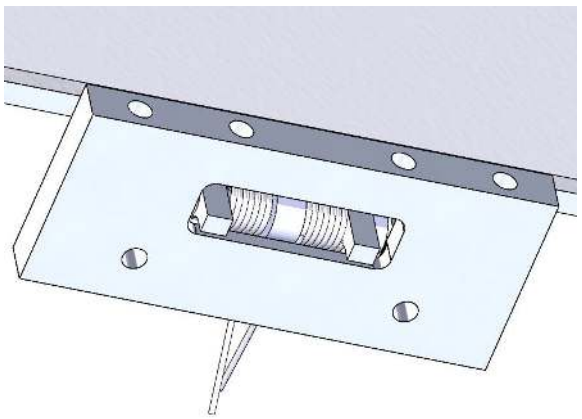

Figure 22: Hinge Stop Bottom View

4.2.1.2 Solar Array Sizing

From the power budget calculations it was determined that 15.3 Watts were required for a typical mission. This was used to determine how many solar arrays were needed, and how large they needed to be. It was calculated that using top, bottom, and front solar arrays as well as a single side solar would supply 22 Watts. This is enough power to supply the expected systems with some margin. This part of the design is greatly dependent on the particular mission. Missions that require more power can add a fourth solar array to the +X face of the CubeSat, or even add a second level to the solar array deployment. These options would, however, require significant redesign work. The system is shown deployed in Figure 24.

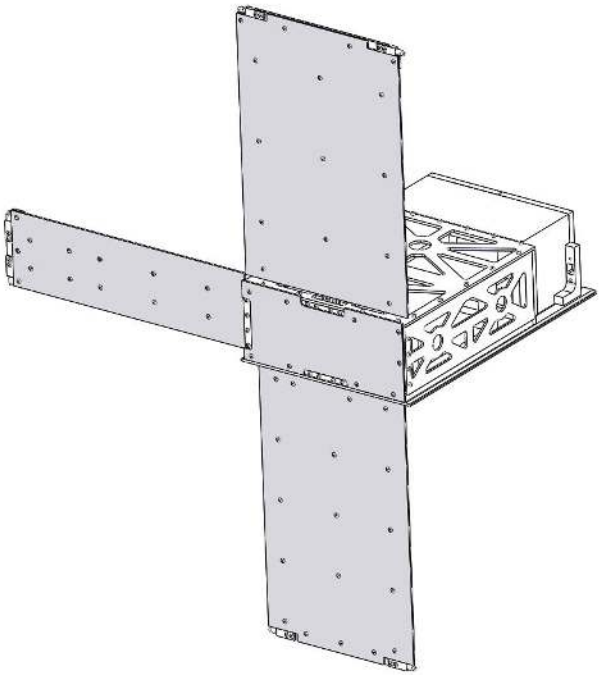

Figure 24: Deployed Solar Arrays

4.2.1.3 Panel Design

Using real solar array assemblies was not necessary for this stage of the project, so panels had to be fabricated to represent the solar arrays. One option was purchasing PCB, but due to the added design effort needed to design the PCB, a simpler alternative was selected. The panels were to be machined out of FR4, a PCB type material. This did cause some challenges when deciding the shape, because most machine shops would prefer to not cut any fiber glass on their machines. This meant when designing the solar arrays they had to be easily manufacturable, and the group needed to use a water jetting company to machine the parts.

When designing the solar arrays, necessary antennas were also considered. The original idea was to place antennas underneath the deployable solar arrays. This was deemed a potential risk item because the communication systems would then be fully dependent on a successful deployment. Despite the calculations and the confidence the solar arrays would deploy, it was decided to avoid the risk altogether by leaving the +X face of the CubeSat open. The power budget proves that this face of the CubeSat does not need to have a solar array. Leaving this side open also has the added benefit of leaving the star tracker independent of the solar array deployment. As it can be seen in Figure 25 there is no solar array on the side to allow for the star tracker hole and space for antennae.

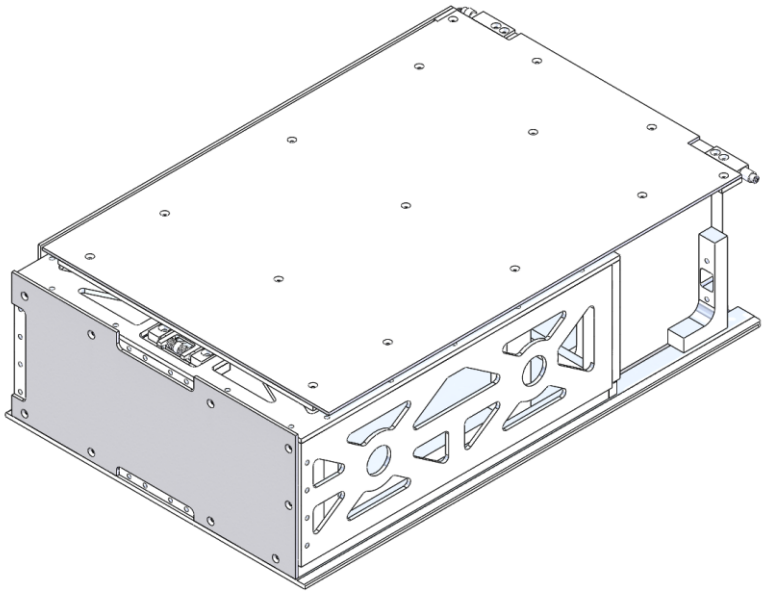

Figure 25: Solar Arrays in Stowed Configuration

4.2.1.4 Solar Array Frames

The solar array panels consist of PCB sections with solar cells affixed to their surface. Because of the size of the panels, the PCB material will not be strong enough to support its own weight during launch loads. To support the panels effectively, the solar panels must be supplemented with an aluminum frame. The solar array frames (P1401, P1406, and P1403) were initially a “T” shaped piece of aluminum used to support the solar arrays, but it was suggested during CDR that the solar arrays must be supported in all corners and must be thicker.

The concept behind this was the corners of the solar arrays may deflect or resonate significantly because of their relatively low fundamental frequency. There is little space for the panels to move within the CSD, but coupling with the vibrations could cause significant damage. After considering these two possibilities, the new design incorporated thicker frames (0.125” instead of 0.090”) and changing the frames so the edges of the solar arrays were supported. These changes were meant to assure the solar arrays could survive the launch environment, and can be deployed later. An example of the new solar array frame is in Figure 26.

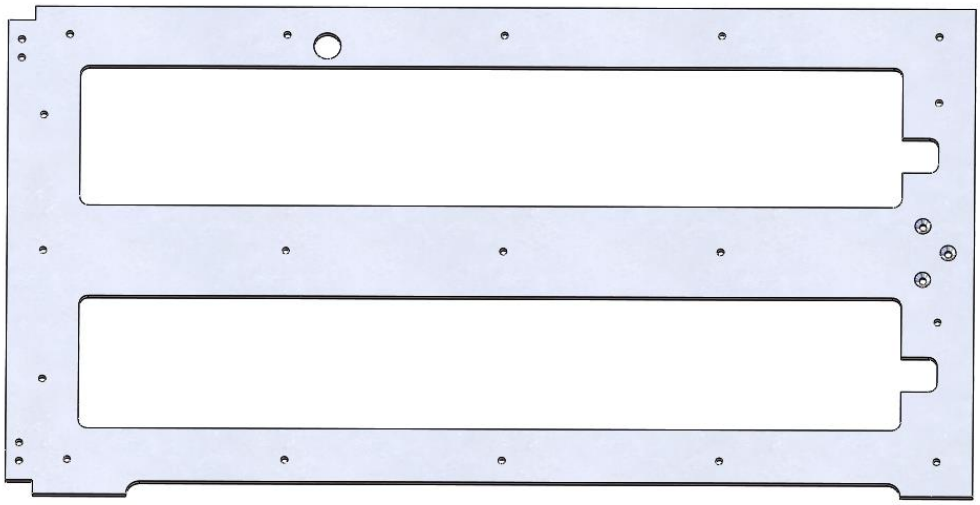

Figure 26: Bottom Frame

4.2.1.5 CSD Interface

Planetary Systems set many of our design drivers, and a hard requirement was to have a bearing or roller on the solar arrays. This was to ensure the solar arrays roll smoothly out of the CSD instead of dragging against the CSD surfaces. The group’s initial solution to this was to use a sleeve bearing or ball bearing to slide out of the CSD. Unfortunately the size required was much smaller than typical bearing sizes, and the dimensions that were required would have to be custom made.

The solution to this was to fabricate simple roller bearings out of delrin. This not only allowed the group to save a significant amount of money, but it was also possible to modify the length of the roller to fit into the specified contact zones. The bearings were then attached to the solar array frames with a simple aluminum seat and a shoulder screw. Overall, this solution allowed the variability that was needed to ensure the proper contact with the CSD. Examples of the delrin rollers can be seen in Figure 27 and Figure 28. Two different sizes were made to fit the contact zones on each face.

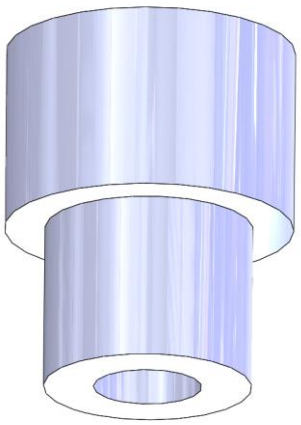

Figure 27: Small Roller Bearing

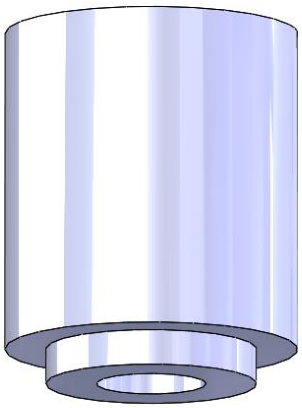

Figure 28: Large Delrin Roller

The bearing seats are all identical, and their fastening position on the solar array frames depended on the contact zone locations. Figure 29 shows the bearing assembly design and integration to the solar array frame.

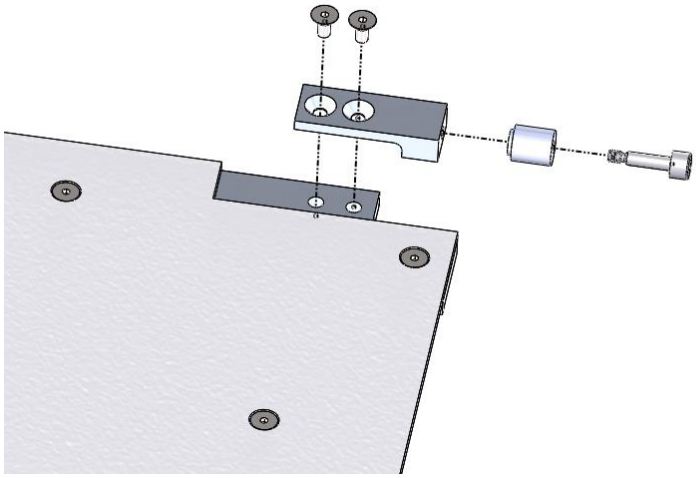

Figure 29: Bearing Assembly Integration

It was fairly difficult to ensure that the solar arrays would be close enough to the CSD walls that only the bearings are in contact, and that the bearings and their seats integrate with the solar array frames and panels. Figure 30 shows how the bearing protrudes slightly from the solar arrays.

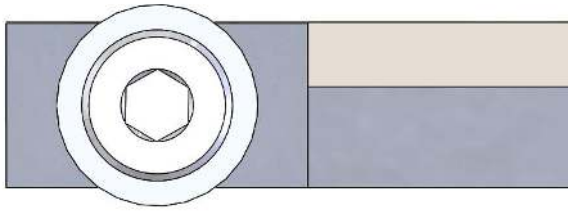

Figure 30: Bearing Side View

If the solar arrays deploy too much, the corner of the bearing seat may touch before the bearing does. It is critical that the bearing protrudes by a significant amount, and there is not too much room for the solar arrays to deploy within the CSD.

4.3 Mass Simulators

4.3.1 Primary Design Elements

In order to test the integrity of the structure and see how it would fare in launch conditions, the team was asked by the client to build mass simulators of subsystems and the payload specified as the design reference mission (DRM). These mass simulators shall replicate the mass, volume and center of mass of all subsystems and payloads. The stretch goal set for the team is to conduct a vibrational test with the structure containing these mass simulators and see how the structure would behave under harsh launch conditions. The mass simulators designed are of two existing systems: the first is the Phoenix Payload, and the second is the avionics stack used in the COSGC ALL-STAR mission. There is a third mass simulator built. The reason it was made is to increase the mass of the structure to its maximum capacity (12 kg set by Planetary Systems CSD specifications). With the addition of the third mass simulator, the structure is now approximately 11.6 kg. This will allow the team to test the structure at its full loading capacity.

The Phoenix payload was initially design to be 1,600 grams to replicate the model that was in progress of being developed as seen in Figure 31. The team was asked to redesign the Phoenix payload to its maximum mass specified by the Phoenix team because developing it was still in progress. The payload, as it stands now, has a mass of 2,639 grams and it replicates the volume and center of mass. It is connected to the bus through tabs that are attached to the payload interface plate.

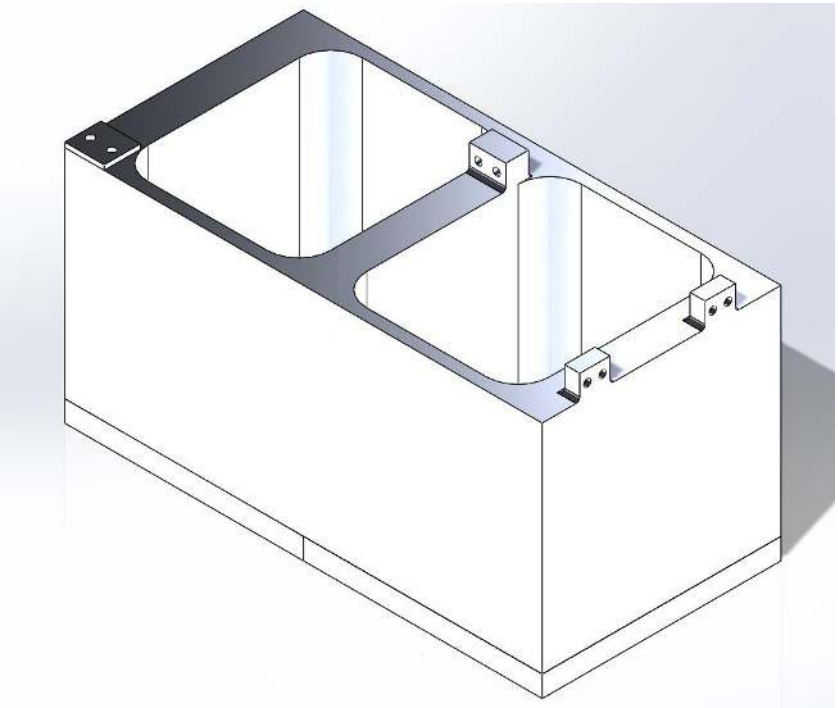

Figure 31: Phoenix Payload

The tabs are shown in Figure 33. Initially, the central tab was 0.15” thick. After the recommendation of the director and the instructor, it was changed to a thicker tab (0.325”). The new thickness can be seen in

the Figure 33 below. Stress analysis using SolidWorks was conducted and hand calculations were made to validate the strength of the tabs.

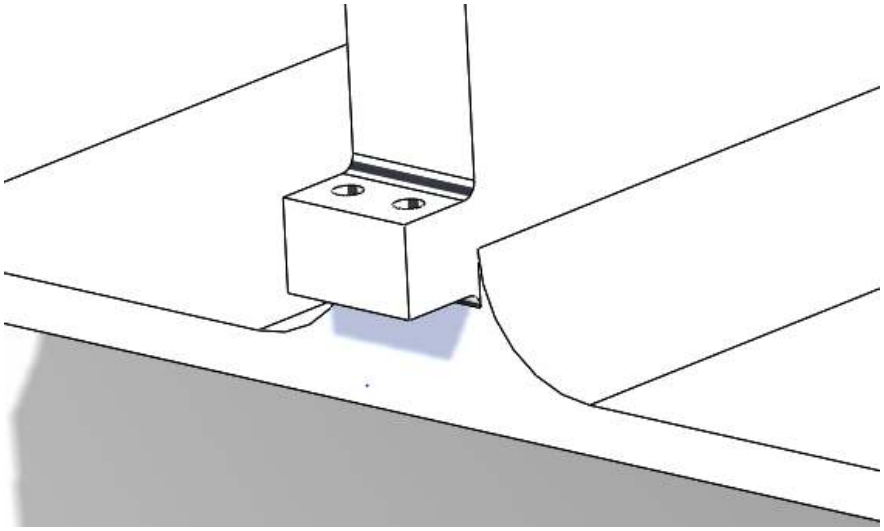

Figure 33: Tab Thickness

Initially, the team specified subsystems to be used for the mission, but was tasked to use the avionics stack from the COSGC ALL-STAR. The avionics stack includes Attitude Determination and Control System (ADCS), COMM, Command and Data Handling (CD&H), Electrical Power System (EPS) and a Global Position System (GPS). A mass simulator replicating the ALL-STAR Avionics stack was made. It is connected to the bottom plate by 7 fasteners in the main bus area. It can be seen in Figure 32 below.

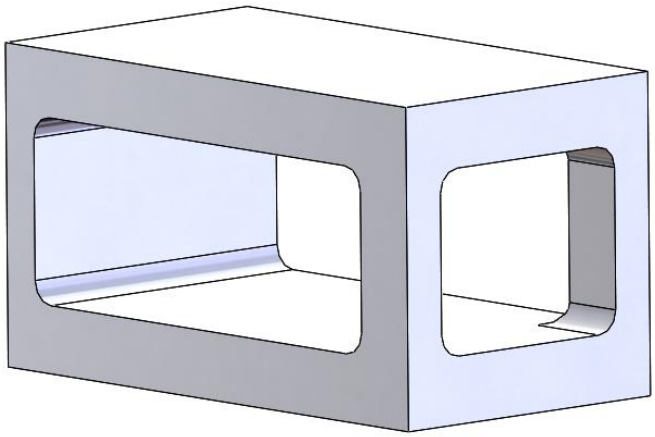

Figure 32: Avionics Stack

The extra mass simulator, called “Additional Volume Mass Simulator”, was built to increase the mass of the structure to its full capacity. That was a team choice to see how the design would fair in a random vibrational test when it is loaded to its allowable limit set by Planetary Systems CSD of 12,000 grams. It can be seen in the Figure 34 below.

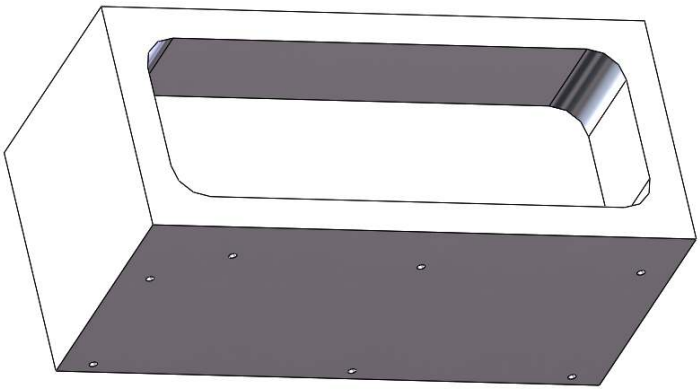

Figure 34: Additional Volume

The additional volume mass simulator weighs nearly 4 kg, and it is fixed to the bottom plate along with the avionics mass simulator.

4.4 Other Design Considerations

4.4.1 Electrical Connector Support

The team was tasked to include an electrical connector support with the structure. The support would house a zero-insertion force electrical connector that would supply the bus with power to charge batteries, communication, and grounding to the CSD once the CubeSat is stowed at launch. The electrical connector is unique in size and location in the structure under the Planetary Systems Corp. specifications. In initial designs, the team was having difficulties in incorporating the electrical connector as it resides in the –Z face of the structure, where the Phoenix Payload is. Therefore, the Payload was shifted to the –X face to allow room for the connector as shown in Figure 35.

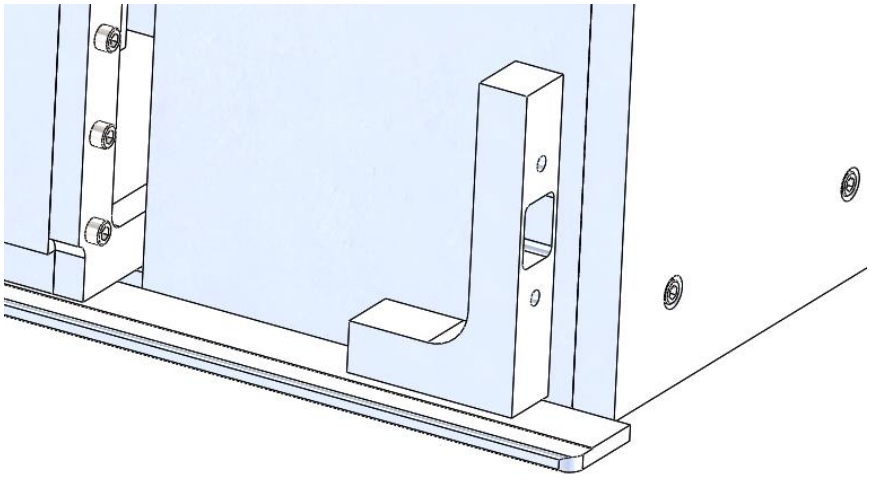

Figure 35: Electrical Connector Support

This support must be located on the –Z face.

5 Analysis

The following section outlines the primary analysis of the 6U-Cubesat structure, and includes a modal analysis, a stress analysis, and a rough thermal analysis of the structure. This section also includes calculations for the payload ejection velocity, the solar array deployment mechanism, and the payload attachment ring.

5.1 Modal Analysis (FEA)

5.1.1 Introduction

One of the principal driving requirements for the design of the structure was the fundamental frequency. In order for the structure to not couple with launch vehicle vibrations, the fundamental frequency must be greater than 100 Hz. The majority of the random vibration generated by the launch vehicle typically occurs within the 0-100 Hz range. Figure 36 is an example quasi-sinusoidal vibration profile for the Atlas V series of launch vehicles.

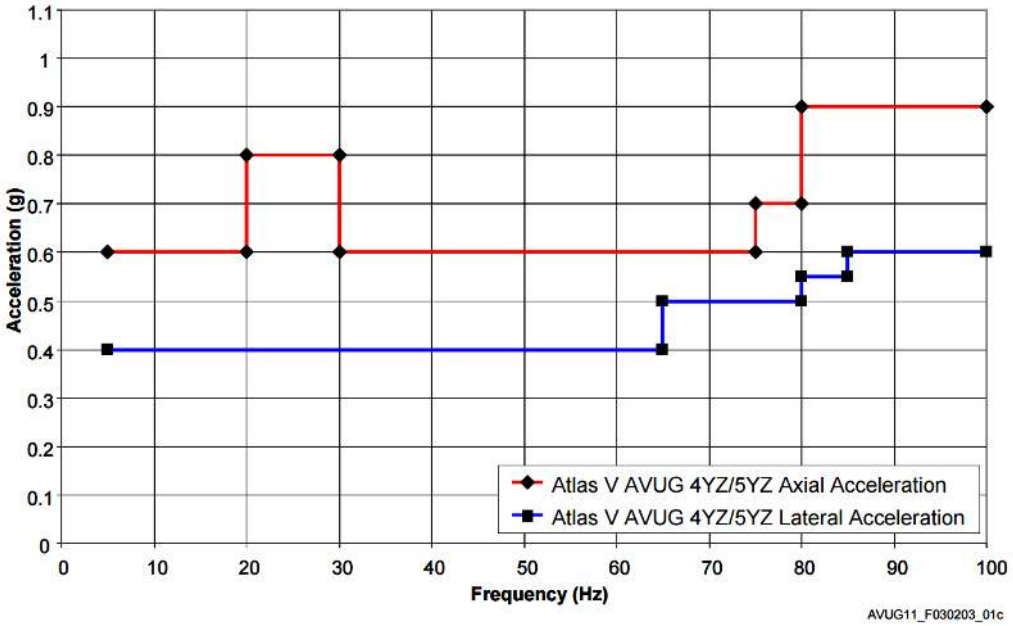

Figure 36: Quasi-Sinusoidal Vibration Levels for Atlas V 400 Series and Atlas V 500 Series [11]

The accelerations are minimal, however, if the payload is coupled at this frequency, the accelerations become amplified significantly. The 0-50 Hz range is typically the design driver for spacecraft structures. However, due to the small size of the CubeSat, the higher 50-100 Hz range is the driver. Staying above 100 Hz provides confidence that no coupling will occur.

Higher frequency random vibration also occurs due to acoustic noise, but only a small portion of this is mechanically transmitted through the spacecraft interface [11]. The vibration levels vary depending on the physical properties of the spacecraft, and an acoustic test is the best way to verify that the spacecraft can survive the environment.

5.1.2 Methods

To determine the resonant modes of the structure and mass simulators, finite element software must be used. SolidWorks simulation was used for this analysis, and a similar approach to the stress analysis was taken for the modal analysis. The solar array deployment system is suppressed from the full assembly for the analysis because the dynamic behavior of the solar arrays and the spring hinge will not be accurately modeled in this way. The assembly is constrained along the tabs of the bottom plate with a fixed geometry condition as shown in Figure 37.

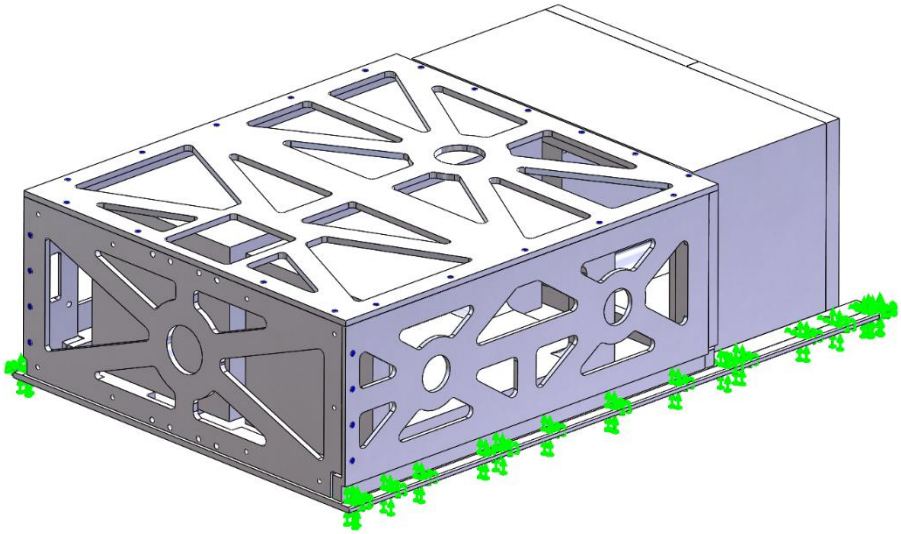

Figure 37: Modal Analysis Constraints

This condition simulates how the tabs will transmit load to the rest of the structure during launch. The CSD clamps the tabs against a surface of continuous bearings. The tabs cannot move in any direction during this clamping, and are thus well modeled by a fixed geometry.

To join each of the parts together, a pin connection is used. This condition joins parts at the location of fasteners, and does not allow any translation. There is no preload, as all that is being studied is the stiffness of the structure and how it responds elastically to impulses.

The final step that is required for the FEA model is building the mesh. Meshing of complex geometries can sometimes be difficult to achieve in the simulation software. Typically, a draft quality mesh must be used with a very fine resolution. If this mesh fails, sometimes a curvature-based mesh works better. Figure 38 demonstrates the mesh created for the modal analysis.

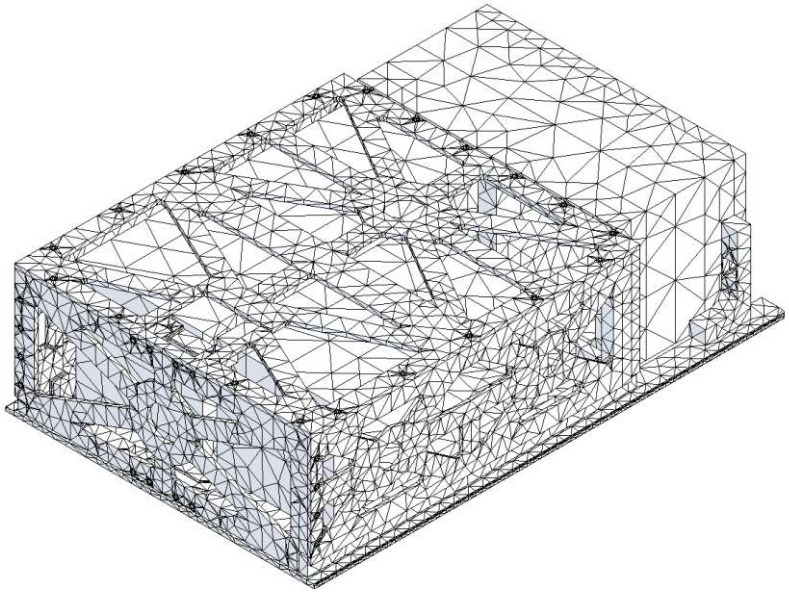

Figure 38: Modal Analysis Mesh

It can be seen how the mesh adaptively adjusts its resolution. Finer details require smaller polyhedra to model their deformation, whereas simple surfaces can get by with large ones.

5.1.3 Resonant Modes

After successfully building a mesh and adding all of the necessary connections and fixtures, the simulation can be run. Table 10 contains the first 10 resonant modes as calculated by the SolidWorks simulation. The first 5 modes have descriptions of the mode pattern.

Table 10: Resonant Modes

Mode No.	Frequency (Hz)	Description
1	293	The +X, -Y, -Z corner of the payload mass simulator is excited. The mass simulator oscillates up and down about the X axis. See Figure x.
2	362	The avionics stack and additional volume mass simulators are excited on their +Y inner Z edge. The two simulators move upwards and rotate outwards as the bottom plate oscillates in a 1-mode drumhead manner. See Figure x.
3	568	The +X, +Y, -Z corner of the payload mass simulator is excited. The simulator is moving away from the rest of the structure in the Z direction. See Figure x.

4	760	The center of the top plate oscillates in a 1-mode drumhead manner. The adjoining structural plates and the payload mass simulator oscillate with the plate.
5	848	The top plate is excited and oscillates along the X-Z plane.
6	895	-
7	951	-
8	997	-
9	1074	-
10	1240	-

Figure 39 through Figure 40 are images of the first 3 resonant modes. These images exaggerate the actual displacement, but are useful for understand which components of the assembly are excited by each mode.

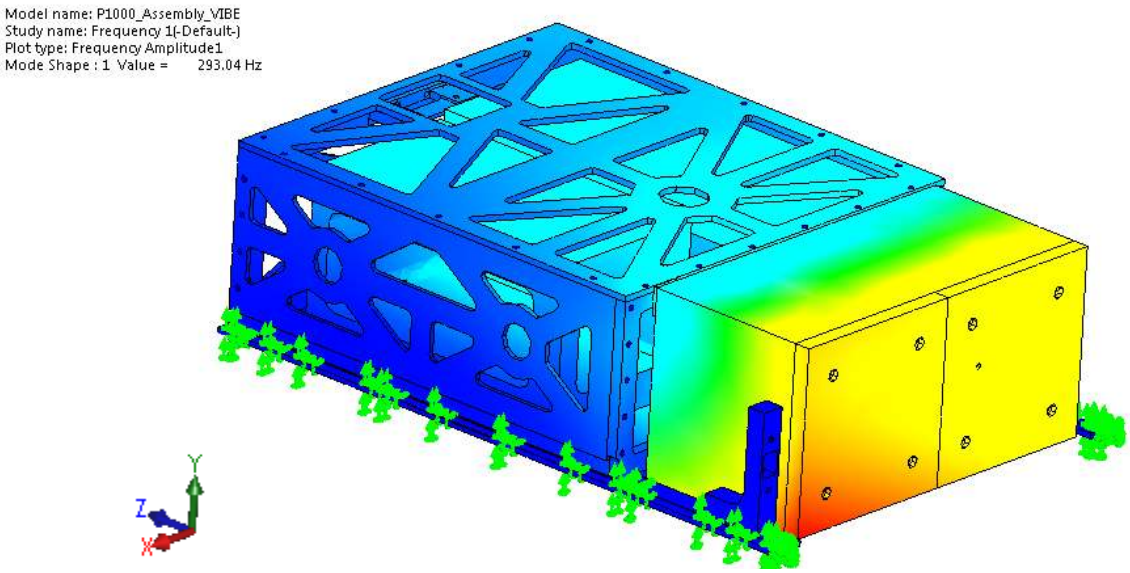

Figure 39: Mode 1, 293 Hz

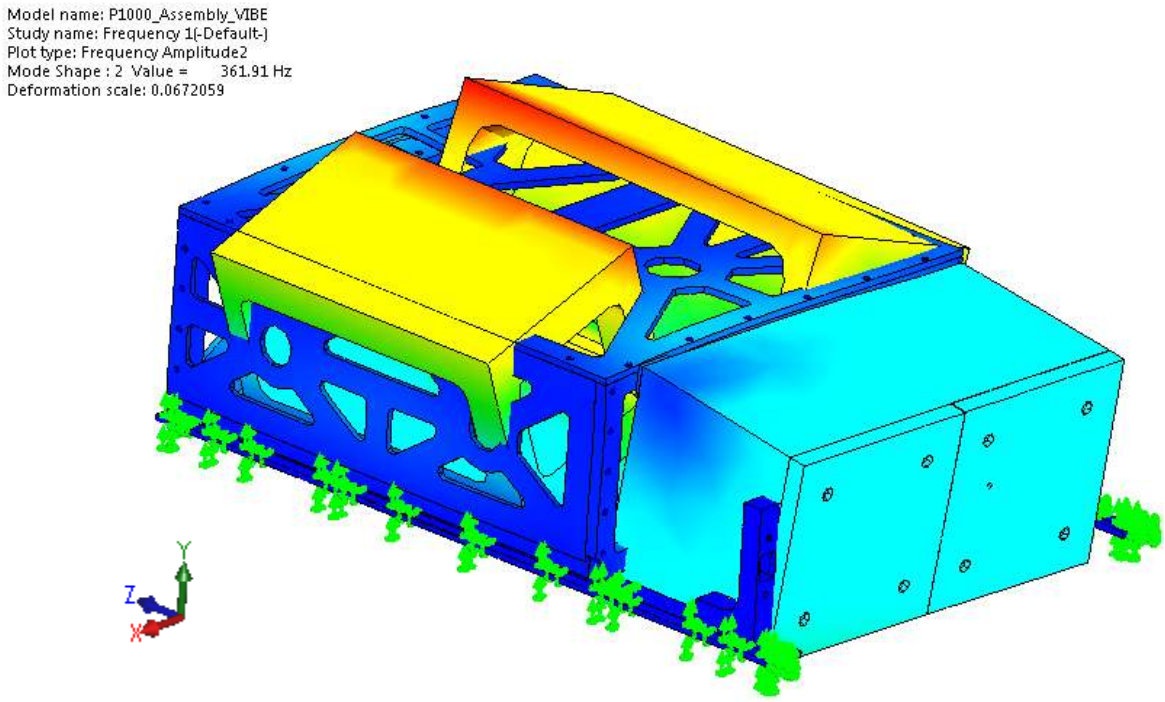

Figure 41: Mode 2, 362 Hz

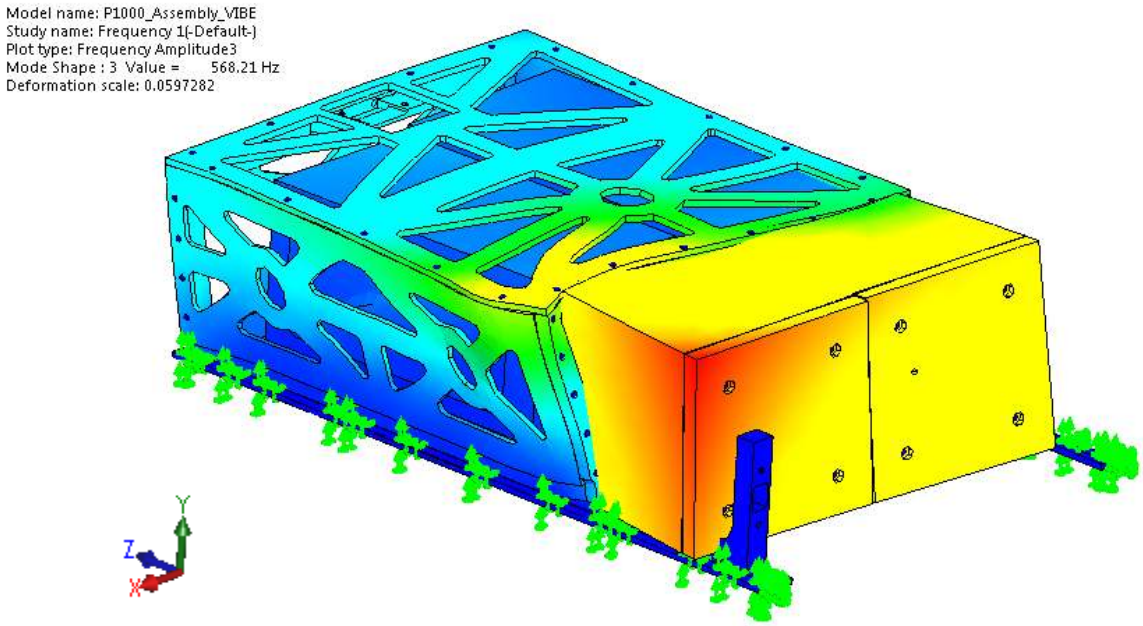

Figure 40: Mode 3, 568 Hz

Note that the color scale is a non-dimensional measure of the amplitude of the excitation. It only has value as a relative comparison to the rest of the component colors. Also, the deformation scale information in each image is not valid. This shouldn't be taken to exhibit any expected deformation scale.

5.1.4 Mass Participation

Another important aspect of modal analysis is the mass participation information. Resonance occurs when an input frequency matches one of the natural frequencies of the structure. Mass participation provides insight into how much mass is activated by the resonance, and subsequently how much energy is being transferred to the object. There may be frequencies at which the structure resonates, but if there is small mass participation, there may be a minimal effect on the structure. Table 11 shows the mass participation for the given modes.

Table 11: Mass Participation

Mode No.	Freq (Hertz)	X direction	Y direction	Z direction
1	293.04	0.025111	0.29357	0.002209
2	361.91	0.015055	0.12658	0.000171
3	568.21	0.18651	0.023405	0.08356
4	759.96	0.086708	0.006949	0.25706
5	847.99	0.00759	0.01382	0.056862
6	895.28	0.19375	0.002965	0.002074
7	950.96	0.023444	0.001312	0.1548
8	997.41	0.029717	0.002362	0.007542
9	1073.7	0.024524	0.000662	0.005559
10	1240.3	0.019486	0.34663	0.007274
		Sum X = 0.61189	Sum Y = 0.81826	Sum Z = 0.57712

These values describe the amount of mass (as a fraction of the whole) that is participating in the given modes in the X, Y, and Z axes. It can be seen that the Y axis has the most mass participation, particularly in the first mode.

The first mode has 2.5% mass participation in the X direction, 29.4% in the Y direction, and 0.2% in the Z direction. Figure 42 shows the cumulative effective mass participation of the first 10 modes.

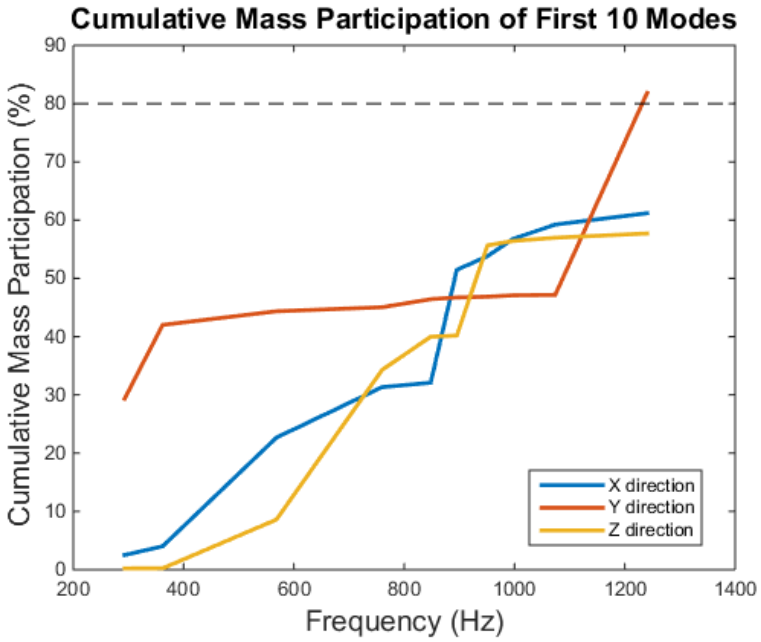

Figure 42: Cumulative Mass Participation Plot

To ensure that the response of the system is adequately modeled, the cumulative mass participation must exceed 80% for the predominate excitation direction. This is shown where the Y curve in Figure 42 goes beyond the 80% mark.

5.1.5 Conclusions

The first resonant mode of the structure and mass simulators is 293 Hz. This meets the requirement for exceeding 100 Hz, so it can be concluded that the design is adequate and ready to be tested empirically for its resonant modes.

It should be noted again that the solar array deployment system was not included in these analyses. The solar arrays have a very small amount of room to move within the CSD constraints, but there is still some room for racking. It is possible that the solar array deployment system has a natural frequency less than 100 Hz. Increasing the preload torque of the hinge mechanism is a possible solution for stiffening this system. More torque would allow the panels to be pressed firmly against the walls of the CSD, making the natural frequency higher.

5.2 Stress Analysis (FEA)

To test the integrity of the structure during launch, a stress analysis was conducted using SolidWorks. The applied static acceleration to the structure during launch varies depending on the launch vehicle. Therefore, the team chose an acceleration of 9 G to account for variability in launch vehicles and mounting locations on the vehicle. The 9 G acceleration was applied to all directions on the structure while constraining the tabs of the structure (fixed geometry condition). This feature is necessary in order to

simulate the clamping system in the Canisterized Satellite Dispenser (CSD). The team set a factor of safety goal of 2.0. The results were promising, with a minimum margin of safety of 1.3.

5.2.1 Preload Conditions

In order to conduct the stress analysis, the preload of each fastener must be set. For an SAE Grade 5 bolt #4-40, with dry conditions (K = 0.2), the torque preloading is 0.64 N-m (8 lb-in). This value was used in the SolidWorks analysis in the design phase, but when the prototype was built, this preloading value changed due to the fact that the fasteners are now locked tight. The torque preloading resulted is 2.5 N-m at lubricated conditions (K = 0.15). In an actual flight hardware, a non-outgassing lubricant would be used [11].

5.2.2 Fixed Geometry Condition

To simulate the loading path and fixture conditions the structure will be exposed to in the Canisterized Satellite Dispenser (CSD) during launch, a fixed geometry condition was applied to the tabs of the structure as shown in Figure 43. The tabs are specified to a specific material and anodization to increase the surface hardness. The type of material (7075-T7 Aluminum or stronger), anodization class and type was specified by Planetary Systems to ensure a clamping strength sufficient to “fix” the structure to the dispenser and avoid crushing the tabs.

5.2.3 Static Loading (Acceleration)

The structure will be experiencing static loading up to 6 G (Delta IV). Due to the variability of the launch vehicles and the mounting location of the CSD on the vehicle, the acceleration used in the stress analysis is 9 G in all primary axes (±X, ±Y, ±Z) as shown in Figure 43.

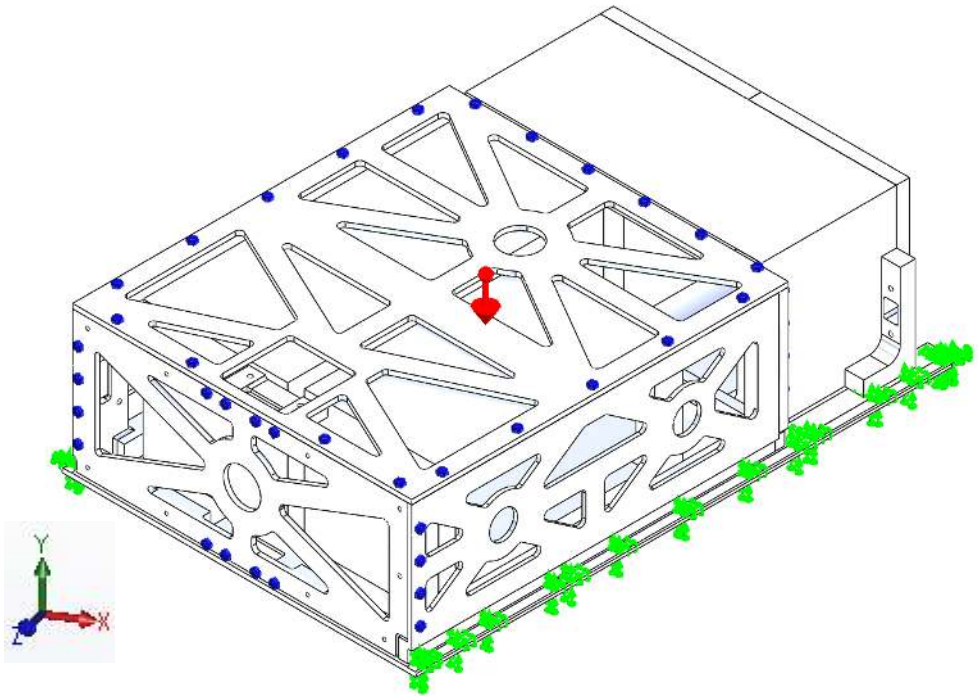

Figure 43: Fixed Geometry Condition and direction of acceleration shown (-y) acting on the center of mass

5.2.4 Mesh

The mesh used in the analysis is a fine curvature based mesh. Figure 44 shows the meshed structure.

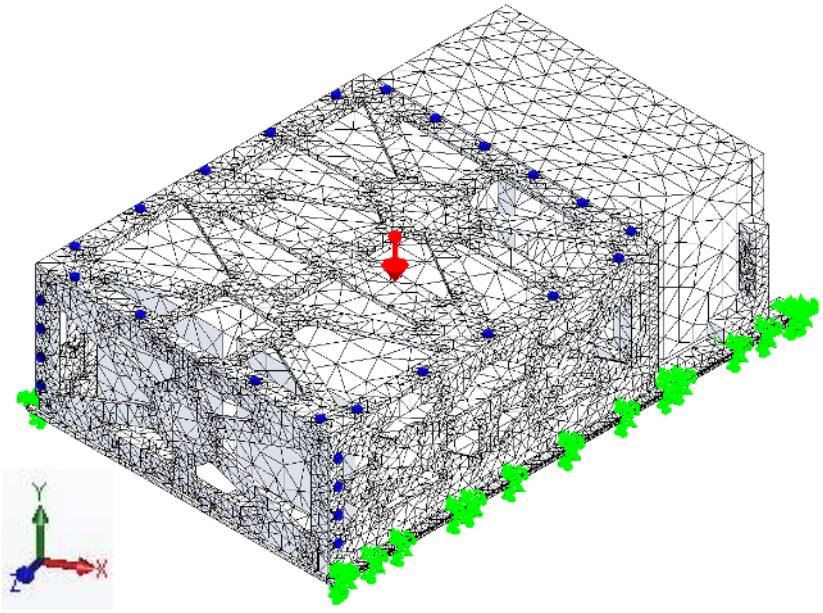

Figure 44: Stress Analysis Mesh

5.2.5 Results

Using the SolidWorks analysis tool, the results in the following images (Figure 45 and Figure 46) were generated. The results show three types of data: stress, deflection, and factor of safety. For the stress, a color map is showing the strength of the structure in multiple regions (red means higher stress concentration). As for the deflection, it is showing an exaggerated view of the deflection (red means higher deflection)

Minimum Factor of Safety: 2.7

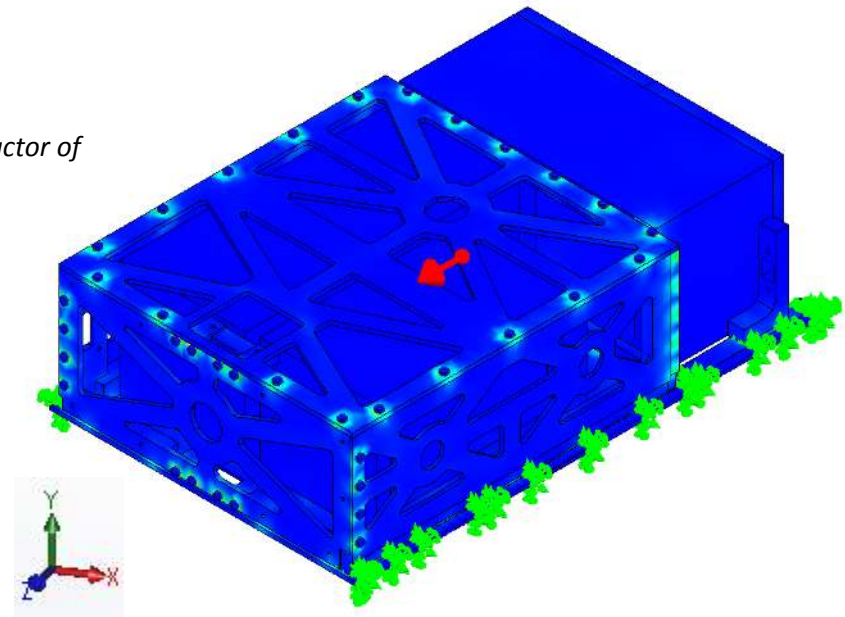

Figure 45: Stress concentration shown with acceleration applied to the (+Z) direction

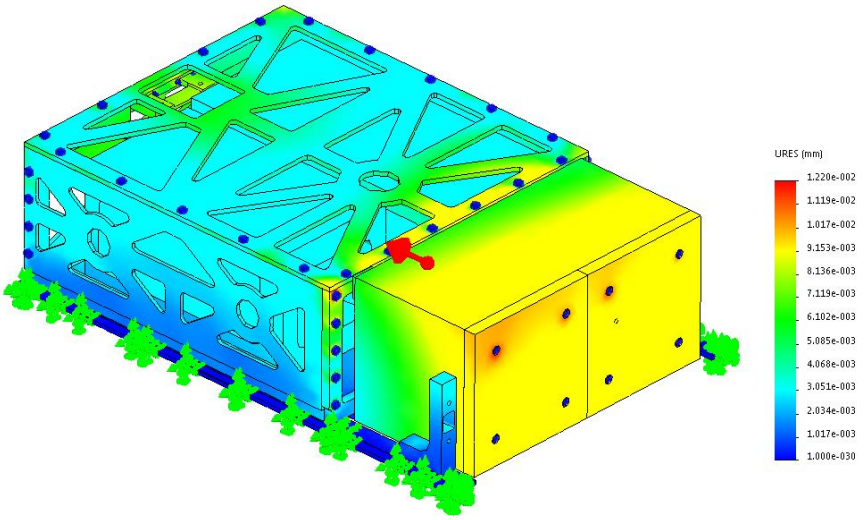

Figure 46: Deflection in the structure with acceleration applied to the (+Z) direction. Deflection is most severe in the Phoenix mass simulator area with a deflection of 12.2 µm which is very small to make a difference.

Table 12 summarizes the stress, deflection and factor of safety for all acceleration directions.

Table 12: Stress, Deflection and Factor of safety each shown with its corresponding direction of acceleration.

Direction	Stress (MPa)	Deflection (µm)	Factor of Safety
X+	104.9	19.9	2.6
X-	100.5	34.5	2.7
Y+	98.84	99.4	2.8
Y-	105.5	28.1	2.6
Z+	101.3	12	2.7
Z-	104	28	2.6

5.2.6 Discussion

The maximum stresses are pretty uniform across the various load directions. Note that use of factor of safety in this table simply refers to the stress margin as compared to the yield stress of the material.

The most impactful acceleration direction is in the -Y, with the highest stress of 105.5 MPa. This is still, however, within the factor of safety set by the team with a minimum margin of safety of 1.3. The highest point of Von Mises stress is in the tab that connects the Phoenix mass simulator to the Payload Interface Plate as shown in figure (5). The stress at the tab is well below the yield tensile strength of aluminum 6061-T6 (276 MPa) [13].

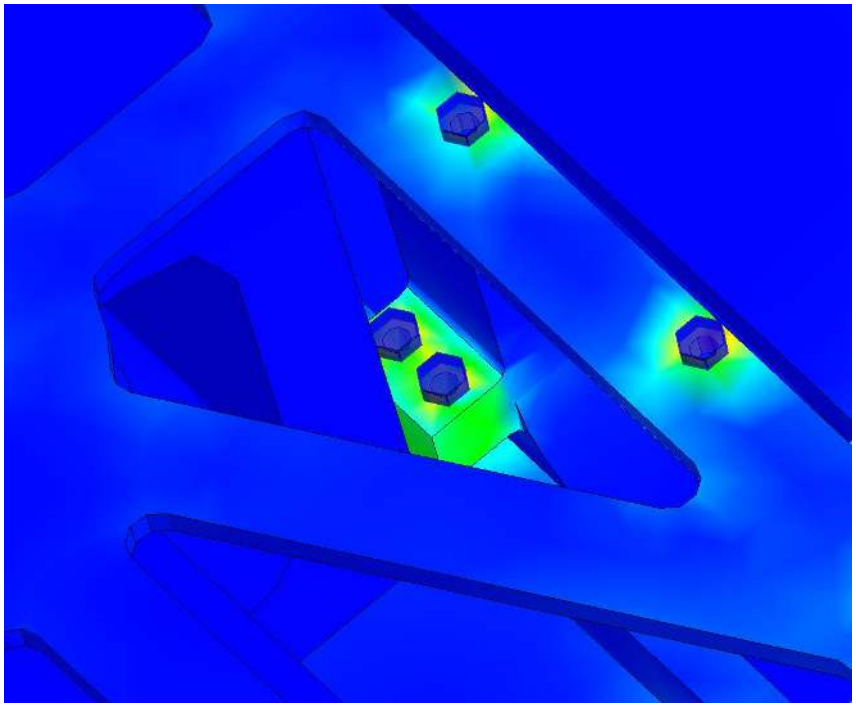

Figure 47: Von Mises stress shown in the payload tab. Most severe when acceleration is applied to the (-Y) direction with 70 MPa (276 MPa is the yield stress of Aluminum 6061-T6)

As for the deflection, the most impactful direction is in the +Y, with the highest deflection of 99.4 μm (about 0.004") which is very small to make a difference.

5.3 Thermal Analysis

5.3.1 Introduction

Although there was no fully defined mission for which the team could model the thermal characteristics of the spacecraft, a rough approximation for the thermal inputs and outputs was performed using preliminary steps as outlined in the text *Elements of Spacecraft Design* by Charles Brown. Figure 48 shows the primary thermal pathways as anticipated by the group.

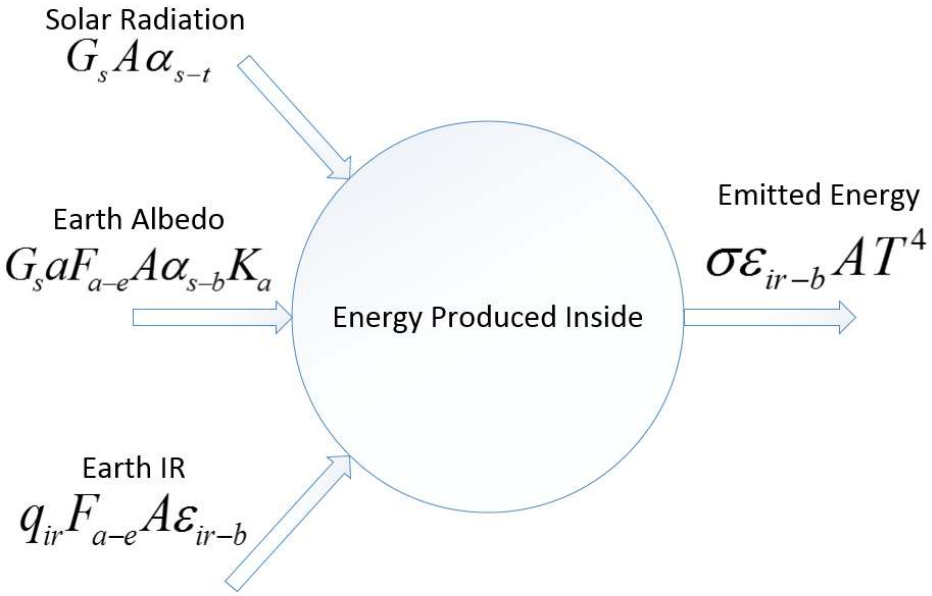

Figure 48: Thermal Analysis

Along with the preceding assumptions, the group also used the following assumptions for the maximum and minimum allowable temperature for each of the primary avionics components. The primary purpose for identifying these constraints was so that the group could plan for a thermal control system if the overall temperature of the satellite were to fall outside one of the specified ranges.

Table 13: Component Temperature Limits

Component	Minimum Temp	Maximum Temp
Battery	-10 °C	50 °C
Command and Data Handling	-40 °C	85 °C
COMM System	-30 °C	70 °C
ACS (Star Tracker)	-40 °C	100 °C

5.3.2 Results

The table of assumptions for the finalized calculations can be found in the Appendix. Figure 49 shows the results as calculated by a specific Matlab script. The Matlab script is also located in the Appendix for future reference. The following graph shows the maximum and minimum internal temperatures expected for the structure with respect to the orbit elevation.

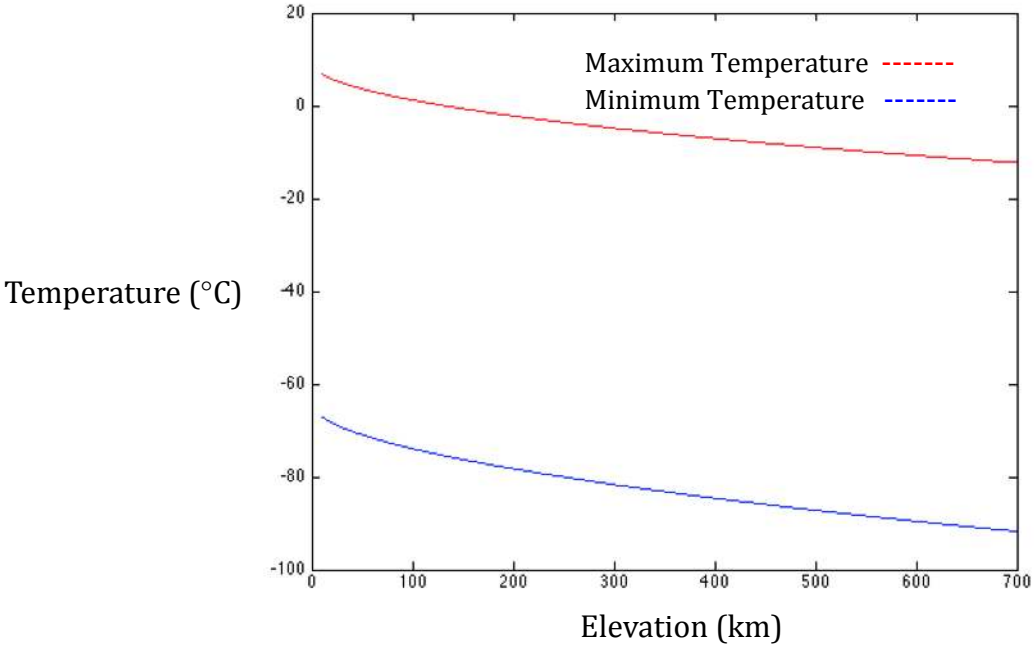

Figure 49: Thermal Analysis Results

Based on the preceding results, the group determined that the primary locations of failure due to thermal constraints were the batteries, the communications system, the command and data handling system, and the star tracker. As such, the group left room around these systems when designing the overall structure, with the anticipation that a thermal control system could be implemented for any future reference missions.

5.3.3 Future Thermal Analysis

While the preceding information shows the very roughly approximated thermal conditions anticipated for the Cubesat, these are entirely subject to change in the future. Once a fully specified mission is established, changes must be made to all assumptions for the structure, and far more specific requirements for an internal temperature range will be established. The primary concern of the SUCCESS team at this point would be the addition of an IR payload like Phoenix, which would require significant thermal isolation in order to properly operate.

5.4 Hand Calculations

Although finite element analysis is convenient and powerful, there were some instances where conventional calculation methods had to be used. The thermal analysis that was carried out for the project was a fairly simple spherical approximation done in Matlab. There was also a series of stress validation calculations done at the location of maximum stress – the single tab shown in Figure 47. These were

intended to validate the FEA results and ensure that the high stress areas were not at any more risk than is demonstrated by the model.

Calculations were also done for determining some of the dynamical aspects of the project. To determine whether there is sufficient torque supplied by the spring hinge to fully deploy the solar arrays, some simple friction calculations were carried out. And to estimate the ejection velocity of the CubeSat from the deployer, some additional calculations were done. The following sections summarize the results of these, but the full calculations are included in the Appendix.

5.4.1 Payload Tab Analysis

From running the full assembly FEA steady acceleration models, it is clear that the highest stress location on the structure is the single tab that connects the payload to the structure and supports the payload in the Y direction. To ensure that this tab is not seeing stress near its yield point, additional stress calculations were carried out.

Analytical beam methods were used to calculate bending stress near the tab, and two different stress concentration effects were considered: stress near the tab fillet, and stress near the fastener hole vicinity. After that, simple shear stress was calculated on the tab. These results were compared to an isolated FEA model of the payload. The tab was constrained and a 9 G load was applied. The results of these analyses are summarized in Table 14. The term MS refers to margin of safety, which is defined as:

$$MS = \frac{Allowable\ Load}{FoS * Load}$$

Table 14: Payload Tab Stress Summary

Method/Location	Load	Limit Load	MS
Hole Vicinity	249 MPa	276 MPa	0.55
Fillet Vicinity	195 MPa	276 MPa	0.71
Simple Shear	10 MPa	207 MPa	10.24
FEA	65 MPa	276 MPa	2.11

Though all of the stresses are less than their corresponding limit loads, the hole vicinity and fillet vicinity stresses have a margin of safety less than 1. The simple shear analysis and the FEA analysis are the more realistic analysis methods, so the result of MS<1 for the other two methods is acceptable.

5.4.2 Solar Array Deployment

Because the solar arrays deploy in microgravity, the primary force that the solar array deployment system must overcome is friction. Determining friction in microgravity is difficult because there is no clear gravitational acceleration that causes normal forces. The normal forces are due to other effects, like the torsional springs pressing against each other along their axes for example. As a conservative assumption to simplify this task, the normal forces will be calculated as they would be in Earth gravity. The normal force will be less during flight deployment. The total frictional force as calculated in this way was 0.045 N.

The total torque output of the springs in each hinge is 0.125 Nm, which translates to a force at the point of rotation of 4.92 N. This gives a margin of safety of 54.7.

5.4.3 Ejection Velocity

To develop an understanding of how quickly the CubeSat ejects from the CSD, some simple calculations were carried out. The friction between the tabs and the interior of the CSD was the primary force opposing the CubeSat ejection. This force was calculated to be approximately 20 N. The maximum force that can generated by the CSD is 46.7 N with all four springs. The springs supply a constant force throughout the ejection.

A force balance was then carried out with the sum of these two forces to determine the CubeSat acceleration. The CubeSat accelerates at 2.3 m/s^2 according to these calculations. Simple kinematics equations can then be used to determine the final velocity after traversing the 14 inches of the CSD interior. The calculated final velocity was 1.31 m/s. This is validated by the ejection velocity curves from the CSD specification document (not the payload specification). These curves are shown in Figure 50.

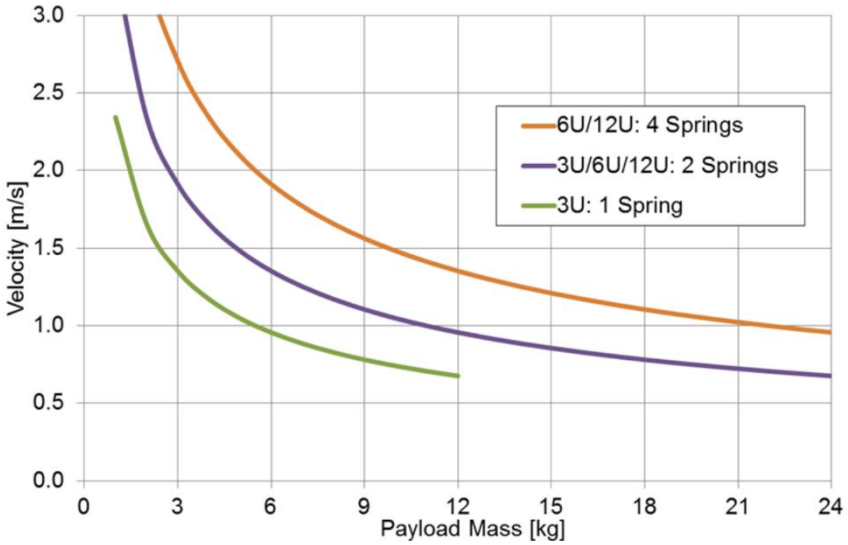

Figure 50: CSD Ejection Curves [4]

With a payload mass of close to 12 kg, the curve for 4 springs (the maximum) shows a velocity of approximately 1.3 m/s.

Note that this velocity applies to a horizontal deployment, not against gravity. The spring force is not enough to eject the full mass vertically.

6 Manufacturing

6.1 Overview

For the purposes of organization and timeliness, the manufacturing of the CubeSat was broken down into three major phases. These phases all have very specific completion dates, and are outlined in the following section. Phase 1 includes the manufacturing of the primary structural plates, and was to be completed by February 14. Phase 2 included the manufacturing of the solar array hinge assembly, and was to be completed by March 1, and finally, Phase 3 was to include the manufacturing of the mass simulators, and was to be completed by April 1. Table 15 outlines the items that were to be manufactured during each of these phases, and the next few sections are first-hand accounts as to what the manufacturing engineers experienced when machining said parts.

The following schedule is the recommended manufacturing process as outlined by the group. It is recommended that any future team follow this schedule in an effort to streamline the manufacturing process and avoid major errors. It should also be noted the group did not always follow these three phases very accurately, as multiple machinists were often working at the same time. Table 15 shows the estimated time frame for a total of roughly 20-25 hours per week of total machining time.

Table 15: Manufacturing Schedule

Phase	Part Number	Part Name	Man. Time	Deadline
Phase 1	P1004	Ext. Top Plate	9 hours	1 Month in
	P1002	Ext. Side Plate	12-14 hours	
	P1006	Ext. Mid Frame Plate	7 hours	
	P1001	Ext.Front Plate	14 hours	
	P1003	Ext Antenna Plate	12 hours	
	P1500	Connector Bottom	4 hours	
Phase 2	P1101	Hinge Rod	15 minutes	2 Months In
	P1102	Hinge Block Left	1 hour	
	P1103	Hinge Block Right	1 hour	
	P1104	HingeArm	4 hours	
	P1105	HingeSpring	NA	
	P1106	HIngeSpacer	20 minutes	
	P1107	SpringSpacer	20 minutes	
	P1408	BearingSeat	1 hours	
	P1409	SA Bearing	20 minutes	
Phase 3	P1300	Mass Phoenix	16 hours	3 Months in
	P1301	Mass Avionics	12 hours	
	P1302	Additional Volume	12 hours	

	P1401	SA BotFrame	5 hours	
	P1406	SA Side Frame	4 hours	
	P1403	SA TopFrame	6 hours	
	P1202	Skel Bot Front	3-4 hours	
Outsourced	P1105	Ext. Bottom Plate	Est. +20 hr.	3 Months In
	P1402	SA Bot Panel	Est. 3 hours	
	P1405	SA Side Panel	Est. 2 hours	
	P1404	SA Top Panel	Est. 3 hours	

The hours estimated in Table 15 for the total machining time are as estimated by the two primary machinists in the group, and are subject to change depending on both the experience and speed of the machinist. All hours mentioned are for the manufacture of a single part; several of the parts have duplicates, so there is additional time to be considered. Also, the hours spent machining in the 3-axis CNC are included, even though it did not require the full attention of the machinists.

Upon closer examination of Table 15, one also notices a significant section of outsourced parts. Outsourcing (as opposed to the group members machining with intermediate skill) is suggested for several parts. The bottom plate requires precise tolerances and an anodization process that could not be completed in the mechanical engineering machine shop. This part should be completed by an expert machinist. The first build of this part for the project was even built incorrectly due to a slip in the inspection process.

The solar array panels also had to be outsourced. The machinist in the mechanical engineering shop and the machinists in all the shops contacted, were not willing to cut any fiber glass with their machines. This made it necessary to outsource the FR4 panels to a water jet machine shop, Rocky Mountain Water Jet. Table 16 shows the prices and locations that the SUCCESS team chose for outsourcing for the reference of any future manufacturers.

Table 16: Outsourced Parts

Part Number	Part Name	Price	Location
P1105	Ext. Bottom Plate	$665.00	St. Vrain Manufacturing
P1402	SA Bot Panel	$26.25	Rocky Mountain Water Jet
P1405	SA Side Panel	$18.75	Rocky Mountain Water Jet
P1404	SA Top Panel	$22.25	Rocky Mountain Water Jet
P1407	SA Front Panel	$13.50	Rocky Mountain Water Jet
P1401	SA BotFrame	$237.50	St. Vrain Manufacturing
P1406	SA Side Frame	$259.50	St. Vrain Manufacturing
P1403	SA TopFrame	$252.50	St. Vrain Manufacturing

An important note on the preceding table: the solar array frame plates were outsourced by the SUCCESS team in an effort to expedite the manufacturing process, because the team had less than the suggested three months to manufacture the entire structure and the team was advised to outsource the parts from the director, client, and class instructors.

6.2 Manufacturing Additions

The following parts were created as additions to the original design, and were justified for several reasons. Each section described below contains an image of the part as well as a justification rationalizing the need for such a part.

6.2.1 Phoenix Mass Sim Additions

As shown in the preceding image, the phoenix mass simulator on the SUCCESS 6U prototype is slightly modified from the version included on the original SUCCESS SolidWorks model. This change is the result of the purchase of the wrong size stock for machining purposes. The group specified the purchase of a 4 x 4 x 8 inch piece of 6061 aluminum, and actually required a 5 x 5 x 8 inch cut of 6061 aluminum. Because of this error, the group was unable to include the required tabs for the payload, and as such had to manufacture a series of two, bolt on additions to the payload. These plates are shown in Figure 51.

6.2.2 Phoenix Contact Point Addition

This addition was actually made the day of the Space Symposium as an important requirement was noted that had been overlooked. The addition was recognized in the Planetary Systems specification document as the group was working on making the necessary measurements to confirm they were to specification for the CSD. The requirement that caused this addition was a third point of contact with the ejection plate of the CSD. It was specified that the three points of contact had to encompass the center of mass of the CubeSat. This is why the third point of contact is located above the center of mass. The following exploded view,

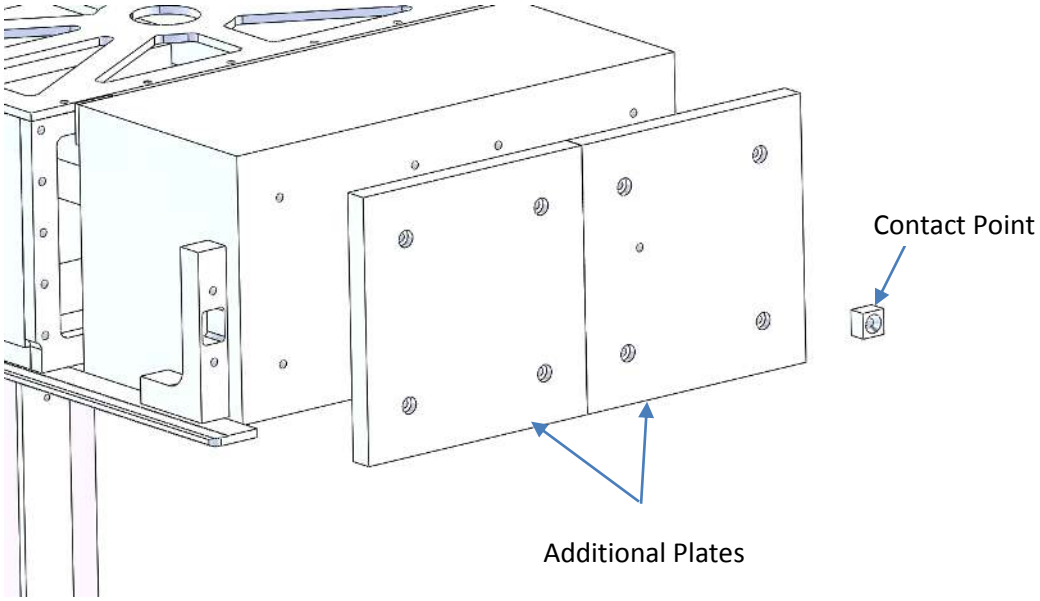

Figure 51, shows the two additions.

Figure 51: Phoenix Mass Simulator showing the plate and the Contact Point addition.

6.2.3 Solar Array Backbones Screw Head Clearances

The team also missed a couple of fastener heads that would cause interference with the solar array frames. After assembly, it was realized that clearances were not included in the frame designs. A simple solution was taken by the team by cutting slots or clearance holes in the solar array backbones as shown in Figure 52.

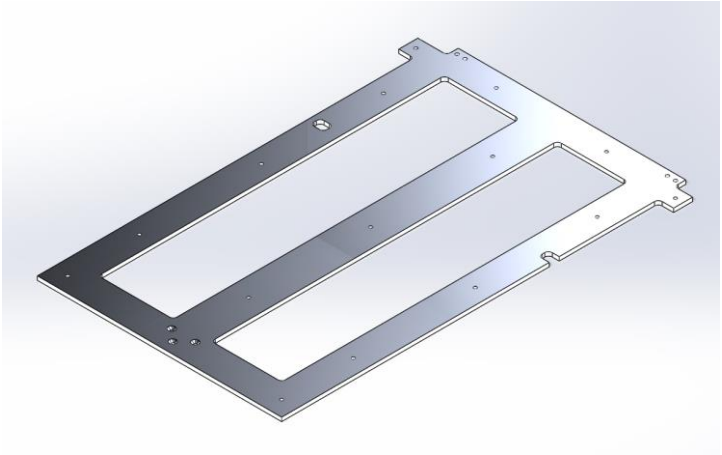

Figure 52: Solar Array Backbone showing modifications made to allow clearance for the fastener heads.

6.3 Manufacturing Errors

The following section outlines the major manufacturing errors that the groups machinist's encountered when manufacturing the various components of the structure. These errors are included for the future reference of anyone who intends to manufacture a similar design.

6.3.1 FR4 Manufacturing

Early in the design process, the group decided to utilize FR4 in an effort to accurately model solar arrays during both vibration and fit tests. While FR4 is a great material to include in any 6U prototype, it is not recommended by any university machine shops because of the damage fiberglass can do to end mills. In response to this problem, the team outsourced our FR4 panels to Rocky Mountain Water Jet for cutting. While the machine shop in question provided the CU group with unbelievable customer service, the countersinks requested on the FR4 panels proved to be difficult to manufacture. The waterjet shop was able to finish all the countersinks requested, but delaminated multiple sheets of FR4 in the process. Therefore, the Rocky Mountain Water Jet chose to outsource the FR4 to be cut in one of their sister machine shops.

When designing a solar array or solar array replica, avoid countersinks on thin (about 0.090") fiberglass sheets if machining them is not an option. This difficulty will likely not be an issue if PCBs are made with functional circuits. It may be preferable in the future to have PCBs made for mass models instead of machining the parts from fiberglass.

6.3.2 Bottom Plate Manufacturing

In order to comply with the specifications laid out in the Planetary Systems CSD specification document, the group was required to meet a very precise set of requirements for the bottom plate and tab interface included on the 6U prototype. Because of these requirements; most notably the anodization and the extremely tight tolerances along the tab interface, the group outsourced the bottom plate to St. Vrain Manufacturing. Whilst the plate was manufactured and anodized with the utmost quality, the tab interfaces were not machined within the specified tolerances. As a result the part was returned to the machine shop and had to be rebuilt.

Whenever the bottom plate or tab interface is manufactured, care should be taken to ensure that the dimensions have been made to the drawing specifications.

6.3.3 Payload Mass Simulator Manufacturing

When machining the payload mass simulator, the mechanical engineering machinist made a mistake while it was in the CNC. The face with the tabs was cut smaller than it should have been. The protrusion that was in the top right corner of the Phoenix mass sim was machined away. The face was 0.0785 inches shorter than it should have been. This meant that the Phoenix payload would not be able to properly interface with the bus.

The Machinist, Greg, decided the best option was to either shorten the entire mass sim by 0.0785 inches to make the protrusion from the mass sim possible, or he could make a small “shim.” The shim, a piece of aluminum that fills the space where the as-designed mass simulator would have had some material, was declared the better option.

7 Assembly

In order to assemble the structure, a procedure to be taken outlining the steps was developed by the team and is detailed in *D01: SUCCESS Assembly Document*. The assembly part consists of four main steps: the structure assembly, the mass simulators integration, the deployment mechanism assembly, and the solar arrays assembly.

All holes in the structure of size #4-40 are tapped for thread-locking Helicoils. The fasteners used shall also be lubricated to prevent galling with the Helicoils. In the development model, Moly lube was used. For space hardware, a non-outgassing lubricants must be used.

7.1 Structure Assembly

The structure assembly is made by starting with the primary plate; the bottom plate is to be used as the base of assembly. The side plates, from plate and payload interface plate with its mass simulator (middle plate) is to be attached to the bottom plate. Next, attach the housing for the deployment mechanism followed by the top plate and lastly, the electrical connector support. Figure 53 shows the structural plates (minus the top plate) assembled together.

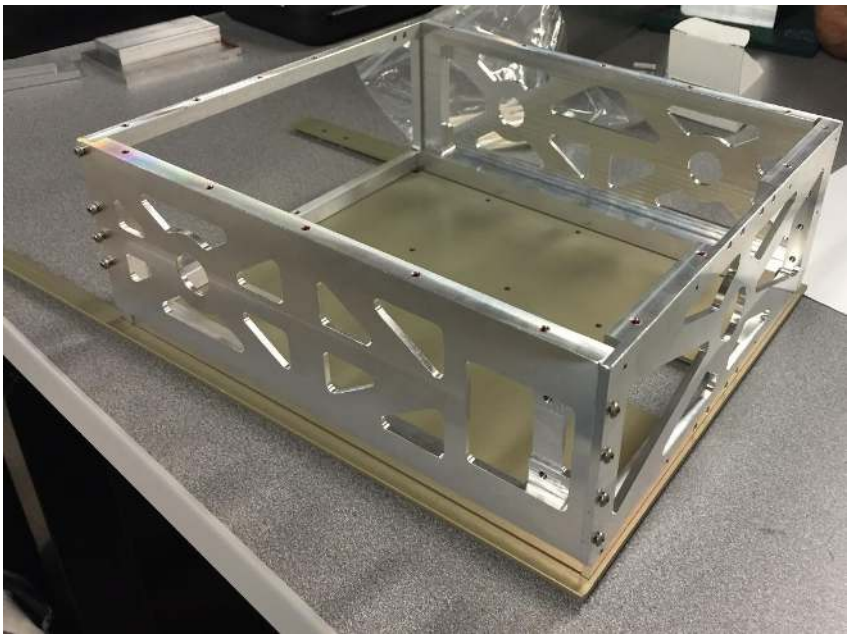

Figure 53: 6U CubeSat Structure with the Bottom Plate, Side Plate, Front Plate and Payload Interface Plate assembled.

7.2 Mass Simulators Assembly

The first step is to attach the Phoenix Mass Simulator to the Payload Interface plate and making sure to fasten the center tab first before the rest. The next step is to place structure assembled on top the Avionics Stack Mass Simulator and the Additional Volume Mass Simulator such that it encloses the mass simulators with the holes aligned. The mass simulators should then be fastened to the structure. Lastly, the Top Plate is attached to the structure and all holes are fastened.

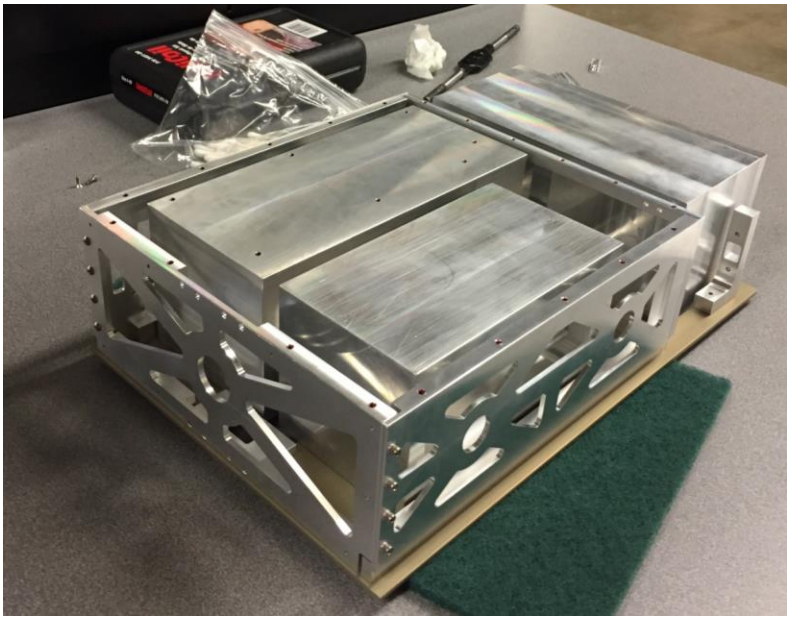

Figure 54: Structure assembly shown with all mass simulators in place.

In the built model, some manufacturing errors occurred and so the team added a shim that connects the Payload to the Payload Interface Plate, a contact point, and two plates to the back of the Phoenix Payload as shown in Figure 55.

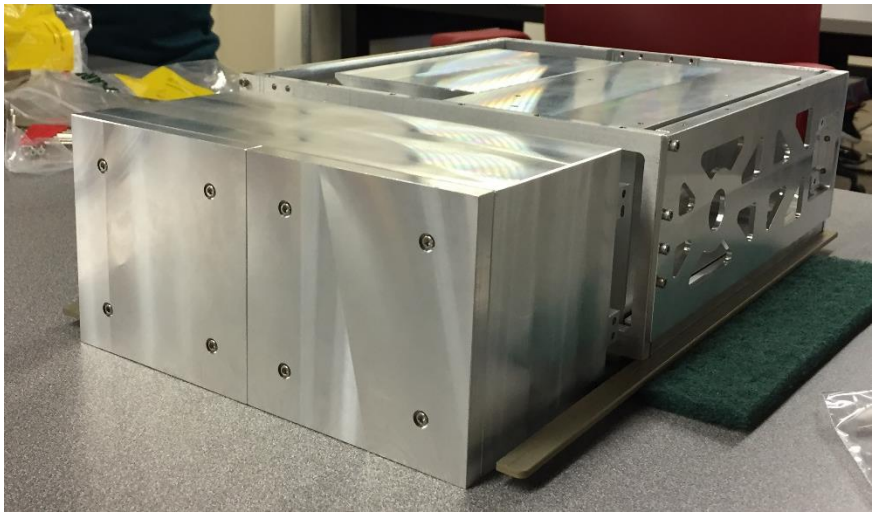

Figure 55: The back plates shown on the Phoenix Mass simulator. The Contact point is not in the picture as it was a last-minute modification to the assembly.

7.3 Deployment Mechanism Assembly

To assemble the mechanism, start with inserting the rod to either hinge blocks. Next, insert the small spacer (hinge spacer) to the rod followed by the hinge arm *partially*, the first spring, the spring spacer, and the second spring. Next, insert the hinge arm *fully* followed by the other small spacer and lastly, the final block. Fasten the blocks to the mechanism housing while ensuring the tip of the hinge arm is in the gap located in the housing. This gap acts as a stopper for the arm at about 95 degrees. The hinge arm default state is *deployed* as shown in Figure 56.

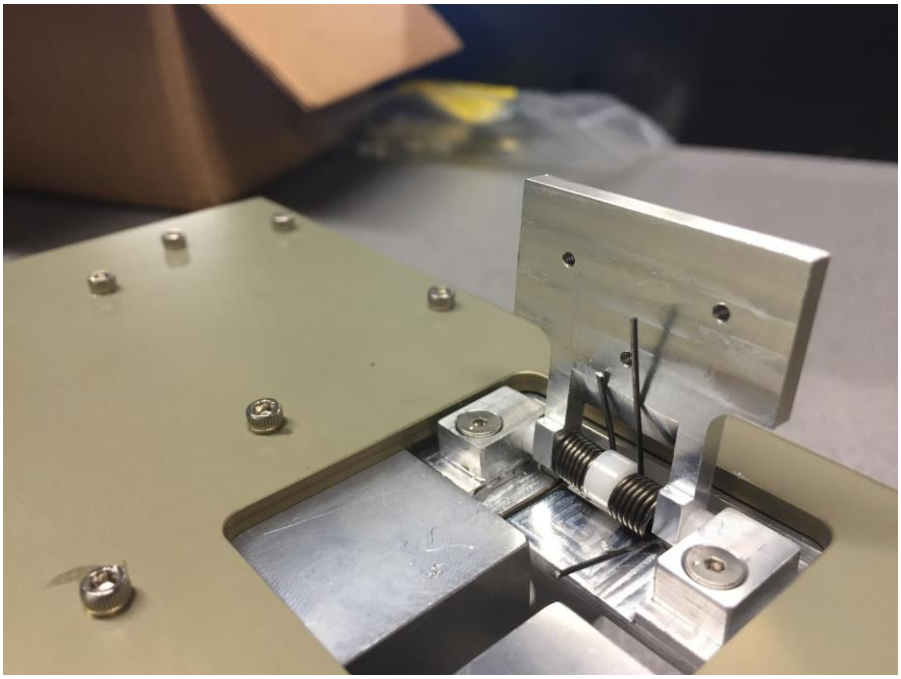

Figure 56: Deployment Mechanism shown in the Bottom Plate side of the structure in its default state: Deployed.

7.4 Solar Arrays, Backbones and Roller Bearings Assembly

The last step of assembly is mounting the Solar Arrays, their Backbones and Roller Bearings that will be housed by the backbones. This starts with placing the backbones, each to its corresponding face of the structure, and fastening them to the hinge arm. The hinge arm shouldn't deploy against gravity. Next, the solar array panels (FR4) are fastened to their corresponding backbones. Lastly, the Delrin Roller Bearings are placed on the shoulder screws and fastened to the Roller Bearing Housings, which are then fastened to the backbones. Figure 57 shows the solar array frames integrated with the primary structure and hinge assemblies.

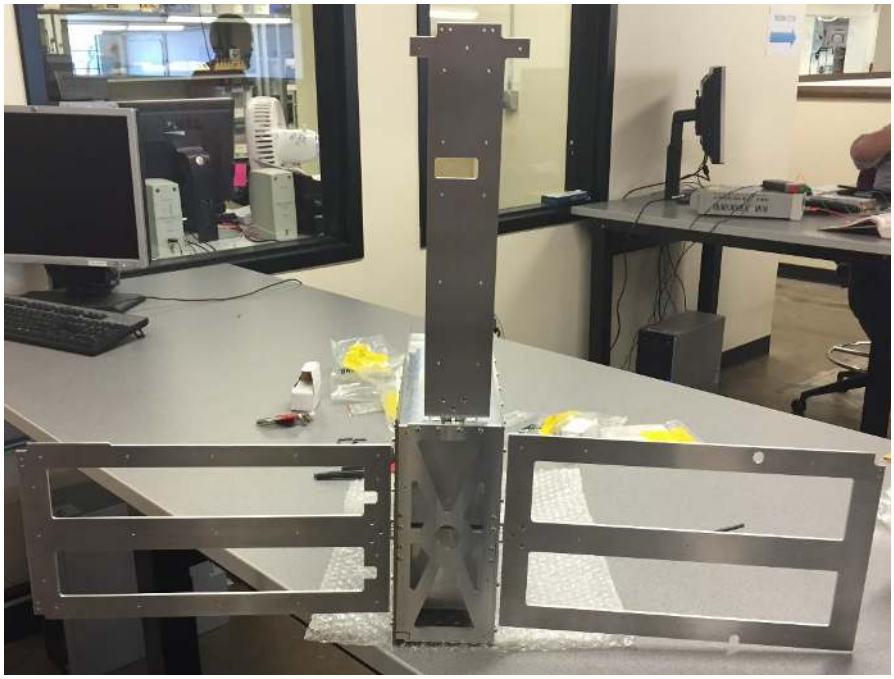

Figure 57: Image showing the solar array backbones deployed on all three faces.

The solar array panels must be attached to the solar array frames after the frames are attached to the hinge assemblies. Figure 58 shows a solar array frame with attached solar array panel and roller bearing assemblies.

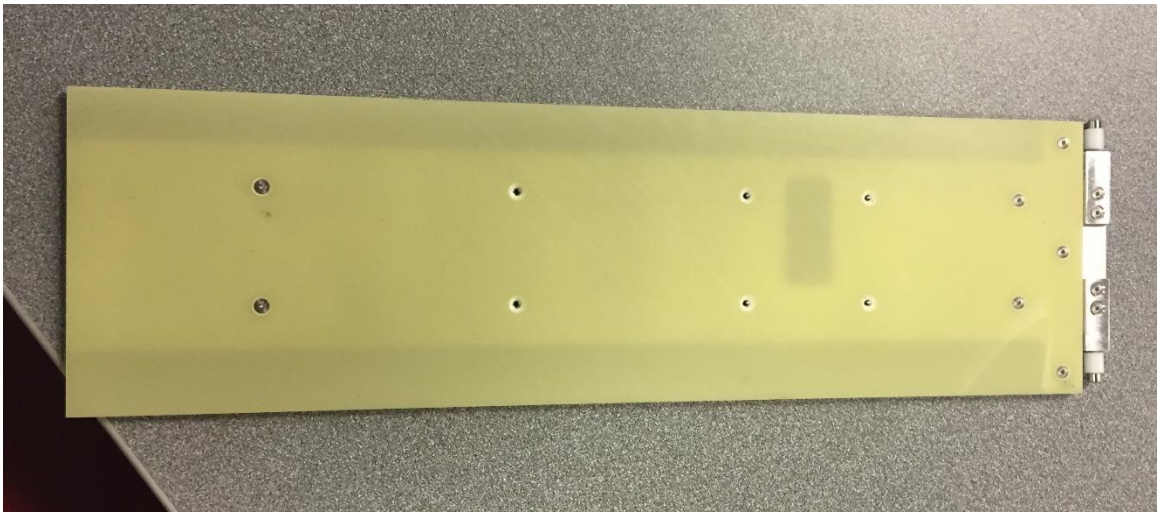

Figure 58: Solar Array (FR4) and Roller Bearings Assembly on the Side Backbone.

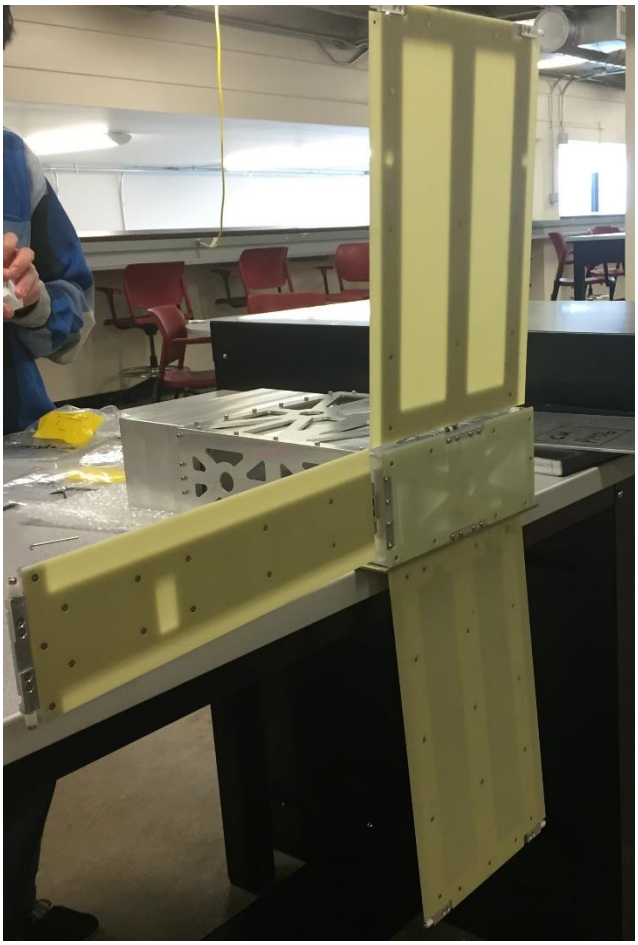

Figure 59: Final Assembly of all parts integrated.

Figure 59 shows the final assembly of all parts. By following the steps, assembly should take about two hours not including Helicoil insertion. With multiple assemblies, the time taken per assembly can be reduced.

8 Testing and Verification

The majority of the team's effort was concentrated in the design and manufacturing phases of the project. Due to the breadth of the CubeSat design, there was little time to do extensive testing. The initial reach goal of the project was to complete a random vibration test of the structure, but it became apparent early in the second semester that it would likely not take place. Between the lead times for the CSD and preparing a time for the vibe test at a nearby facility, the logistics proved to be too challenging. That being said, there are opportunities for the vibration test to take place sometime this summer.

Most of the testing and verification that took place for the project was in the form of checking the masses, center of masses, and dimensions of the built parts. There was also functional verifications of systems and full assembly dimensional and functional verifications. This culminated with the fit check and deployment tests with a test CSD at the 2015 Space Symposium. A more extensive account of the testing and verification is seen in *D02: Testing and Verification Document*.

8.1 Mass Verification

To determine whether any manufacturing errors occurred and make sure that total mass targets are met, each part was massed and verified. The criteria for acceptance for the part masses was 5% of the total mass or 1 gram, whichever is larger. This allows the larger parts more variability, and does not limit the small parts to a tight mass limit when their impact to the total mass is minimal.

All of the manufactured parts met this criteria with the exception of the solar array panels, solar array frames, and the top plate. The solar array panels are made of FR4 fiberglass, and the material density is somewhat variable. Additionally, the parts were made to a different thickness than as designed. This is explained further in the manufacturing errors portion of the report, but essentially the original stock material was damaged due to delamination, and thinner stock that was readily available had to be used. This compromise was necessary for meeting schedule goals.

The solar array frames and top plate differ by approximately 10% from their designed masses. This difference can be explained in part by inaccuracies with SolidWorks material properties, and small variations due to machining tolerances. The parts still fulfill their functional roles without issue, and the total mass is within the required range, so these discrepancies are acceptable.

8.1.1 Center of Mass

The locations of the mass simulators center of mass is essential in adequately simulating the systems they are intended to represent. These locations were measured by finding the tipping points for each of the three axes of the mass simulators with a small fulcrum. This process is shown in Figure 60.

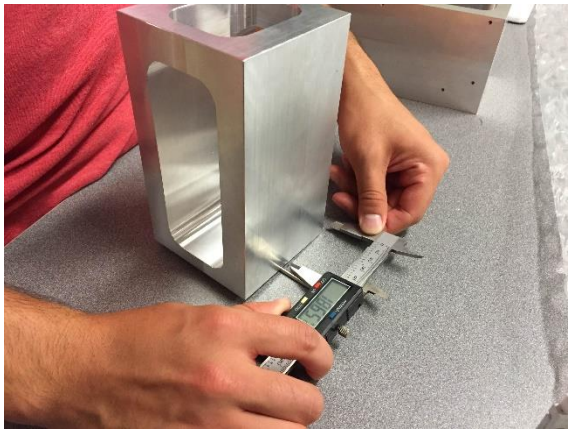

Figure 60: Center of Mass Measurement

The mass simulator is guided along a thin rod, and the point at which the mass simulator tips and balances is measured with respect to the reference axes. All of the mass simulator centers of mass came within 0.25 cm of the designed locations. This ensures that their locations are accurate representations of the spacecraft systems, and are valid to use for further testing.

8.2 Functional Verifications

The primary functional verifications that needed to be carried out pertained to the solar array deployment system. It needed to be verified that the spring hinge assemblies functioned as intended, and there were no foreseeable issues in their function.

This was done through inspecting the hinge assemblies and evaluating the friction among their components. It is a fairly tight fit on the hinge rod with the various spacers and springs, so it is important to check that there is enough room to not restrict the motion. The large interior hinge spacer had to be filed down from its designed width to tailor it to each hinge assembly. Once it was determined that the hinges allowed adequate movement, they could be tested with the solar arrays attached. Test deployments of each of the solar arrays were carried out and filmed. These deployments proved adequate for the project purposes. The torque output by the spring hinges is enough to deploy the solar arrays with ease, but is not enough to induce shock loads when the stopper is hit. The deployment videos are available as part of the deliverables package in the photos and videos folder.

8.2.1.1 Final Deployed Angle

Another element of the solar array deployment verification was the final deployed angle. It is essential for proper power generation that the solar arrays are deployed perpendicular to the sun's rays. These angles were measured with a protractor as shown in Figure 61.

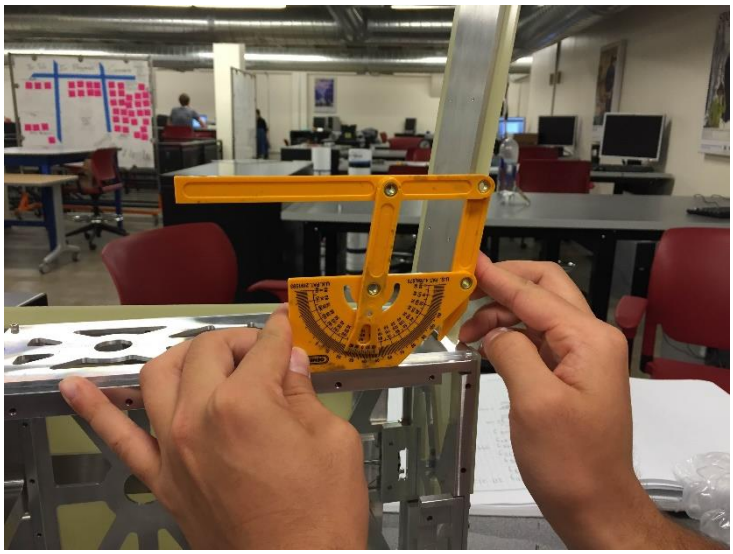

Figure 61: Deployment Angle Measurement

Each of the solar arrays is over-deployed by about 5°. The measured angles were 95°, 94°, and 96° for the top, bottom, and side solar arrays respectively. These angles are within the established limits of 90° ± 10°, but future iterations of the design should seek to bring this number as close to 90° as possible.

8.3 CSD Dimensions and Functional Verifications

The success of the project hinged on the final fit check and test deployments from the CSD. In order to develop full confidence that these verifications would be successful, an extensive dimensioning process was carried out. All of the dimensions and requirements that were relevant to the fit check and deployment were fully verified from the CSD specification document. The testing document lists all of these and their respective measurements.

8.3.1.1 Dimensional Verification

These dimensions are also mentioned in more detail in the driving requirements section of the report. They pertain primarily to the dynamic envelope of the CubeSat, contact locations with the ejection plate, and contact zones for the solar array deployment system. Some of the measurements were fairly difficult to gather, and required reference plates to accurately verify. This concept is demonstrated in Figure 62.

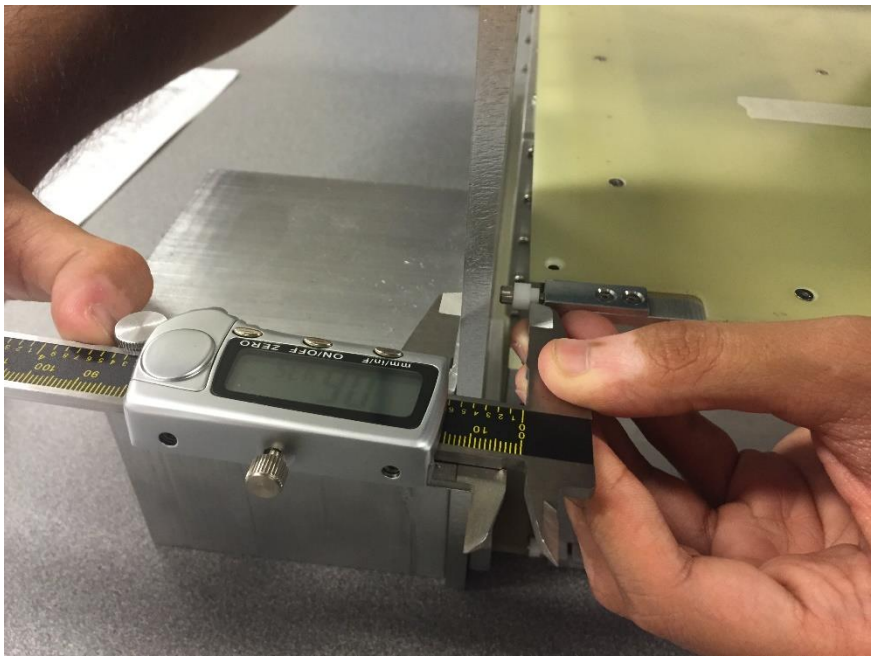

Figure 62: Dimensioning Method

The example shows the measurement of the location of one of the roller bearings. A reference plate of known thickness was used to tie the measurement to the outer extent of the bottom plate, which was used to determine the distance to the reference origin. Care was taken to ensure the reliability of these measurements, and it paid off during the final test.

8.3.1.2 Fit Check and Deployment

On April 15, 2015 the team attended the Space Symposium in Colorado Springs, where representatives of Planetary Systems were showcasing their technologies. A 6U test CSD was present and available for testing purposes. The full assembly was loaded into the CSD without issues, and the fit of the assembly was tested qualitatively. The solar arrays interface well with the CSD contact zones – there is very little space for them to move, yet the assembly slides out smoothly with the roller bearing interface. Figure 63 shows the full CubeSat assembly integrated with the CSD. The image on the left shows the assembly simply resting in the enclosure, and the image on the right shows the CSD with the door shut and latch locked.

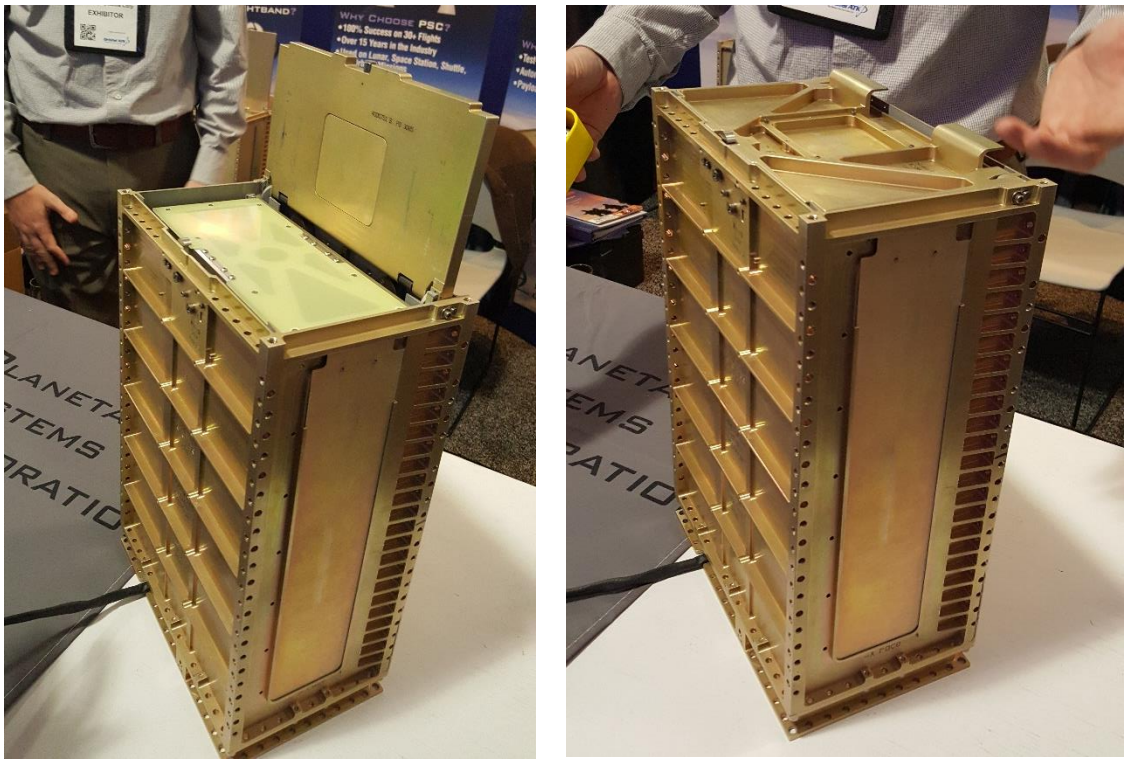

Figure 63: Full Assembly within CSD

Six deployment tests were carried out with the assembly, though two of the mass simulators had to be removed. This was necessary because there were concerns that the fully loaded assembly would damage the CSD interior on ejection due to gravity. The assembly would have ejected at a slight downward angle, and may have scraped along the ceiling of the dispenser. A future test of the full mass would require a continuation of the series of rollers seen inside the CSD. The CubeSat would eject and continue moving along the conveyer.

9 Scheduling

The following section contains an outline of the primary milestones faced by the team during the SUCCESS 6U Cubesat development effort. These milestones were integral steps in the design process, and culminated in the design expo on April 24th. A schedule overview is shown Figure 64.

Over the entirety of the design process, the group tried multiple different programs in an effort to remain organized and on time. The first semester the group utilized Microsoft project, but strayed away from project as the client and director did not have access to the program themselves. During the second semester, the group utilized an excel document to track manufacturing progress. It is highly recommended that groups use excel for scheduling because of its simplicity and universal use.

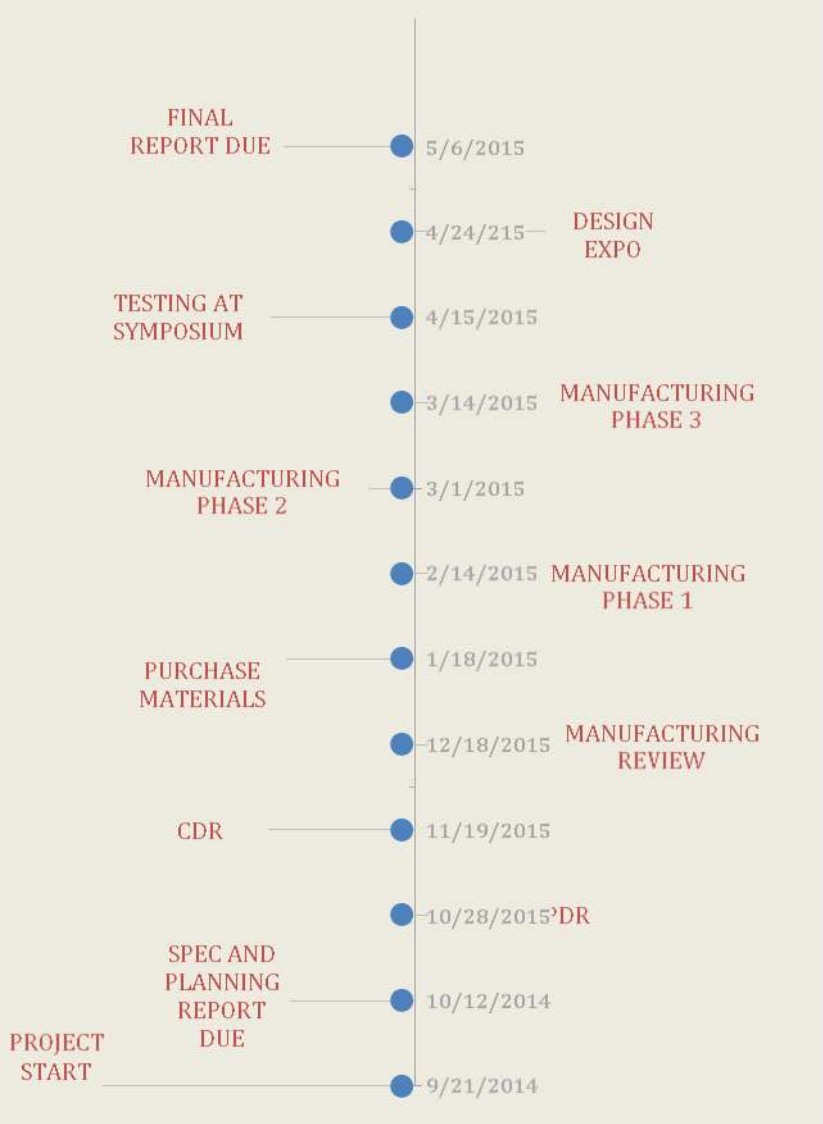

Figure 64: Schedule Overview

Only the major milestones and deliverables are included in this overview. Figure 65 is an excerpt from the excel document that was used to track tasks by the team.

Part Numbe	Part Name	Machining	Machining L	Stock Material	Stock	Responsible	Date Due	Updates	Comments	Estimate	Percentage
P1001	Front Plate	CNC	In House	Aluminum 6061-T6		Andrew Oh	3/7/2015	100%	Drilling and Tapping holes needed	12	9.84%
P1002	Left Side Plate	CNC	In House	Aluminum 6061-T6		Andrew Oh	3/7/2015	100%	Drilling and Tapping holes needed	12	9.84%
P1003	Right Side Plate	CNC	In House	Aluminum 6061-T6		Andrew Oh	3/7/2015	100%	Drilling and Tapping holes needed	12	9.84%
P1004	Top Plate	CNC	St. Vrain Par	Aluminum 6061-T6		Khalid Al Dc	3/7/2015	100%	Stock delivered - Mid March expe	0	0.00%
P1005	Bottom Plate	CNC/Anod	St. Vrain Par	Aluminum 7075-T7		Nicholas Me	TBD	100%	Quotes are in, just need to make a	0	0.00%
P1006	Mid Frame Support	CNC/Mill	In House	Aluminum 6061-T6		Khalid Al Dc	3/14/2015	100%	Tapping holes needed	10	8.20%
P1101	Hinge Rod (Axle)	Lathe	In House	Aluminum 6061-T6		Khalid Al Dc	2/14/2015	100%	Need validation and de-burring	2	1.64%
P1102	Hinge Block	Mill	In House	Aluminum 6061-T6		Khalid Al Dc	2/14/2015	100%	Need validation and de-burring	3	2.46%

Figure 65: Scheduling Tool Excerpt

10 Finances

Despite initial preconceptions, financial aspects of the project had a significant effect on design, manufacturing, and overall scheduling processes.

At the start of the project, the budget sources consisted of two parts: $750 from the Colorado Space Grant and $1500 from the Mechanical Engineering department. Financial costs did not really start until second semester when material procurement began. Comparing initial plan and the final plan, the team needed to request $1200 from the overrun fund to meet schedule goals. The total cost for the project was $2792.72. The final budget total for the project was $3450 ($1500 + $1200 + $750). So the balance credit is $657.28 including contingency and other margin.

10.1 Budget Sources

There were three financial sources for this project. These sources are listed with their totals in Table 17.

Table 17: Budget Sources

Mechanical Engineering Department	$ 1,500
Colorado Space Grant Consortium	$ 750
STOP Fund	$ 1,200
Total	$ 3,450

The primary budget source was the $1500 provided by the Mechanical Engineering Department. After that, the budget provided by Colorado Space Grant was utilized. It was determined that additional funds were required to meet project goals on schedule, so additional funds were requested from the STOP overrun fund. These sources are further demonstrated in Figure 66.

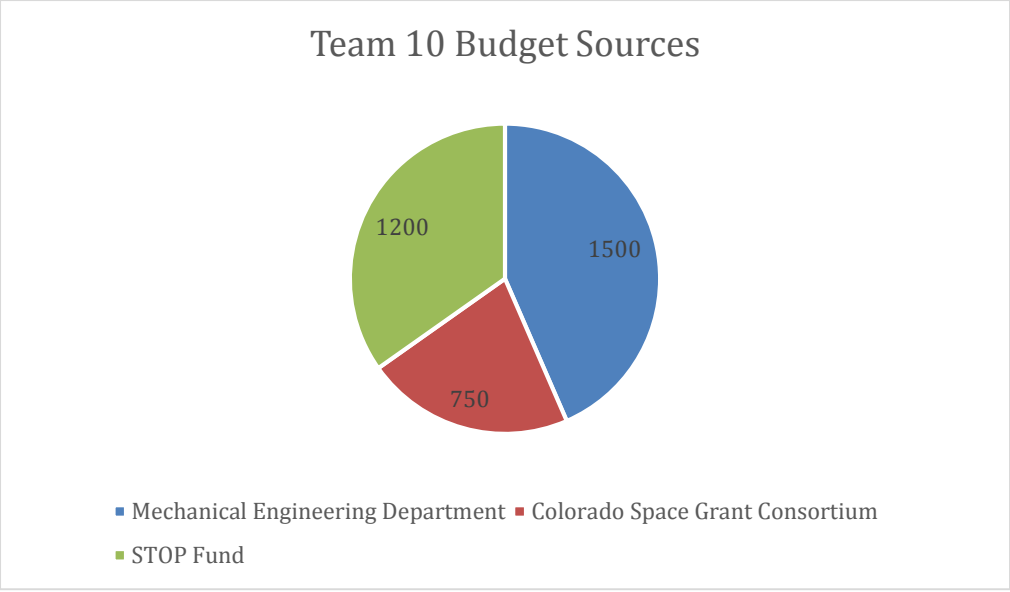

Figure 66: Budget Sources

10.2 Budget Overview (Project Closure Phase)

Table 18 details the final status of the budget. This encompasses all of the costs that were necessary for project completion.

Table 18: Cost Table

Total Cost	$ 2,792.70
Contingency	$ 450.00
Miscellaneous	$ 5.00
Balance	$ 203.00

$450 was initially allocated for contingency, and this amount was not needed after all. $150 was allocated initially for poster printing and other miscellaneous costs. $5 remains of this section. The left over balance from the STOP Fund comes to $200. Table 19 contains all of the project costs, organized by their category.

Table 19: Financial Costs by Category

Category	Source	Costs	Total
Stock Material	Olympic Metals	$ 431.30	$ 528.85
	Colorado Plastic Product Center	$ 10.00	
	ePlastics	$ 87.55	
Machining	St. Vrain Manufacturing PO1	$ 665.00	$ 1,848.43
	St. Vrain Manufacturing PO2	$ 1,022.68	
	Rocky Mountain Waterjet	$ 160.75	
Fasteners and Components	MSC Direct	$ 138.34	$ 263.35
	McMaster-Carr	$ 142.22	
	MSC Direct*	-$ 125.80	
	Mcmaster-Carr*	-$ 21.70	
	Mcmaster-Carr	$ 99.43	
Miscellaneous	McGuckins	$ 7.45	$ 152.09
	Poster	$ 45.00	
	Fedex Printing	$ 79.20	
	UPS	$ 20.44	
		Grand Total	2792.72

* Negative costs were due to product returns.

By far the largest portion of the financial costs was from machining. The majority of the parts for the project were machined in house, but there were so many parts that it was not feasible to finish them all on schedule. Some of the outsourced parts required tight tolerances, or could not be machined in house. Figure 67 demonstrates the differences in categories graphically.

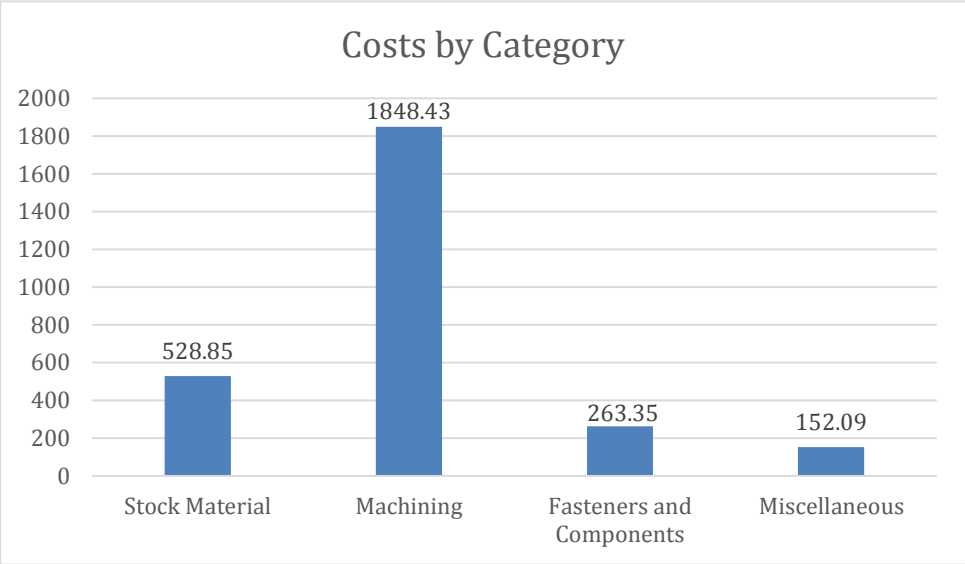

Figure 67: Financial Costs by Category

Table 20 shows the costs that were incurred each month of the second semester of the project. There were no expenses during the first semester.

Table 20: Cost Distribution by Time Phase

Month	Source	Costs	Total
January	Colorado Plastic Product Center	$ 10	$ 441.30
	Olympic metal	$ 431.30	
February	MSC	$ 138.34	$ 311.42
	Mcmaster-Carr	$ 30.86	
	Mcmaster-Carr	$ 142.22	
March	MSC	-$ 125.80	$ 1,734.61
	McMaster-Carr	-$ 21.70	
	McGuckins	$ 7.45	
	St. Vrain Manufacturing PO1	$ 665	
	St. Vrain Manufacturing PO2	$ 1,022.68	

	ePlastics	$ 87.55	
	McMaster-Carr	$ 99.43	
April	Rocky Mountain Waterjet	$ 160.75	$ 305.39
	Poster	$ 45.00	
	Fedex	$ 79.20	
	UPS	$ 20.44	

This distribution is demonstrated further by Figure 68.

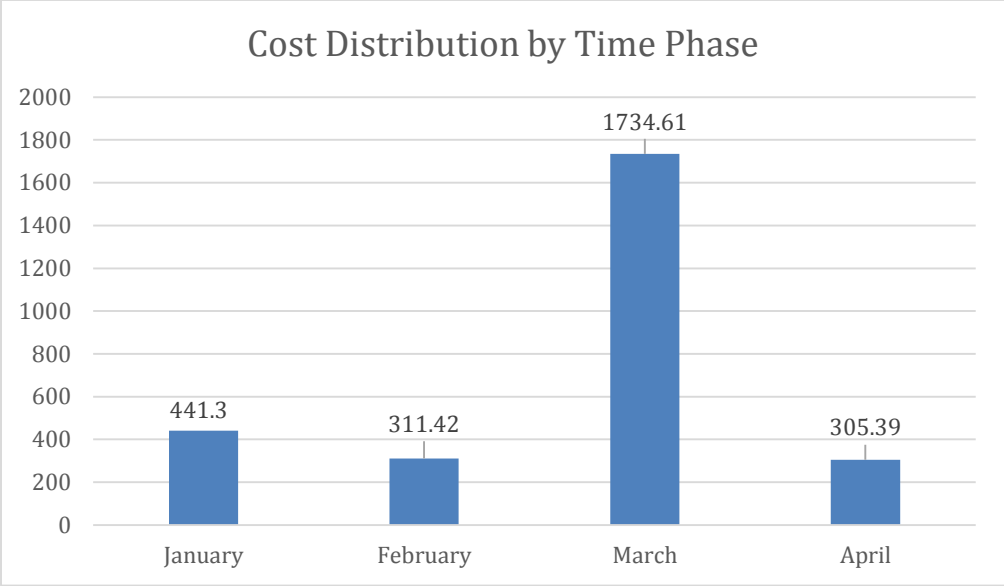

Figure 68: Financial Costs by Time Phase

Table 21 shows the cost distribution by subsystem.

Table 21: Costs by Subsystem

Subsystem	Source	Costs	Total
Structural Parts	Olympic Metals	$ 431.30	$ 2,118.98
	St.Vrain Manufacturing PO#1	$ 665	
	St.Vrain Manufacturing PO#2	$ 1,022.68	
Fasteners and Components	MSC Direct	$ 138.34	$ 270.80
	McMaster-Carr	$ 30.86	
	McMaster-Carr	$ 142.22	
	MSC Direct	-$ 125.80	
	McMaster-Carr	-$ 21.70	
	McGuckins	$ 7.45	
	McMaster-Carr	$ 99.43	
Deployment System	ePlastics	$ 87.55	$ 248.30
	Rocky Mountain Waterjet	$ 160.75	
Roller System	Colorado Plastic Product Center	$ 10	$ 10
Expo	Poster	$ 45.00	$ 144.64
	Fedex	$ 79.20	
	UPS	$ 20.44	

All purchases were done through the senior design project purchasing card provided by the department of mechanical engineering. The card works like a credit card, but it is tax free and does not accumulate interest.

Some issues were encountered with purchasing. Some vendors had transactions declined because they were not listed as approved vendors through the University of Colorado. In these occasions, the financial manager had to speak to the program financial director to resolve the issue. The financial director had to open the card transaction code for a short period so the vendors were able to complete the transaction during that period.

11 Next Steps

Although the design team is graduating and the project is coming to an end, there are still many requirements that need to be met and steps that need to be taken in order to assure that the efforts of this project translate to future successful 6U CubeSat missions. The following section discusses the future of the CubeSat design and the steps that need to be taken in the continuation of the project.

11.1 Bottom Plate Re-Manufacture

The bottom plate of the CubeSat has strictly specified dimensions from Planetary Systems in order to assure a smooth deployment from the CSD and sufficient preload through the CubeSat tabs. The bottom plate was outsourced to St. Vrain Manufacturing, but was received with a tab thickness outside of the specified tolerance. The part was returned to the shop for a rebuild, and the first step for the project in the near future is to receive the new part, and verify that the dimensions are within the stated tolerance within the Planetary Systems CSD payload specification. The CubeSat mass model will not be able to be used in a vibration test if the tabs are not within this specified range. If the tabs are too small, not enough preload will be applied to adequately support the structure. If the tabs are too large, the clamps will not be able to fully actuate, and the door will not shut.

11.2 Random Vibration Test

The designed CubeSat has been theoretically examined to survive a random vibration test with a fundamental frequency over 100 Hz. However, the structure itself has not undergone any actual vibrational testing. The next part of the prototyping process would be to bring the hardware to a facility that can host a random vibration test to simulate the launch conditions that the CubeSat would be expected to withstand. The vibration test would then verify the theoretical analysis performed and confirm the CubeSat's structural integrity.

11.3 Pheonix Payload Integration

Pheonix's payload section is another project under Colorado Space Grant Consortium and does not yet have an official way to interface with the 6U CubeSat designed by SUCCESS. In order to assure successful integration of the Pheonix Payload, the CubeSat team must contact team Pheonix and retrieve their current payload model. The "payload interface plate" can be easily re-designed to accommodate the different fastening methods the Pheonix team may have in mind.

11.4 Solar Array Hinge Redesign

Although the structure is expected to pass a random vibration test without yielding, there is much speculation around the solar array hinge's ability to withstand the forces present throughout launch. The team recommends that the solar arrays be fastened to the structure with two hinges on each panel, reducing the amount of rotation the solar panels experience during launch.

12 Lessons in Design

Over the course of the project there were many opportunities to learn about design in general, and in particular, spacecraft design. These lessons were not just limited to technical aspects, however. The team learned many things about how to work professionally and interact with people in the workplace. This section serves to summarize the major takeaways from the project, but there were too many to put in words.

12.1.1 Adapting to the Planetary Systems Canisterized Satellite Dispenser

When designing to the specific constraints of the planetary systems CSD, the group encountered several problems and unexpected issues. While all of these issues were evaluated and mitigated prior to the testing phase, the following section outlines most of these for the reference of any group that may either design a ground up CubeSat or modify the SUCCESS bus.

When designing to the planetary systems CSD, one of the largest design constraints is the tab interface system. While the size and tolerances of the tabs are very closely defined in the design specification document, the group found out that holding these tolerances through a manufacturing process was extremely difficult. The major takeaway from this error was that the tabs should always be verified after the plate is received from the manufacturer.

The team did not do a good job of verifying these dimensions immediately, as it was assumed that for the price, the part would be made perfectly. It is important to always double check outsourced work, and don't accept errors. Most shops will gladly rebuild parts if they are not made to the drawing.

Another crucial component of the CSD interface that the group almost overlooked was the ejection plate contact zone. Although it is not that obvious from the specification document, the importance of maintaining the appropriate contact points with the ejection plate cannot be overstated. As specified, the pusher plate must contact the structure in at least three separate locations, and these three (or more) locations should encompass the entire structure.

Key Takeaways:

- When designing to planetary systems design specifications (or any other specifications), always read each and every page of the document, and do not make any assumptions about what is stated.
- Always have each and every member of the team verify the design constraints in the literature provided to ensure no requirement is overlooked.
- Always verify that the dimensions of any outsourced part match the dimensions provided in the drawing before assembling the part or using it in any way.
- Acquiring a CSD for testing purposes can be difficult, so make sure to reserve such a test device at least 6 months in advance.

12.1.2 Revision Control

While the final SolidWorks iteration of the 6U CubeSat bus may look very clean and organized, the group had very inadequate revision control throughout most of the design process. The original SolidWorks drawings often had features included in assembly files, rather than features being included exclusively in part files, and the revisions were not organized in numerical order every time. This lead to extensive amounts of "wasted" time trying to identify the correct revision to change. Rather than backtracking and trying to fix problems, it is much easier to just follow a strict system.

Key Takeaways:

- Always establish a revision control system at the beginning of the design process, and stick with it throughout the design process.
- Utilize CAD specific cloud storage locations if possible; controlling revisions on SolidWorks can turn into an extreme mess in short order. The group recommends using GrabCad or similar whenever possible.
- Include a name and date for each and every revision to maintain traceability in the design changes.

12.1.3 Finite Element Analysis

In an effort to validate our design ahead of time, the group decided to utilize finite element analysis in SolidWorks. While most of the lessons learned are included in the FEA sections of the report, the key takeaways associated with computerized FEA models are listed below.

Key Takeaways:

- When performing modal analysis, pin constraints that do not allow translation are appropriate for the fasteners. In SolidWorks, there is a separate connection constraint called “bolt,” but this is not an option for the frequency analysis.
- When designing to planetary systems specifications, make sure to constrain the tabs when performing both the modal and stress analysis. Sometimes results can be generated that may look reasonable, but are basically garbage.
- When performing a modal analysis in SolidWorks, the first five modes (more or less) are often due to numerical issues and read as 0 or close to 0 Hz. This shouldn’t be taken as an indication that the model is wrong – simply look at the modes beyond those.
- When performing a Modal analysis in SolidWorks, the output image can be misleading. The scale given is essentially meaningless, and the deformation scale shouldn’t be taken seriously. Just look at the resonant modes and mass participation.
- It is important to validate FEA models with other methods, and also run FEA tests of subassemblies and components to build further confidence in the models.

12.1.4 CDR and Other Presentation Lessons

The following section contains important information regarding the presentation of information at an aerospace industry level CDR and presenting in general. The SUCCESS team’s CDR included approximately 8 industry professionals, each of which had extensive knowledge regarding the engineering of spacecraft. It is very important to note that an aerospace CDR is far more detailed than a typical CDR or what is expected for a senior design group.

Key Takeaways:

- Perform several mock-CDR presentations for as many different people as possible, this is to prepare the team for the types of questions asked in a CDR situation, and become familiar with all of the presentation content.
- Include all key information in the PowerPoint, and have a plethora of back-up slides to fall back on during questioning.
- The design process should be complete prior to CDR, and ideally the group should be able to build the structure and fly it with no major changes after the CDR is passed. The level of design completeness for an aerospace CDR is very high.

- Be prepared for challenging questions from the CDR panel, and don't be afraid to say "I don't know, we will look into that." It is better to say that than respond with an incorrect or poorly though out response.
- Know the audience – a presentation for professional engineers is way different from a presentation for people at the design expo. The terms used and the level explanation needed has to be tailored to this audience.

12.1.5 Manufacturing Lessons

The following section includes the major lessons learned by members of the team with regards to the manufacturing of the SUCCESS 6U structure. Most of the important lessons are included in the manufacturing section of the report, but several of the key takeaways.

Key Takeaways:

- Always overestimate machining time, as machining a student project involves as much waiting for a machine as it does actually machining.
- If anyone on the team has prior machining knowledge, make sure to include them on every aspect of the design. Knowing how things are made is essential for designing a useful part.
- When machining with Greg Potts, always use a maintain a docile nature and accept his word as law whenever working in his machine shop.
- Avoid making parts out of FR4 or fiberglass. A conventional machine shop will not make parts out of fiberglass, and water jet cutters even have difficulty.
- Do not let complex manufacturing processes hold you back, as it is standard in the aerospace engineering industry to spend large sums of money to use additive manufacturing processes.

12.1.6 Lessons Learned About Aerospace

When compared to many other engineering industries, the aerospace engineering world can be drastically different. The following section includes lessons learned by the team regarding any project in the aerospace engineering industry.

Key Takeaways:

- Because of the high manufacturing costs, multiple prototypes are far less common in the aerospace industry. This means that significant emphasis is placed on the design phase. As a result, expect to have your client and director be highly critical of your design work.
- Always overdress for any occasion, you never know when a high level government or company representative is present.
- Share your design with as many industry professionals as possible (excluding any design with significant protected intellectual property) as each professional may have valuable insight on your design.

13 Conclusions

The goal of the project was to develop a design foundation for a 6U CubeSat bus to be used on future missions by Colorado Space Grant Consortium. The 6U form factor opens the door to many new missions that would be otherwise impossible with a smaller design.

This project encompassed the design, manufacture, and verification of a full structure, solar array deployment system, and mass simulators for spacecraft systems and payload. The entirety of the preceding document outlines a proposed bus structure design for a 6U CubeSat that conforms with the Planetary Systems Canisterized Satellite Dispenser. The structure was designed, built, and verified to meet all of the relevant constraints listed in the CSD specifications document. A modal analysis of the structure in SolidWorks identified the fundamental frequency as approximately 293 Hz, and a stress analysis confirmed the structure could function in a launch environment exceeding 9 G of static loading to a factor of safety of 2.0. The solar array deployment system is capable of producing 22 Watts of power to support payload and spacecraft systems. This system interfaces directly with the interior of the CSD with a roller bearing interface.

Over the course of just 9 months, a tremendous amount of design and fabrication was accomplished by the part-time student team. The critical design review occurred just three months after the start of the project in September of 2014, where the first full iteration of the design was scrutinized by a panel of industry engineers. The design was further refined and reviewed once more at a manufacturing review in December, and was approved for continuation into the manufacturing phase.

The majority of the parts were fabricated in house with Mechanical Engineering resources. Several parts had to be outsourced due to machine shop limitations. The full assembly consists of 26+ unique parts, and in order to meet schedule goals, it was decided to outsource additional parts. The total cost of the project including all material and machining costs was $2,793. Cleanliness and certifications that would be needed for flight were not considered, as this is an engineering development unit. Fabricating equivalent hardware for flight would likely cost significantly more than this listed cost. Additionally, COSGC paid to have this project as a Mechanical Engineering senior design project, so there is additional cost that may be equivalent to labor costs.

After extensive dimensional verification and some redesign and rework, the model was ready for a fit check and deployment. This took place on April 15, 2015 at the Space Symposium in Colorado Springs. The full mass unit was tested for fit and a mass relieved version was successfully deployed from the Planetary Systems CSD. The next step for the project is a random vibration test. This will hopefully be carried out by a Space Grant team over the summer.

Through this extensive design program, the team learned an enormous amount about the engineering process and spacecraft design. This project has directly influenced the team members' career goals and decisions, and will continue to benefit the members in the years to come.

14 Appendix

14.1 Hand Calculations

14.1.1 Thermal Analysis

Assumptions

Assumption	Value
Altitude	10-700km
Solar Emissivity	0.316
Solar Constant	1371 W/m^2
Albedo (a)	0.30 +/- 0.05
Earth IR emission	237 W/m^2
Collimation Factor	Varies with Altitude
Infrared Emissivity	0.8

Matlab Script

```
% The following is a rough estimate of the thermal analysis%
clc
clear all
close all

% Temperature ranges %

Tmin_QBC = -40;
Tmin_ACS = -40;
Tmin_EPS = -40;
Tmin_Batt = -10;
Tmin_Solar = -40;
Tmin_UHG = -30;

Tmax_QBC = 85;
Tmax_ACS = 100;
Tmax_EPS = 85;
Tmax_Batt = 50;
Tmax_Solar = 80;
Tmax_UHG = 70;
```

```
% Electrical Power Dissapation %
Q_wmax = 5; %Electrical Power Dissapation in Watts%
Q_wmin = 15; %Minimum Power Dissapation%

% Surface area %

Surface_area = 2*(10*20)+2*(30*20)+2*(10*30);
Radius_Sphere = sqrt(Surface_area/pi);
D = 2*(Radius_Sphere);
%D = 2.07;

% Radiation Surface Property Values %

Alpha_s = 0.316; % Solar absorbtivity %
Epsilon_ir = 0.8; % Infrared_emmissivity %

% Other Constants
H = 600:0.1:800; %Altitude in km%
R_e = 6378; %Radius of Earth km%
F_se = 0.5.*(1-((H.^2 + 2.*H.*R_e).^(0.5))./(H+R_e)); %Radiation View Factor%
K_a = 0.657 + 0.54.*(R_e./(R_e+H))-0.196.*(R_e./(R_e+H)).^2; %albedo
correction%
Q_irmax = 258; % maximum earth IR emission
Q_irmin = 216; % minimum earth IR emission
G_s = 1376; % Maximum direct solar flux value
A = .35; %Albedo percentage (maximum value for worst case hot condition)
Sigma = 5.67e-8; %Stefan Boltzmann constant%

% Calculate the best-case and worst-case hot temperature

T_maxs = ( (((G_s.*Alpha_s)./4) + (Q_irmax.*Epsilon_ir.*F_se) + ...
    (G_s.*A.*Alpha_s.*K_a.*F_se) +
(Q_wmax./(pi.*D^2)))./(Sigma.*Epsilon_ir)).^(1/4);

T_mins = (( (Q_irmin.*Epsilon_ir.*F_se) +
(Q_wmin./(pi.*(D.^2))))./(Sigma.*Epsilon_ir)).^(1/4);

T_maxs = T_maxs-273; %Changes the temperature from Kelvin to Celsius
T_mins = T_mins-273; %Changes the temperature from Kelvin to Celsius


if T_maxs > 50
    disp('Radiator Needed')
else if T_mins < -10
        disp('Heater/Body Mounted Radiator Needed!!')
    end
end


disp('the maximum temperature at 800km altitude is')
T_maxs(800)
disp('the minimum temperature at 800km altitude is')
T_mins(800)
```

```
plot(H,T_maxs,'r')
xlabel('elevation km','fontweight','bold')
ylabel('temperature Celsius','fontweight','bold')
grid on
figure()
plot(H,T_mins,'b')
xlabel('elevation km','fontweight','bold')
ylabel('temperature Celsius','fontweight','bold')

grid on

% %Calculation for Body Mounted Radiator area
% theta = 0.0005
% T_radiator = 40-5
% A_r = Q_wmax./(Sigma.*Epsilon_ir.*(T_radiator.^4)-
G_s.*Alpha_s.*cos(theta));
```

14.1.2 Payload Tab Analysis

The reference origin for this analysis is the corner of the payload mass simulator on the +Y, +X, -Z corner with respect to the given axes. The origin is shown in Figure 69 along with the position of the center of mass of the assembly.

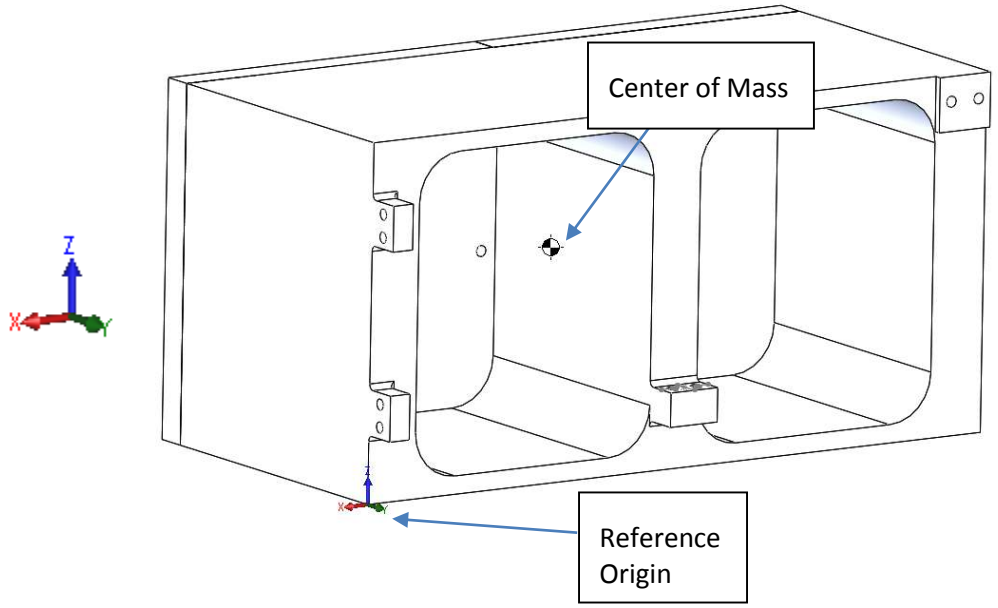

Figure 69: Tab Analysis, Reference Origin and Center of Mass

The position of the center of mass is calculated in SolidWorks with respect to the origin. The coordinates of the center of mass (in mm) are $(x_{COM}, y_{COM}, z_{COM}) = (-100.559, -62.230, 49.987)$.

The maximum stress the tab experiences will either be due to the stress concentration about the fastener holes or at the fillets at the base of the tab. Both cases will be analyzed to determine the absolute maximum stress. The tab will be approximated as a beam though it is very short, and as such the equations derived from Euler-Bernoulli are less accurate.

14.1.2.1 Stress in Fastener Vicinity

The through holes in the tab for fasteners act as stress concentrators. The two holes are of equal size, so the stress concentration factor will be calculated for one hole, and the other hole diameter will be subtracted from the width of the tab. This is demonstrated in Figure 70.

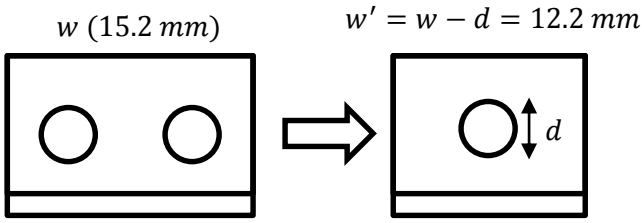

Figure 70: Tab Analysis, Hole Concentration Approximation

It is assumed that the width reduction is symmetric, and the resulting single hole is centered on the approximated tab. This means that the position of the center of the hole is equivalent to the center point of the original tab.

The diameter of each hole is $d = 0.120$ inches (3.05 mm), the width of the tab is $w = 0.600$ inches (15.2 mm), and the height of the tab is $h = 3/8$ inches (9.53 mm). The transformed width is then $w' = 0.600 - 0.120 = 0.480$ inches (12.2 mm).

This position can be generated using the un-altered geometry in SolidWorks with center lines. Figure 71 is an overhead view of the assembly demonstrating the location of the hole as well as its distance from the center of mass.

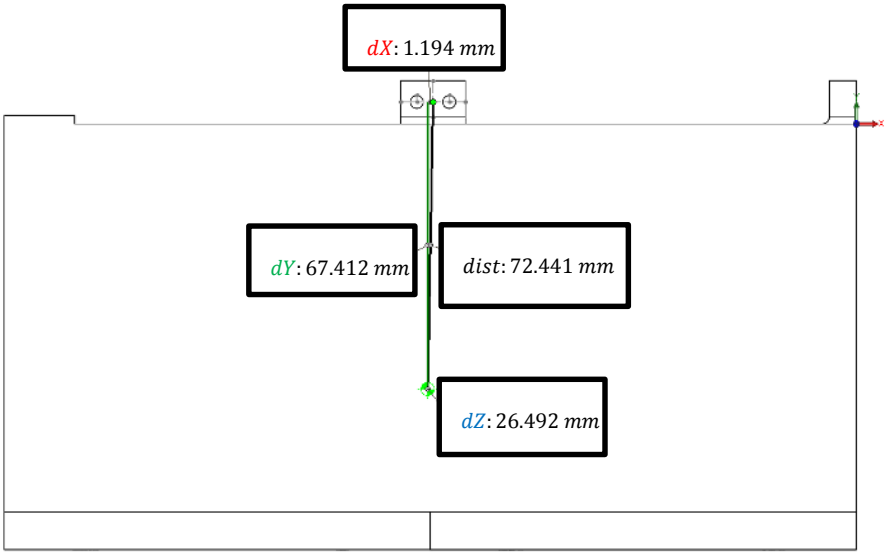

Figure 71: Tab Analysis, Overhead View of Assembly with Distance

The distance vector (in mm) that is given is $(dX, dY, dZ) = (1.194, 67.412, 26.492)$ with respect to the center of mass position. The total distance is 2.852 inches (72.441 mm).

The tab will be considered as a rectangular beam under a moment imposed by static acceleration through the center of mass of the payload assembly. To take the most conservative case, an acceleration of 9 G will be considered perpendicular to the Y distance vector between the two points (2.654 inches, 67.41 mm).

The mass of the assembly is 2.638 kg (not including fasteners and helicoils). The fasteners used will be stainless steel 4-40 socket-head cap screws with a threaded length of 0.75 inches. The mass calculated with Solidworks of the fastener geometry (316 stainless steel) is 1.02 grams. Similarly the mass of each helicoil insert is calculated to be 0.16 grams. There are 8 fastener locations on the back of the assembly, so the total mass is $m = 2.638 + 8(0.00102 + 0.00016) = 2.647$ kg. The resulting moment at the tab fastener hole is thus:

$$M = (2.674\ kg)(9)\left(9.81\frac{m}{s^2}\right)(0.0674\ m) = 15.91\ Nm$$

The stress at that location is calculated:

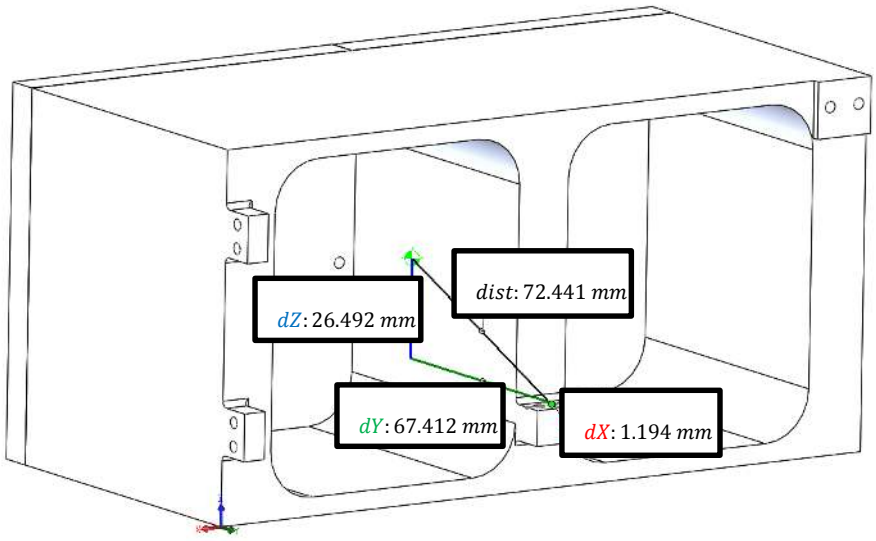

Figure 72: Tab Analysis, Distance from COM to Hole

$$\sigma = \frac{Mc}{I} = \frac{\frac{Mh}{2}}{\frac{1}{12}(w' - d)h^3} = \frac{(15.91\ Nm)(0.00476\ m)}{\left(\frac{1}{12}\right)(0.0122\ m - 0.00305\ m)(0.00953\ m)^3} = 114.8\ MPa$$

An additional factor must be considered due to the stress concentration of the transverse hole. This factor is calculated with [13]:

$$K_t = Ae^{b\left(\frac{d}{w}\right)} \text{ for } \frac{d}{h} \geq 0.25$$

d/h	A	b
0.25	2.68750	-0.75128
0.50	2.46620	-0.77215

Where d is the diameter of the hole, w is the width of the beam, and h is the height of the beam. The ratios: $\frac{d}{w} = \frac{0.120}{0.480} = 0.25$, and $\frac{d}{h} = \frac{0.120}{0.375} = 0.32$. A linear interpolation is used to calculate A and b from the above table.

$$K_t = Ae^{b\left(\frac{d}{w}\right)} = (2.625536)e^{(-0.7571236)(0.25)} = 2.173$$

The transformed stress is then:

$$\sigma = K_t\sigma_{nom} = 2.173 * 114.8\ MPa = 249.4\ MPa$$

14.1.2.2 Stress Near Fillet

The same loads are used in this case to calculate the maximum stress. The nominal stress is taken as 114.8 MPa. Instead of the factor for the hole concentration factor, there is a factor for the stress concentration due to the fillet. This factor is given by [13]:

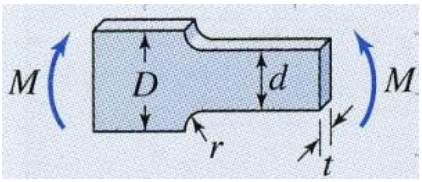

$$K_t = B\left(\frac{r}{d}\right)^a$$

D/d	B	a
6.00	0.896	-0.358

Where D is the height of the beam before the size change, d is the height of the beam after the size change, t is the width of the beam, and r is the radius of the fillet. Because the tab is more of a cantilever attached to a fixed wall than a beam with a changed height, this treatment is approximate. The heighest D/d ratio in the source was 6, though this does not reflect the geometry exactly. The radius of the fillet is 1/16 inches (1.59 mm).

$$K_t = 0.896\left(\frac{0.00159}{0.00953}\right)^{-0.358} = 1.70$$

The transformed stress is then:

$$\sigma = K_t\sigma_{nom} = 1.70 * 114.8\ MPa = 195.16\ MPa$$

14.1.2.3 Simple Shear Stress

Due to the size of the beam and the nature of its loading, the most accurate model for the stress that it will undergo is simple shear stress.

$$\tau = \frac{VQ}{It}$$

Where V is the total shear force at the location, Q is the statical moment of area, I is the moment of inertia of the cross-section, and t is the thickness of the of material perpendicular to the shear. The material cannot shear at the cross-section of the holes, so the full tab area will be considered.

$$Q = (A)\left(\frac{h}{2}\right) = (15.2\ mm * 9.53\ mm)\left(\frac{9.53\ mm}{2}\right) = 690.24\ mm^3 = 6.902 * 10^{-7}\ m^3$$

$$I = \frac{wh^3}{12} = \frac{(15.2\ mm)(9.53\ mm)^3}{12} = 1096.33\ mm^4 = 1.096 * 10^{-9}\ m^4$$

Let $V = (2.764\ kg)(9)\left(9.81\frac{m}{s^2}\right) = 244.03\ N$, and $t = 15.2\ mm$.

$$\tau = \frac{(244.03\ N)(6.902 * 10^{-7}\ m^2)}{(1.096 * 10^{-9}\ m^4)(0.0152\ m)} = 10.11\ MPa$$

14.1.2.4 SolidWorks FEA

The tab is modeled with a fixed geometry boundary condition on its bottom side with a 9G gravity load applied to the payload assembly. Figure 73 is the result of this static loading.

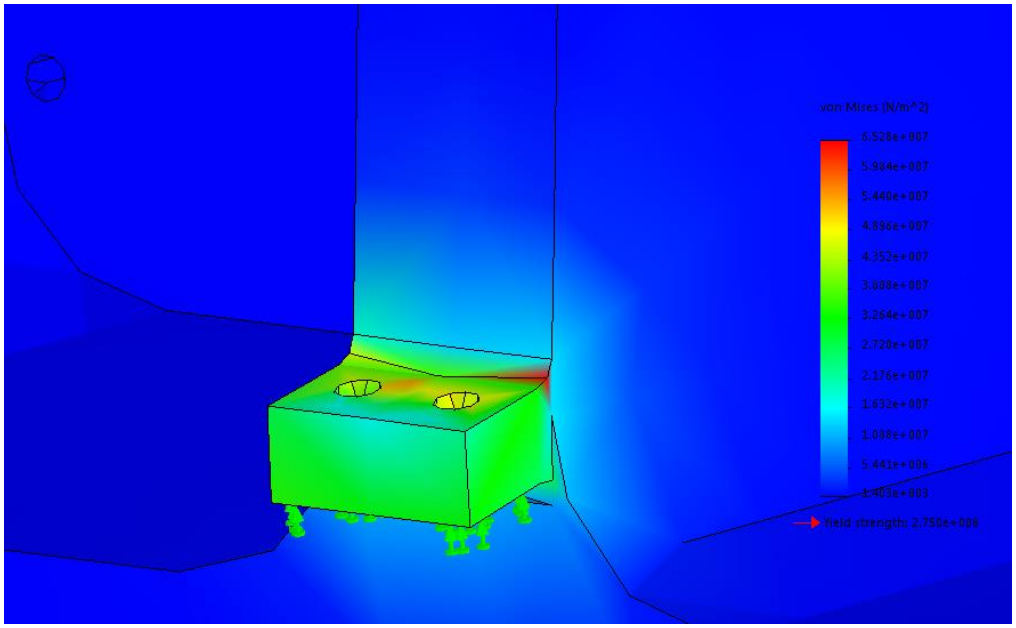

Figure 73: Tab Analysis FEA Result

The scale at the right shows a maximum stress of 65.28 MPa in the vicinity of the fillet.

14.1.2.5 Standards and Acceptance

GEVS (GSFC-STD-7000A) requires a factor of safety of 1.25 for metallic yielding in static loads, but for loads qualified by analysis only, a factor of safety of 2.0 is required. Therefore a factor of safety of 2.0 will be used in evaluating the calculated stresses. Margin of safety is defined by [5]:

$$MS = \frac{Allowable\ Load}{FoS * Load}$$

The margin of safety for each analysis is given in Table 22. The yield stress for 6061-T6 aluminum is 276 MPa and the shear strength is 207 MPa [12].

Table 22: Tab Analysis Summary

Method/Location	Load	Limit Load	MS
Hole Vicinity	249 MPa	276 MPa	0.55
Fillet Vicinity	195 MPa	276 MPa	0.71
Simple Shear	10 MPa	207 MPa	10.24
FEA	65 MPa	276 MPa	2.11

Though all of the stresses are less than their corresponding limit loads, the hole vicinity and fillet vicinity stresses have a margin of safety less than 1. The simple shear analysis and the FEA analysis are the more realistic analysis methods, so the result of MS<1 for the other two methods is acceptable.

14.1.3 Solar Array Deployment

Because the solar arrays will be deploying in microgravity somewhere near low earth orbit, the primary force the hinge mechanism must overcome is friction. There is a small amount of atmosphere that causes drag on the solar arrays, however, the magnitude of this force is negligible.

To quantify the friction the springs must overcome, all of the contact faces in the mechanism must be identified. These are on the hinge arms, hinge blocks, and delrin spacers in contact with the hinge rod, as well as the friction among the spring coils. Table 23 shows the coefficients of static and dynamic friction for the materials in contact.

Table 23: Coefficients of Friction with Steel

Material	Static	Dynamic
Delrin [14]	0.20	0.35
Aluminum [15]	0.61	0.47

The mechanism was designed such that none of the parts are fixed. All parts are built to a slip fit on the precision ground stainless steel rod. This has the benefit that if any parts are experiencing unusually high friction due to debris or surface defects, some other part will be able to move instead. To most accurately model the dynamics of the deployment, a built hinge was observed. As the hinge deploys:

- The hinge arm slides against the hinge rod.
- The large spacer slides against the hinge rod.
- The small spacers slide against the hinge rod.
- The hinge rod remains static within the hinge blocks.

Therefore, the spring forces must overcome the sliding friction between the rod and the hinge arm, and all of the spacers. It is difficult to model friction in microgravity, but an estimation can be made by the dynamic friction experienced in a gravity environment. The friction forces are determined by:

$$F_f = \mu F_N$$

Where μ is the coefficient of dynamic or static friction (whichever is greater), and F_N is the normal force of the parts against each other. It is assumed that this normal force will be less than the normal force seen in gravity – calculating this friction will serve as an upper bound.

For the spacer parts, the only normal force is the weight of those parts. For the hinge arms, the solar arrays are attached as well. It will, however, be approximated that that mass is not present. In microgravity, the normal force present will not be near the magnitude of the full solar array mass. Table 24 lists each of the parts with their corresponding masses that will be used to calculate normal force.

Table 24: Part Masses

Part	Mass (g)
Hinge Arm	7.31
Large Spacer	0.13
Small Spacer	0.028

The total normal force is then calculated as:

$$F_{N1} = (0.00731\ kg)\left(9.81\frac{m}{s^2}\right) = 0.072\ N$$

$$F_{N2} = (0.00013\ kg + 2 * 0.000028\ kg)\left(9.81\frac{m}{s^2}\right) = 0.0018\ N$$

Where F_{N1} is the normal force for the hinge arm, and F_{N2} is the normal force for the spacers. From this, the friction can be calculated.

$$F_f = \mu_1 F_{N1} + \mu_2 F_{N2} = (0.61)(0.072\ N) + (0.35)(0.0018\ N) = 0.045\ N$$

The total torque output of the springs in each hinge is 1.104 in-lbs (0.125 Nm). The length of the leg on each spring is 1 inch (0.0254 m). The force at the hinge rotation point from the spring is:

$$F = \frac{0.125\ Nm}{0.0254\ m} = 4.92\ N$$

This gives a margin of:

$$MS = \frac{4.92\ N}{2.0 * 0.045\ N} = 54.7$$

This margin is very large, and it will encompass a lot of potential variation in the friction experienced.

14.1.4 CSD Ejection

To develop an understanding of the ejection velocity from the CSD, some brief calculations were done and verified with the CSD specification document.

Figure 74 is a free-body diagram for the moment of ejection from the CSD.

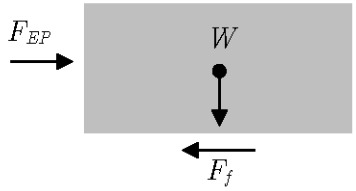

Figure 74: CubeSat Ejection FBD

Where F_{EP} is the ejection plate force in N, W is the weight of the CubeSat in N, and F_f is the frictional force between the CubeSat tabs and the CSD.

The ejection plate exerts a constant force on the CubeSat throughout ejection. This force can be in the range 15.6 - 46.7 N depending on the spring that is installed [4].

The weight of the CubeSat is simply:

$$W = mg = (12\ kg)(9.81\ m/s^2) = 117.72\ N$$

And the frictional force is described by:

$$F_f = \mu F_N = (0.17)(117.72\ N) = 20.01\ N$$

Where F_N is the normal force along the friction axis (in this case it is just the weight of the CubeSat), and μ is the coefficient of static friction for hard-anodized aluminum on hard-anodized aluminum [16]. The coefficient of kinetic friction may be more appropriate, but for dry metals there is little difference.

To determine the ejection velocity of the CubeSat, a force balance must be carried out.

$$\sum F = \sum ma$$

$$F_{EP} - F_f = ma$$

Assuming the maximum spring force,

$$46.7\ N - 20.01\ N = (11.6\ kg)a$$

$$a = 2.30\ m/s^2$$

From this acceleration, the final exit velocity can be calculated.

$$v_f^2 = v_0^2 + 2 * a * d$$

The initial velocity, v_0, is zero as the CubeSat starts at rest. The distance, d, is the length of the tabs, $d = 14.7$ in (0.373 m).

$$v_f^2 = 2 * \left(2.30 \frac{m}{s^2}\right) * (0.373\ m)$$

$$v_f = 1.31\ m/s$$

This value is in family with what is expected from the CSD specification document. Figure 75 is the ejection velocity plot from the CSD specification document.

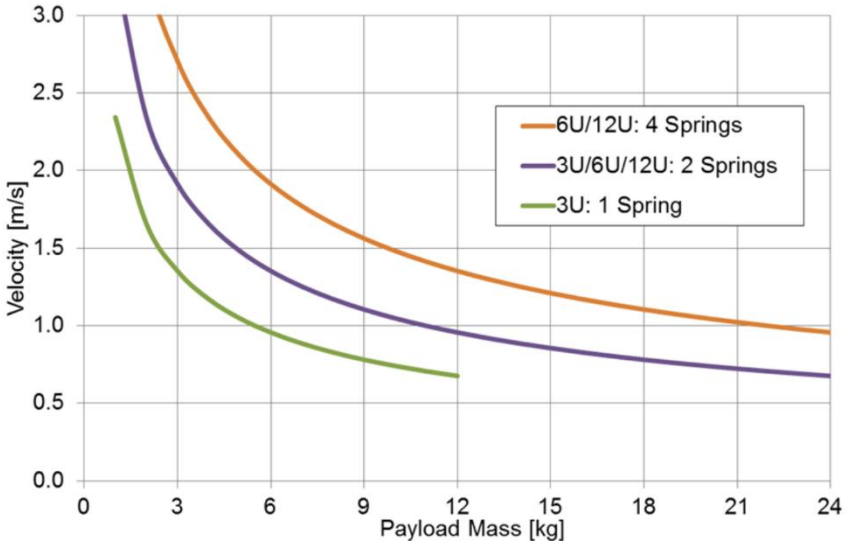

Figure 75: CSD Ejection Velocity [4]

With a payload mass of close to 12 kg, the curve for 4 springs (the maximum) shows a velocity of approximately 1.3 m/s.

Note that this velocity applies to a horizontal deployment, not against gravity. The spring force is not enough to eject the full mass vertically.

15 References

[1] Dunbar, Brian. "NASA's Cubesat Launch Initiative." *NASA*. NASA, 10 Feb. 2011. Web. 06 May 2015

[2] "6-Unit CubeSat Structure." *CubeSat Shop*. Innovative Solutions in Space, n.d. Web. 06 May 2015.

[3] *6U SUPERNOVA Structure Kit Owner's Manual*. Rep. San Francisco: Pumpkin Space Systems, 2014. Print.

[4] CANISTERIZED SATELLITE DISPENSER (CSD) DATA SHEET. Tech. no. 2002337B. N.p.: Planetary Systems Corporation, 2014. Print.

[5] Brown, Charles D. *Elements of Spacecraft Design*. Reston, VA: American Institute of Aeronautics and Astronautics, 2002. Print.

[6] *Falcon 9 Launch Vehicle Payload User's Guide Rev. 1*. Tech. Hawthorne, CA: Space Exploration Technologies, 2009. Print.

[7] *Delta IV Launch Services User's Guide*. Tech. Centennial, CO: United Launch Alliance, 2013. Print.

[8] *Atlas Launch System Mission Planner's Guide, Atlas V Addendum*. Tech. San Diego, CA: International Launch Services, 1999. Print.

[9] GENERAL ENVIRONMENTAL VERIFICATION STANDARD, GSFC-STD-7000, 2013-04-22

[10] Holemans, Walter. "PAYLOAD SPECIFICATION FOR 3U, 6U, 12U AND 27U." (n.d.): n. pag. Planetary Systems Corporation. *Planetary Systems Corporation*, 21 July 2014. Web. 1 May 2015.

[11] *Atlas V Launch Services User's Guide*. Tech. Centennial: United Launch Alliance, 2010. Print.

[12] "Suggested Tightening Torque1 Values To Produce Corresponding Bolt Clamping Loads." (n.d.): n. pag. *Spaenaur*. Spaenaur. Web. 6 May 2015. <http://www.spaenaur.com/pdf/sectionD/D48.pdf>.

[13] "Aluminum 6061-T6; 6061-T651." *ASM Material Data Sheet*. Matweb, n.d. Web. 06 May 2015. <http://asm.matweb.com/search/SpecificMaterial.asp?bassnum=MA6061t6>.

[14] Shigley, Joseph Edward., and Charles R. Mischke. Mechanical Engineering Design. Boston: McGraw-Hill, 2001. Print.

[15] Delrin Acetal Resin: Design Guide Module III. Rep. N.p.: Dupont, n.d. Print.

[16] "Friction and Coefficients of Friction." *Friction and Coefficients of Friction*. The Engineering Toolbox, n.d. Web. 06 May 2015. <http://www.engineeringtoolbox.com/friction-coefficients-d_778.html>.

[17] "Coefficient of Friction between Anodized Aluminum and Steel." *Anodizing World*. N.p., n.d. Web. 06 May 2015. <http://aluminumsurface.blogspot.com/2011/02/coefficient-of-friction-between.html>.